Behaviour of a falling apron
Final Report

January 2002

M.Sc. Thesis
M.A. van der Hoeven
St. no. 9347276

Graduation Committee:

Prof. ir. K. d'Angremond	*(DUT, Chairman)*
Dr. ir. H.L. Fontijn	*(DUT)*
Ir. H. Oostinga	*(BHD)*
Ir. H.J. Verhagen	*(DUT)*

Delft University of Technology
Faculty of Civil Engineering and Geosciences
Hydraulic and Geotechnical Engineering Department
Hydraulic Engineering Section

Ballast Ham Dredging bv
Engineering and Research Department

Preface

This is the final report of a thesis study on the behaviour of a falling apron. It has been written within the scope of a graduation project, as part of the master’s study, at the Faculty of Civil Engineering and Geosciences at Delft University of Technology.

The subject of study was put forward by Ballast Ham Dredging bv, a company which has a broad experience in the field of hydraulic engineering. As the contractor for the Jamuna Bridge River Training Works, this company was involved in the construction of a falling apron, which consisted of a considerable quantity of rock. The knowledge, gathered during the construction of the project was very useful in this study.

The author wishes to thank the graduation committee for their advice and supervision. Their patience in carefully reading and commenting on the preliminary report and the various draft reports have contributed to this final report.

Special thanks go to Ir. H. Oostinga, who was closely involved in the construction of the JB-RTW and therefore has much knowledge on the subject, to Prof. ir. K d’Angremond and Dr. ir. H.L Fontijn for their supervision and useful comments and especially to Ir. H.J. Verhagen, who was prepared to help at any time.

Thanks are also due to Geert Mulder, of Joosten Bouwstoffen bv, Werkendam, for his help in obtaining the different rock grades needed in the experiments.

Further gratitude is due to members of the staff of Ballast Ham Dredging bv, who provided an interesting thesis subject and a pleasant working environment. Their support in various fields was encouraging. Two who special mention here: Klaas Klein and Fred Aleven. During the period when the experiments were in progress they were very good company and always ready to help.

Delft, January 2002

Mark van der Hoeven

Abstract

In 1997 the Jamuna Bridge was finished and came into use. As this bridge is a shore connection for one of the largest rivers in the world, extensive river training works were designed and built, mainly to avoid outflanking of the bridge by the river. It was especially the braiding character of the river with its ever-changing pattern, which made it difficult to predict the morphological behaviour. The river training works incorporated two guide-bunds, which lead the river through the contraction at the location of the bridge. This made it possible to cross the flood plain by constructing earthen abutments, leaving a bridge span of 5km instead of 15km.

The narrowing of the river will lead to morphological changes. Deepening of the riverbed by means of local scour can be expected. To protect the toe of the revetment against this scour, a more or less traditional solution has been applied: the falling apron. A falling apron is a stack of granular material at the toe of a revetment, which will launch onto the slope of the scour hole when the revetment is undermined. The established slope will then be protected by a layer of rock, which will retain the bed material and prevent the formation of a slope that is too steep.

To understand more about the setting process and to determine the resulting slope, a physical model was built and tested in a flume. Three different rock sizes were examined and two different initial configurations. It was found that the slope angle after setting was 1:2 for all experiments.

Surprisingly, only a small amount of apron rock was actually used. This was because just a single layer of material covered the scour slope. This single layer does not retain the material like a properly designed filter, but it does slow down the erosion of sand from under the apron. Two parts of the falling apron were discerned: the ‘waiting part’ consisting of the stack of unused material and the ‘launched part’, which is the rock layer covering the slope.

This single layer has important consequences for the functioning of the apron. The grading used at the Jamuna Bridge was extra wide. The idea was that when a thick layer was launched on the slope, the fines would wash out of the top layer. A filter structure would then develop with large grains in the upper layer and fines (and large grains) in the lower layer. This theoretical case was not found in the model.

The resulting slope appeared to have settled evenly and over the complete scour depth. No unprotected sand slope was observed during the experiments. The rock layer follows the bed level and extra rock is added from the waiting part of the apron when the layer slides down. This mechanism of scour at the toe and rock launching at the top implies that sand transport through the layer also occurs. The consecutive phases in the setting process showed that at different times the apron slopes lie parallel and retreat as a whole with the edge of the waiting apron.

Resulting slope angles found in the model

	FT01	FT02	FT03	FT04	UNIT
rock size	15/30	15/30	30/60	8/16	[mm]
apron height	18.5	12.5	11.7	13.6	[cm]
Slope	26.6	26.6	25.6	27.0	[º]
V:H	1:2.0	1:2.0	1:2.1	1:2.0	[-]

The survey data, retrieved since the Jamuna Bridge was built, were used to compare the model results with a prototype. These profiles also showed an apron slope of 1:2. However the thickness of the layer cannot be determined from the data. It can be seen that the apron slope follows the edge of the waiting part as it does in the model.

Notation

α	=	coefficient	[-]
β	=	empirical coefficient ($\beta \approx 3.0$)	[-]
γ	=	scour coefficient	[-]
Δ	=	relative density $(\rho_s-\rho_w)/\rho_w$	[-]
η	=	ripple height	[m]
φ	=	angle	[°]
κ	=	Von Kàrmàn constant	[-]
λ	=	ripple length	[m]
ν	=	viscosity	[m^2/s]
θ	=	angle, stability parameter	[rad, -]
ρ_r	=	density of rock	[kg/m^3]
ρ_w	=	density of water	[kg/m^3]
τ	=	shear stress	[N/m^2]
τ_c	=	critical shear stress	[N/m^2]
ψ_s	=	Shields parameter	[-]
a	=	model factor	[-]
B_0	=	initial width	[m]
B_c	=	constricted with	[m]
C	=	Chézy coefficient	[$m^{1/2}$/s]
c	=	coefficient (see Table 5.1)	[-]
d	=	diameter	[m]
d_b	=	characteristic diameter of bed material	[m]
d_{b50}	=	characteristic diameter of bed material (50% smaller)	[m]
d_f	=	characteristic diameter of filter material	[m]
d_{f15}	=	characteristic diameter of filter material (15% smaller)	[m]
e	=	empirical coefficient; $e=c*Re^{-m}$	[-]
f		silt factor	[-]
G	=	weight of soil mass	[kg]
g	=	gravitational acceleration	[m/s^2]
h	=	water depth	[m]
h_0	=	initial water depth	[m]
h_c	=	water depth in constriction	[m]
h_c	=	water depth in the centre of the river	[m]
h_{init}	=	initial depth at start of local scour	[m]
h_{max}	=	maximum depth of scour hole	[m]
h_r	=	Lacey regime depth	[m]
h_s	=	scour depth (below water level)	[m]
i	=	water level gradient	[-]
i_c	=	water level slope in the middle of the river	[-]
i_{cr}	=	critical gradient	[-]
k	=	grain roughness	[m]
m	=	coefficient (see Table 5.1)	[-]
n	=	porosity	[-]
Q	=	discharge	[m^3/s]
R	=	radius of curvature	[m]

r	=	radius	[m]
r	=	relative turbulence (r=0.1 to 0.15)	[-]
R_c	=	radius of curvature in the centre of the river	[m]
t	=	time	[hours]
t	=	layer thickness	[m]
u	=	flow velocity	[m/s]
$\bar{u}$	=	average velocity	[m/s]
u_{*cr}	=	critical shear velocity	[-]
u_{cr}	=	critical flow velocity	[m/s]
u_f	=	flow velocity in filter	[m/s]
$u_{f,c}$	=	critical filter velocity	[m/s]
V	=	volume	[litre]

Abbreviations

CC-blocks	Concrete Cement blocks
EGB	East Guide Bund
FA	Falling Apron
FAP	Flood Action Program
FT	Flume Test
JB-RTW	Jamuna Bridge River Training works
PWD	Public Works Datum, all levels used are relative to PWD, which is 0.4599m below New Mean Sea level.
SPT	Suction Pipe Test
WGB	West Guide Bund

List of figures

Figure 1.1 Different alternatives for scour protection. 13
Figure 1.2 Severely attacked guide bund.. 15
Figure 2.1 Bangladesh transportation network.. 18
Figure 2.2 Frequency distribution for mean daily discharge measured at Bahadurabad between 1956 and 1989.. 19
Figure 2.3 Theoretical relationship for estimating outer bend scour [JANSEN 1979]............. 23
Figure 2.4 Scour depth development in time 25
Figure 3.1 Decrease of pore volume.. 29
Figure 3.2 Flow slide result 30
Figure 3.3 Slip circle failure with rotation centre RC 31
Figure 4.1 Falling apron design according to Spring, Gales and Rao 34
Figure 4.2 Steepness of sand slope beneath a sand-tight mattress, re-drawn from: [DE GROOT 1988].. 37
Figure 4.3 Shields diagram 42
Figure 4.4 Angle of internal friction for different grain diameters acc. to Lane.................... 44
Figure 5.1 Relation between different types of filters 46
Figure 5.2 Decrease of apron thickness during setting... 51
Figure 6.1 Sand transport at different locations of the cross-section.................................... 55
Figure 6.2 Attack scenarios.. 56
Figure 6.3 Different geometrical configurations.. 57
Figure 7.1 Scour development 66
Figure 7.2 Method of approach of scour development... 67
Figure 7.3 Curvature of flow lines (top view).. 67
Figure 7.4 Filling rack with its 5 compartments 70
Figure 7.5 Co-ordinate system 71
Figure 8.1 Development of scour depth FT01 74
Figure 8.2 Erosion around an individual stone and along the apron edge (on the right)........ 75
Figure 8.3 Settled apron at t=420min 76
Figure 8.4 Settled apron at t=420min with lines to accentuate the difference in slope angle (initial sand level in red) 76
Figure 8.5 Profile of apron and sand before and after setting (FT01, x=2.50m).................... 77
Figure 8.6 Development of scour depth FT02 78
Figure 8.7 Profile of apron before and after setting (FT02).. 79
Figure 8.8 Top view of setting FT02 (x=2.50m).. 80
Figure 8.9 Side view of setting FT02 81
Figure 8.10 Development of scour depth FT03 83
Figure 8.11 Profile of apron before and after setting (FT03).. 83
Figure 8.12 Development of scour depth FT04 85
Figure 8.13 Profile of apron before and after setting FT04 86
Figure 8.14 Cross-section of apron after run #4 (FT04).. 86
Figure 8.15 a&b Measuring of average rock level 88
Figure 9.1 Secondary flow in river bend 96
Figure 9.2 Change of bank steepness as result of secondary flow 97
Figure 9.3 Outfanning of apron in bend. 98
Figure 10.1 Setting process of the apron 99
Figure 10.2 The expected (A) and the observed (B) setting result...................................... 100
Figure 10.3 Retreat of slope... 102

List of tables

Table 2.1 Maximum discharge and water level of Jamuna River at Bahadurabad 17
Table 3.1 Grading of bed material [10^{-6}m]. 27
Table 3.2 Relation between fall velocity and grain diameter.. 28
Table 4.1 Comparison of costs* per m^1 of guide bund for various levels of the falling apron 35
Table 4.2 Types of materials used at different locations 40
Table 4.3 Empirical relations for Ψ_c according to Van Rijn.. 43
Table 5.1 Parameters according to Klein Breteler... 49
Table 6.1 Ripple sizes for sand 100μm and different flow velocities 61
Table 6.2 Sand and rock size.. 61
Table 6.3 Critical velocities for proposed rock sizes (h=0.50m).. 62
Table 6.4 Comparison of test alternatives.. 63
Table 7.1 Rock characteristics 65
Table 7.2 Relation between rock gradings and sand size 65
Table 7.3 Theoretical bed form and roughness for different depths..................................... 68
Table 7.4 Experiment Outline.. 69
Table 7.5 Location and time of different measurements 72
Table 8.1 Characteristic parameters from experiment FT01 74
Table 8.2 Characteristic parameters from experiment FT02 78
Table 8.3 Characteristic parameters from experiment FT03 82
Table 8.4 Characteristic parameters from experiment FT04 84
Table 8.5 Deviations in measured planes 89
Table 8.6 Summary of experiment results 89
Table 9.1 Falling apron parameters of JB-RTW 91
Table 9.2 Main scale factors 93
Table 9.3 Scour characteristics from survey data October 2000... 96

Table of Contents

Preface 2
Abstract 3
Notation 5
List of figures 7
List of tables 9
Table of Contents 10
1 Introduction 13
1.1 General description of the Falling Apron concept 13
1.2 Scope of the subject 14
1.3 Problem definition and aim of the project 16
2 Hydraulic aspects 17
2.1 Introduction 17
2.2 The Brahmaputra/ Jamuna River 17
2.3 Discharge 19
2.3.1 Bed forming discharge 19
2.3.2 Bank-full discharge 19
2.4 Velocity 20
2.5 Scour 20
2.5.1 Different types of scour 20
2.5.2 Combination of scour along guide bunds 24
2.5.3 Scour development in time 24
3 Geotechnical aspects 27
3.1 Introduction 27
3.2 Soil characteristics Jamuna River 27
3.3 Slope stability 28
3.3.1 Micro stability 29
3.3.2 Macro stability 29
3.4 Presence of clay 31
3.5 Presence of mica 32
4 Common design practice 33
4.1 Introduction 33
4.2 Design 33
4.2.1 Thickness of apron section 33
4.2.2 Length of apron section 33
4.2.3 Slope after setting 35
4.2.4 Construction depth 35
4.2.5 Grading of rock 36
4.3 Alternative materials 36
4.3.1 Mattresses 37
4.3.2 Granular material 38
4.3.3 Description of some applications 39
4.4 Stability of apron rock 40

4.4.1 Izbash ... 40
4.4.2 Shields ... 41
4.4.3 Sloping bed ... 43

5 Granular filters ... 45
5.1 Introduction ... 45
5.1.1 Filter function of a falling apron ... 45
5.1.2 Geometrically closed filters ... 46
5.1.3 Geometrically open filters ... 46
5.2 Basic equations ... 47
5.2.1 Navier Stokes ... 47
5.2.2 Forchheimer ... 48
5.3 Calculation of gradient inside the filter ... 48
5.4 Stability of bed material ... 49
5.4.1 Critical gradient ... 49
5.4.2 Thickness ... 50

6 Model ... 52
6.1 Introduction ... 52
6.2 Information required from the model tests ... 52
6.3 Extent of the model ... 53
6.3.1 Borders ... 53
6.3.2 Boundary conditions ... 53
6.4 Similarity ... 54
6.5 Considerations on suction pipe tests ... 55
6.5.1 Suction distance ... 55
6.5.2 Scenarios ... 56
6.5.3 Apron material ... 56
6.6 Considerations on flow tests ... 57
6.6.1 Froude ... 57
6.6.2 Reynolds ... 58
6.6.3 Bed material ... 58
6.6.4 Roughness ... 59
6.6.5 Apron material ... 61
6.6.6 Thickness of apron section ... 62
6.7 Choice of model ... 63

7 Experiment Set-up ... 64
7.1 Introduction ... 64
7.2 Test facility ... 64
7.3 Materials used ... 64
7.3.1 Sand ... 64
7.3.2 Rock gradings used ... 64
7.4 Test conditions ... 66
7.4.1 Water depth ... 66
7.4.2 Curvature of flow lines ... 67
7.4.3 Roughness and bed features ... 68
7.5 Experiment programme ... 68
7.6 Description of experiment outline ... 69
7.7 Measurements ... 70
7.7.1 Co-ordinate system for measurements ... 70
7.7.2 Velocity ... 71

7.7.3 Bed profile *71*
7.7.4 Water depth *71*
7.7.5 Discharge *72*

8 Description and interpretation of results 73
8.1 Introduction 73
8.2 Experiment FT01 (rock: 15/30 mm, thickness: 0.20m) 73
8.2.1 Set-up *73*
8.2.2 Development of scour *73*
8.2.3 Behaviour of apron *74*
8.3 Experiment FT02 (rock: 15/30 mm, thickness: 0.12m) 77
8.3.1 Set-up *77*
8.3.2 Development of scour *77*
8.3.3 Behaviour of apron *78*
8.4 Experiment FT03 (rock: 30/60 mm, thickness: 0.12m) 82
8.4.1 Set-up *82*
8.4.2 Development of scour *82*
8.4.3 Behaviour of apron *83*
8.5 Experiment FT04 (rock: 8/16 mm, thickness: 0.12m) 84
8.5.1 Set-up *84*
8.5.2 Development of scour *84*
8.5.3 Behaviour of apron *85*
8.6 Influence of measuring errors 87
8.6.1 Reading error *87*
8.6.2 Deviation of measuring device *87*
8.6.3 Deviation in measured planes *88*
8.7 Model observations 89

9 Relation between model and prototype 91
9.1 Introduction 91
9.2 Parameters of prototype 91
9.3 Scaling effects 92
9.4 Survey information Jamuna Bridge 93
9.4.1 Satellite images *93*
9.4.2 Survey results *95*
9.5 Considerations on secondary influences 96

10 Description of apron behaviour 99
10.1 Apron dynamics 99
10.2 Filter function 101
10.3 Durability 102

11 Conclusions and recommendations 104
11.1 Introduction 104
11.2 Conclusions 104
11.3 Recommendations 105

Bibliography 107

1 Introduction

1.1 General description of the Falling Apron concept

When a revetment is applied as a bank protection in a bend of a meandering or braiding river, it can be expected that erosion will continue, or even increase, after construction of the revetment. The same holds for river training works that locally constrict the river, i.e. at the location of a bridge. This scour can be due to general degradation of the riverbed, meandering, seasonal variations or constriction. When considerable scour is expected (say more than a few meters) there are several possible ways to counteract this (see Figure 1.1).

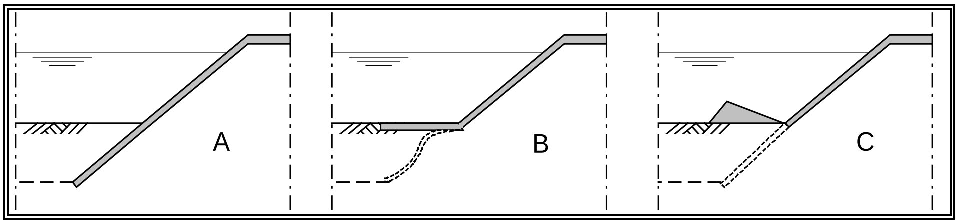

Figure 1.1 Different alternatives for scour protection.

The first possibility is to install the protection down to the expected scour depth and to cover it with the original bed material (A). This is a good solution, but often very expensive. When the expected scour depth is more than 25-30m below water level, technical difficulties with dredging might arise.

Another option is to cover the toe of the revetment with a flexible mattress, which can follow the scour slope and thus retain the bed material (B). Nowadays mattresses are made of geotextile for strength and sand-tightness and concrete blocks for ballast. Traditionally, fascine mattresses were made of willow saplings or bamboo and ballasted with rock.

Another possible solution is the ‘falling apron’ (C), which is often applied in rivers in India and Bangladesh. The falling apron is a toe protection that can adjust to scour and follow any bed erosion downwards, thus continuing to protect the toe of the bank protection. The idea is to store an amount of stones at the toe of the revetment during construction. Scour will cause the stones to roll down; preventing the formation of an erosion slope that is too steep. When the scour starts to develop, the material is launched onto the developing slope. The loose elements are assumed to cover the slope to a thickness large enough to retain the bed material.

In this study the term *falling apron* is used. The reader can substitute *launchable apron*, which has the same meaning. In Figure 1.1 the alternatives B and C are located at original bed level. Of course, it is also possible to choose a lower level. This will generate higher dredging costs, but a smaller falling height.

1.2 Scope of the subject

A flexible toe protection in the form of a falling apron finds many applications in India and Bangladesh. The idea of dumping concrete cement blocks (CC blocks) or rock at the low waterline when a river endangers a village is copied for large structures. The first major application was at the Hardinge Bridge in India[1] in 1912. Usually design rules formulated on the basis of experience, are made and applied in other river training works. The scour depth that they are to withstand is often scaled up, the design for river training works at the Paksey Bridge being the most striking example. In the design, an expected scour depth of approx. 55m is anticipated and the falling apron section consists of 180 m^3/m^1.

These enormous quantities, rock being scarce in Bangladesh, generate high costs and logistical difficulties. It is therefore important that the result should justify the expenditure.

A falling apron can be applied as a toe protection along revetments, at the head of a groyne or along a guide bund. In the case of the bridge works a guide bund system to keep the river under the bridge is very suitable. Two banana-shaped revetment works are built on the flood plains at the head of two spur dykes, which decrease the length of the bridge span. The width of the river is constricted and deepening of the riverbed can be expected. In Figure 1.2, a guide bund with the falling apron at the toe is shown.

The structure of the river training works for the Jamuna Bridge[2] (finished in 1997) also included a falling apron. These works were executed by a joint venture of two Dutch dredging contractors; HAM and Van Oord ACZ (HAM-VOA JV). Data is available from the execution of these works and from surveys conducted since the construction. This provides an opportunity for research on this protection method and comparisons with prototype data.

First a simple 2-dimensional situation such as that used along a revetment or guide bund was investigated. The flow direction in these situations is parallel to the falling apron, which simplifies the scour and setting mechanism.

---

[1] In 1912, Bangladesh was still part of the Indian territory, under English administration. After the independence of Pakistan in 1947, it was known as East Pakistan. In 1971, after the liberation war, it became independent and known as the Peoples Republic of Bangladesh. The Hardinge Bridge now lies in the territory of Bangladesh, crossing the Ganges River.

[2] In this study, the name Jamuna Bridge is used. The official name is Bangabandhu Jamuna Multipurpose Bridge, named after Bangabandhu Sheikh Mujibur Rahman (1920-1975), founder of the nation of Bangladesh. Bangabandhu is an unofficial title meaning Friend of Bengal.

Figure 1.2 Severely attacked guide bund

1.3 Problem definition and aim of the project

In design practice for Bangladesh, in addition to rock, alternative materials are used. Besides concrete blocks of uniform size and granular material with a very wide grading, articulated concrete mats and geocontainers are also used.

The wide grading is supposed to be more sand-tight than a normal (narrow) grading, because it has a more compact granular skeleton. In all designs, the slope after the falling process is assumed to be 1:2. It is very likely that the different materials will influence the establishment of the slope and the final protection. For sand-tight materials, such as geotextile, this has already been proven by tests at WL|Delft Hydraulics [DE GROOT 1998].

The aim of this project is:

- To gain insight into the falling process and the successive phases (what happens?),
- To determine whether different configurations influence the final slope (special care during dumping necessary?),
- To determine how an apron with insufficient rock should be re-strengthened,
- To determine whether the use of a falling apron will provide a durable protection against scour.

On design drawings only the beginning and anticipated final situations are shown. The successive phases during the process are neglected or unknown. This project, being a preliminary exploration, should initially give insight into the process of falling, the successive phases and the final slope.

2 Hydraulic aspects

2.1 Introduction

In this chapter the hydraulic aspects that are relevant to the subject are described, starting with a description of the hydraulic conditions of the Jamuna[3] River. The objective of this study was to consider this particular river, but to interpret the survey results it is necessary to give an idea of the scale of operations.

After this description of a natural system, the more theoretical background of the scour process is described. Therefore first the discharge parameters are given.

2.2 The Brahmaputra/ Jamuna River

The Brahmaputra, like the Ganges, originates on the northern slopes of the Himalayas in Tibet. From its source, the river flows eastward through China for about 1,700km before turning to the south, cutting through the Himalayas to enter India (See Figure 2.1). In India the river completes a large horseshoe bend and flows some 720km to the west. Close to the border of Bangladesh, the Brahmaputra turns to the south and flows as Jamuna River in this direction up to the confluence with the Ganges at Goalundo. Downstream of this confluence the rivers (Ganges and Jamuna) are referred to as Padma River. The total length of the river is 2,880km. The catchment area upstream of Bahadurabad is approximately 560,000km^2 (see Appendix 1).

The river level starts to rise in March owing to the melting of snow in the Himalayas, which causes a first peak in May or early June. Subsequent and higher peaks occur in July-August in quick response to heavy monsoon rainfall in Assam (India) and Bangladesh. The recorded maximum discharge is approximately 90,000m^3/s (see Table 2.1). The maximum width and depth are about 15km and 20m respectively. In Bangladesh the average slope of the course of the Jamuna River decreases gradually from 10cm/km to 6cm/km.

Table 2.1 Maximum discharge and water level of Jamuna River at Bahadurabad

FREQUENCY [1/year]	DISCHARGE [m^3/s]	WATER LEVEL [m+PWD]
1:100	91,000	21.26
1:50	87,000	20.99
1:10	76,000	20.36
average	65,000	19.73

The flow frequency distribution (Figure 2.2) was made on the basis of daily discharge records over the period 1956 to 1988. Data came from the Bangladesh Water Development Board (BWDB) gauging station at Bahadurabad.

[3] Jamuna River is a local name used in Bangladesh for the Brahmaputra River.

Figure 2.1 Bangladesh transportation network

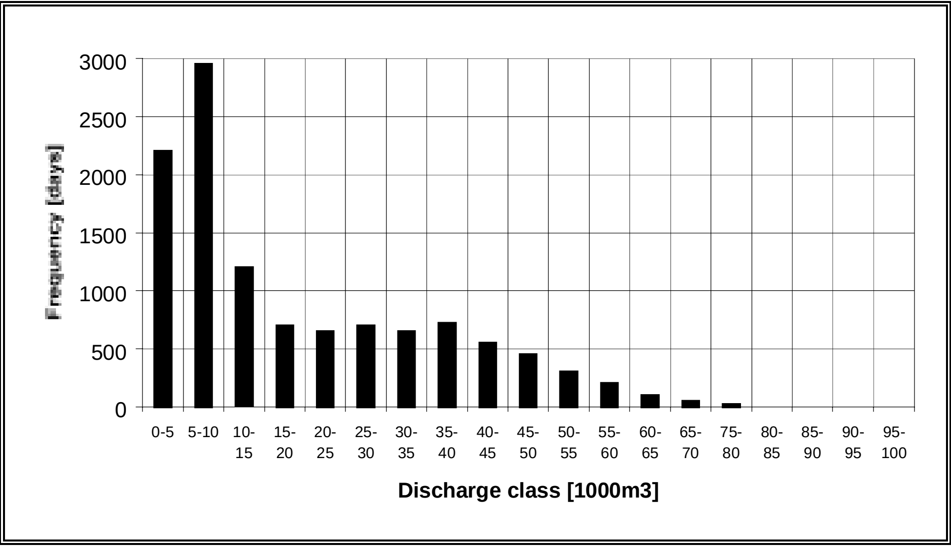

Figure 2.2 Frequency distribution for mean daily discharge measured at Bahadurabad between 1956 and 1989.

“In most years between 20 and 30% of Bangladesh is flooded and this is quite acceptable to the population [BEST ET AL. 1993, PP. 257]”. However, on occasion the Jamuna peaks late, coinciding with the Ganges and leading to catastrophic flooding that is far more extensive. The last major occurrence on this scale was in 1988, when nearly 60% of the nation was inundated. The disasters caused by the floods of 1987 and 1988 led to the establishment of the Flood Action Plan (FAP). This is concerned with the development of a strategic overall plan for water management in Bangladesh.

2.3 Discharge

Two different discharge parameters are used in calculations of scour depth: bank-full discharge and bed formation discharge. Both are described in this section.

2.3.1 Bed forming discharge

Bed forming (or dominant) discharge is a characteristic discharge that can be substituted for the discharges that determine the bed formation. In other words, if the river had this discharge constantly, the riverbed would maintain the same shape. Bed formation discharge is used to determine the channel morphology for mean flow. Methods of calculating for bed forming discharge require the maximum sediment transport rate, bank-full discharge and average discharge in flood season.

Bed forming discharge includes the strength and duration of bed formation. The strength of bed formation relates to the sediment transport capacity.

2.3.2 Bank-full discharge

Bank-full discharge is referred to as the stage in which the river is full but just fails to spill onto the flood plain. For the Jamuna River the bank-full discharge can be estimated on 60,000 m^3/s.

When this flood of 60,000 m^3/s occurs, parts of the high flood plain will probably be inundated to a shallow water depth. The annual probability of the discharge of 60,000m^3/s is only 2%, with a duration of 7-8 days.

2.4 Velocity

For scour calculations and also for the determination of protective material stability, the velocity must be known. In the cross-section the velocity will differ from place to place. The average velocity is presented here as:

$$\bar{u} = C \cdot \sqrt{(h \cdot i)} \qquad \textit{Equation 2.1}$$

in which,

$\bar{u}$	=	average velocity	[m/s]
C	=	Chézy coefficient	[$m^{1/2}$/s]
h	=	water depth	[m]
i	=	water level gradient	[-]

The velocity close to the riverbed (or at the bed protection) is lower than the average velocity in a vertical. However, the average velocity is usually used in design formulae for slope protection elements.

The Chézy coefficient will not have the same value on the riverbed as on the bed protection. Using the riverbed value will lead to a higher flow velocity, as the roughness of the riverbed will be less than the roughness of a slope protection. This is therefore considered a safer approach. Of course, the river configuration will also have an influence. For the design of the Jamuna Bridge-River Training Works (JB-RTW), a maximum velocity of 3.0m/s was used.

2.5 Scour

Scour can be described as local erosion of bed material and can have different causes. In this section the different forms of scour are described. Because this study does not emphasise the morphological behaviour of the river, the different forms of scour are only mentioned and not worked out completely. The different contributions can be calculated separately and some tools for the calculations are given. How the overall scour at a specific location can be estimated depends on the different scour contributions and is described in §2.5.2. The development of the scour process is presented in §2.5.3.

2.5.1 Different types of scour

Hydraulic structures that obstruct the flow pattern in the vicinity of a structure may cause local erosion or scour. Changes in flow characteristics (velocity and/ or turbulence) lead to changes in sediment transport capacity. This introduces a difference between actual sediment transport and the capacity of the flow to transport sediment. The scour depth is usually generated by a combination of different causes. As a first approximation, the scour caused by each separate process may be added linearly to obtain the resulting scour. Although formulas are used (and described in this chapter), only estimates of the scour depth can be made on this basis. For the design of river training works, it is still necessary to conduct model tests In this section a summary of the different forms of scour is given.

General scour

General scour is the scour that must be anticipated in the long term, irrespective of the construction of a bridge or structure. Factors influencing the general scour are:

- Change in sediment supply into the river,
- Change in discharge,
- Construction of flood embankments,
- Diversion of water and/or sediment into other rivers,
- Change in sea level.

In Bangladesh, there may be a rise of both riverbed and water level of approx. 0.50m in the next 100 years, because of the sea level rise, so in this case it would be better to speak of accretion instead of scour.

Constriction scour

Constriction scour is the result of narrowing of the river. It occurs if the width of an alluvial river is constricted over a substantial length. This may be caused by e.g.:

- Bank protection works
- Bridge approaches in the floodplains (as at the Jamuna Bridge site)
- Houses or even towns on the floodplains of the river

The effect of the constriction will be that the depth increases and usually the slope in the constricted river reach decreases. For constant discharge and steady conditions simple expressions for the increased depth and the related reduced slope can be derived [JANSEN 1979].

$$\frac{h_c}{h_0} = \left(\frac{B_0}{B_c}\right)^{\frac{b-1}{b}} \qquad \textit{Equation 2.2}$$

and,

$$\frac{i_c}{i_0} = \left(\frac{B_c}{B_0}\right)^{1-\frac{3}{b}} \qquad \textit{Equation 2.3}$$

in which,

h_c	=	water depth in constriction	[m]
h_0	=	initial water depth	[m]
B_0	=	initial width	[m]
B_c	=	constricted width	[m]
b	=	power of a simple transport formula ($s = a*u^b$)	[-]
		in which,	
		s = Sediment transport per unit width	[m^2/s]
		a = Coefficient	[-]

Confluence scour
Confluence scour occurs in the reach downstream of the junction of two river reaches, such as the branches of a braiding river or the confluence of a tributary with the main river.

Bend scour
Outer bend scour is the type of scour that develops in the outer part of river bends. The maximum depth resulting from scour at a natural outer bend (not influenced by a local obstruction) can be expressed as a function of the average depth (h_{av}) of the river. River bends are characterised by helical flow, causing sediment particles to move to the inner bend. This causes scour in the outer bend and deposition in the inner bend. The variation of the bed level in transverse direction is given by Equation 2.4 [Jansen 1979]:

$$\left(\frac{1}{h(y)} - \frac{1}{h_c}\right) = \left(\frac{1}{R(y)} - \frac{1}{R_c}\right)\frac{1.5 \cdot \alpha \cdot i_c \cdot R_c}{\Delta \cdot D} \qquad \textit{Equation 2.4}$$

in which,

$h(y)$	=	Water depth at the transverse location y	[m]
h_c	=	Water depth in the centre of the river	[m]
$R(y)$	=	Radius of curvature at the transverse location y	[m]
R_c	=	Radius of curvature in the centre of the river	[m]
α	=	Coefficient	[-]
Δ	=	Relative density $(\rho_s-\rho_w)/\rho_w$	[-]
D	=	Size of bed material	[m]
i_c	=	Water level slope in the middle of the river	[-]

It can be shown that in a first approximation the relative outer bend depth (the depth in the outer bend h_b normalised by dividing it by the average water depth h_{av}) can also be written as a function of the following two parameters:

Relative width B/R_c, and
Bend parameter $A\sqrt{\Theta}$,

in which,

B	=	width of river	[m]
R_c	=	radius of curvature in the centre of the river	[m]
Θ	=	stability parameter, defined as:	

$$\Theta = \frac{h \cdot i}{\Delta \cdot D} \qquad \textit{Equation 2.5}$$

in which,

h	=	water depth	[m]
Δ	=	relative density $(\rho_s-\rho_w)/\rho_w$	[-]
D	=	size of bed material	[m]
I	=	hydraulic gradient	[-]

A = coefficient (about 10), defined as:

$$A = 2\kappa^{-2}\left(1-\frac{\sqrt{g}}{\kappa C}\right)\cdot 0.85 \qquad \textit{Equation 2.6}$$

in which,

κ	=	Von Kàrmàn's κ (about 0.4)	[-]
g	=	Gravitational acceleration	[m/s²]
C	=	Chézy coefficient	[m^{1/2}/s]

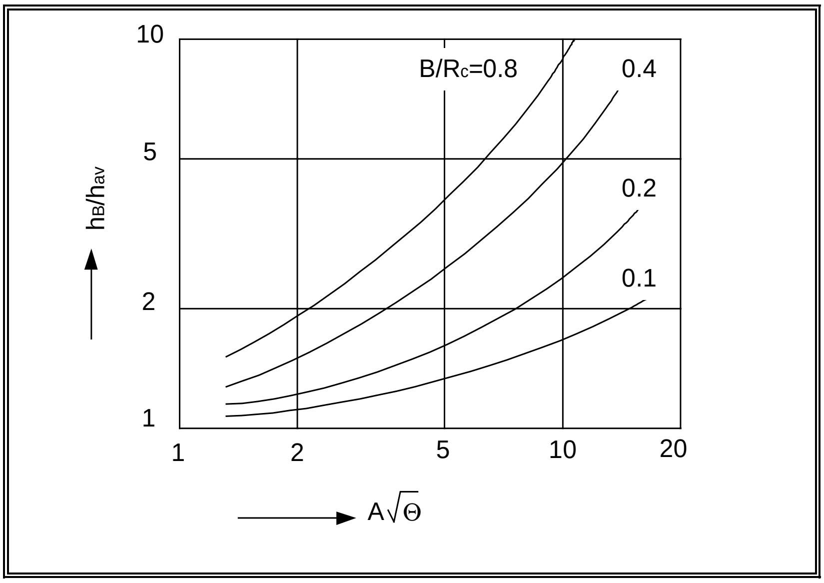

Figure 2.3 Theoretical relationship for estimating outer bend scour [JANSEN 1979]

This graph is derived for bed-load only; it can therefore be assumed that deviations occur in real situations. However, it does give an idea of how the different parameters relate to each other. Furthermore:

- The transverse bed level is apparently dependent on the value of the stability parameter, which in turn is determined by the discharge via the water depth. Apparently, the transverse bed-level slope in bends varies throughout the year.
- Not only does the transverse bed level slope depend on discharge, but this transverse bed level is also adapting itself with some delay.
- The derived formulae hold for the downstream part of a bend where the initial effects are not noticeable.

Local scour
Local scour results directly from the impact of the structure on the flow. For local scour near a guide bund, substantially more insight has been gained through local scour model tests [TE SLAA 1995, NEDECO 1996]. The local scour depth can be determined with Equation 2.7 [NEDECO 1996]:

$$h_s = h_{init} + h_r \cdot (a-1) \qquad [m] \qquad \textit{Equation 2.7}$$

in which,

h_s	=	scour depth (below water level)	[m]
h_r	=	Lacey regime depth	[m]
h_{init}	=	initial depth at start of local scour	[m]
a	=	model factor	[-]

The Lacey's regime scour depth, h_r ,can be computed with Equation 2.8:

$$h_r = 0.47(Q/f)^{1/3} \qquad [m] \qquad \textit{Equation 2.8}$$

in which,

Q	=	Bed forming (or dominant) discharge	[m^3/s]
f	=	silt factor (for very fine to fine sand with little silt, 0.40 is used)	[-]

A general tendency is that the maximum local scour depth near a steep slope of the revetment is deeper than the maximum local scour depth near a gentle slope [NEDECO 1996]. This advantage of a gentle slope has to be balanced against the disadvantage of more material being required for the top layer of the revetment. The formula for the Lacey regime depth is only valid for sand diameters (between 0.06 mm and 2.0 mm). For both clay and pebbles, the depth will be smaller.

2.5.2 Combination of scour along guide bunds

For river training works, the local scour seems to be dominant over all other forms of scour [NEDECO 1996]. However, it should be realised that the local scour is a function of the initial depth, which in turn is a function of scour in an outer bend and constriction scour. Only general scour has to be added to the local scour along a guide bund. (For bridge piers, the confluence scour is the dominant mode.)

It is clear from the above that the combination of the different contributions is difficult to predict. Even with model tests the predicted scour depth will only be an estimate. In a natural system like a braided river with fluctuating discharges and onstantly changing courses this prediction will even be more difficult to make.

Therefore, a worst case scenario is adopted in the design. This is an important aspect for the design of the falling apron. The scour depth at which level the apron should function is considered to be the maximum likely depth. It is not expected that the apron will have to function over the entire lifespan of the hydraulic structure. The discharge of the river also contributes to this phased loading.

2.5.3 Scour development in time

In general, the time scale of local scour is relatively short [WL|DELFT HYDRAULICS 1998]. For the development of scour, an empirical relation for use in preliminary design exists, see Equation 2.9:

$$\frac{h_{\max}}{h_0} = \left(\frac{t}{t_1}\right)^{\gamma}$$ *Equation 2.9*

with,

$$t_1 = \frac{330 \cdot h_0^2 \cdot \Delta^{1.7}}{(\alpha u - u_{cr})^{4.3}}$$ *Equation 2.10*

in which,

α	=	Scour coefficient	[-]
γ	=	Scour coefficient	[-]
Δ	=	Relative density of sediment	[-]
t	=	time	[hours]
t_0	=	time when $h_{max}=h_o$	[hours]
h_{max}	=	max. depth of scour hole	[m]
h_0	=	Original water depth	[m]
u	=	flow velocity	[m/s]
u_{cr}	=	Critical flow velocity	[m/s]

The coefficients α and γ can be found experimentally. The number of measuring points has to be enough to give accurate values. In Figure 2.4, the development of the clear water scour depth is given in a schematic way; the scour depth develops asymptotically. This development is valid for clear water scour. For live bed scour, the development will be faster and when the maximum is reached will fluctuate around the equilibrium.

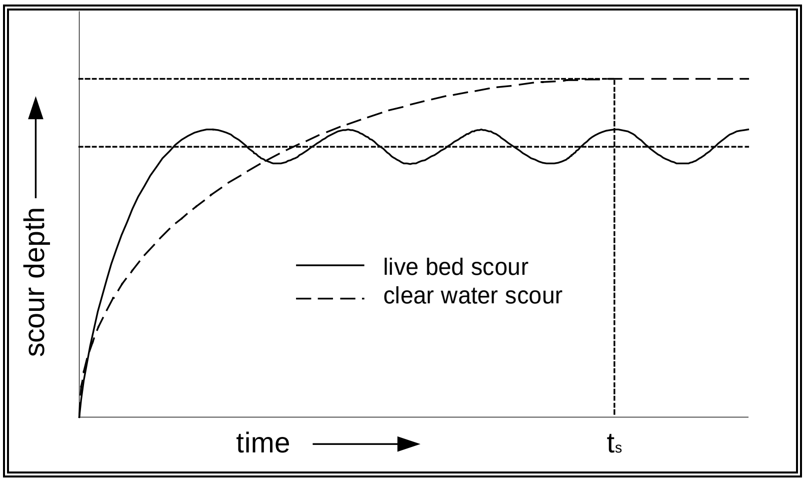

Figure 2.4 Scour depth development in time

In the Jamuna River the critical mean flow velocity for the initiation of sediment transport is between 0.2 and 0.4 m/s in shallow water. It is much less than the mean flow velocity during the floods (order of 3.0 m/s) and therefore the maximum scour depths can be reached within one season.

In the development of the live bed scour four phases can be distinguished:

- Initiation phase
- Development phase
- Stabilisation phase
- Equilibrium phase

In the initiation phase, the flow in the scour hole is nearly uniform in the longitudinal direction. This phase of the scour process can be characterised as the phase in which the erosion capacity is highest. Observations with fine sediments showed that at the beginning of the scour hole development some bed material near the upstream scour slope goes into suspension. Most of the suspended particles follow convectional paths within the main flow and remain in suspension due to the internal balance between the upward diffusive flux due to turbulence and the downward flux due to gravity. Some of the particles will settle and will be re-suspended owing to the large bursts of the turbulent flow near the bed, while some particles are transported as bed load.

During the development phase, the scour depth increases considerably, but the shape of the scour hole does not change. In this phase, the ratio between the maximum scour depth and the distance between the end of the bed protection and the point where the scour hole is at its maximum is more or less constant.

In the stabilisation phase, the rate of the development of the maximum scour depth decreases. The erosion capacity in the deepest part of the scour hole is very small compared to the erosion capacity downstream of the point of reattachment. Because of this, the dimensions of the scour hole increase more in the longitudinal direction than in the vertical direction. The longer the scour process continues, the more the flow velocities above the lower part of the upstream scour slope decreases. In the stabilisation phase, the equilibrium situation for both the upstream scour slope and the maximum scour depth is almost achieved.

3 Geotechnical aspects

3.1 Introduction

When a falling apron is installed, it will be located on the riverbed or in the floodplain area. Geotechnical boundary conditions will determine the stability of slopes and the above lying structures. In this chapter the different geotechnical aspects, which relate to the falling apron, are described.

3.2 Soil characteristics Jamuna River

The Jamuna River catchment supplies enormous quantities of sediment from the actively uplifting mountains in the Himalayas, the erosive foothills of the Himalayan Foredeep and the great alluvial deposits stored in the Assam Valley. Consequently, the Jamuna River carries a heavy sediment load, estimated to be over 500 million tonnes annually. Most of this is in the silt size class (suspended load) but around 15 to 25 percent is sand (bed load). This sand is deposited along the course of the river and the clay fraction is transported to the delta region.

The banks of the Jamuna River consist of fine cohesionless silty sand. The composition of the bank materials is remarkably uniform.

The primary process of unprotected bank erosion is toe scouring leading to mechanical collapse. “Typically eroding banks display slab-type failure of the upper bank above the water surface generated by toe erosion and over-steepening due to undercutting at depth” [BEST ET AL. P.269]. These ‘slabs’ disintegrate quickly after sliding and fall apart in to primary particles. These are washed away with the current and therefore do not stabilise the slope.

Angle of internal friction

For the determination of stability of slopes, the angle of internal friction (ϕ) is a relevant parameter. For the Jamuna River it can be estimated at approximately 30°. It is however dependent on the mica contents, this is described in §3.5.

Grading

Because of the varying location of the river branches, much of the sediment has been eroded and accreted many times. The sand size sediment is relatively uniformly graded. The grading is summarised in Table 3.1. The range of d_{50} values could be taken as lying between 0.21mm to 0.14mm. Overall, the material has to be categorised as highly erodible.

Table 3.1 Grading of bed material [10^{-6}m].

SIZE	JAMUNA	JAMUNA*	PADMA[4]
d_{15}	110	120	100
d_{35}	120	190	124
d_{50}	150	200	140
d_{85}	210	250	185
d_{90}	220	300	220

(* Depth of 20-25m)

[4] After the confluence with the Ganges, the Jamuna River is called Padma River.

Fall velocity
The fall velocity is important for use in transport formulae. For a spherical particle the fall velocity is:

$$w = \sqrt{\frac{4}{3C_w} g d \Delta}$$ *Equation 3.1*

in which,

C_w	=	drag coefficient	[-]
g	=	Gravitational acceleration	[m/s^2]
Δ	=	relative density	[-]
d	=	Diameter	[m]

Average values for quartz sands in water at 20° appear to fit reasonably well to the relationships [RAUDKIVI 1993]:
$w=663\ d^2$ [mm/s] $\quad$ d<0.15 mm
$w=134.5\ d^{1/2}$ [mm/s] $\quad$ d>1.5 mm
For the transition, the following values can be used:

Table 3.2 Relation between fall velocity and grain diameter

d[mm]	0.15	0.2	0.3	0.4	0.5	0.8	1.0	1.5
w[mm/s]	14.8	21.1	36.1	50.0	64.0	99.0	121.0	166.0

Cohesion
For non-cohesive sediments the particle or grain size and weight, are the dominant parameters for sediment movement and transport. Non-cohesive sediments have a granular structure and do not form a coherent mass. In cohesive soils, the electro-chemical interactions dominate and the size and weight of an individual particle are of little importance.

Because the bed material consists of sand with a diameter between 0.21mm to 0.14mm, the cohesion can be neglected.

3.3 Slope stability

The most common process of bank failure along the river is due to shearing, caused by flow attacking the bank (Chapter 2), or over-steepening of the bank by a *thalweg* approaching the bank. The scour processes remove the sediment from the toe, resulting in over steepening of the riverbank and causing the bank failure by slumping. Bank material properties determine the cohesiveness of the bank, which is an important parameter for how quickly erosion products are transported by the current and thus determines the time needed for the typical toe scour failure. It will be clear that when a riverbank slides, the moved soil will stabilise the newly established slope. However, when the current transports this soil, the bank will still be very steep. In areas where the clay content of the bank material is low, the bank lines are very sensitive to bank erosion.

Regarding riverbank stability, a distinction can be made between macro and micro stability. With macro stability, the stability of a certain volume of soil is considered. As with micro stability, the stability of a single grain is considered. This is worked out in the following.

3.3.1 Micro stability

The micro stability concerns the individual grains or protection elements on the slope. These can be loaded from inside the revetment, or by external forces. The micro stability is influenced by water level difference (gradient through the revetment), or by current forces.

When water levels in the river are falling, the direction of the seepage force will be directed outwardly. The ground water table will lag behind the falling river level and, depending on the permeability of the soil, ground water might escape at the slope surface. The resulting uplift forces will reduce effective stresses and consequently reduce stability. Total reduction of effective stresses will result in dislodging of particles, causing local instability and removal of material.

In addition to the internal loads, external loads can also lead to micro instability. The current forces can lift individual grains and/or the protective cover layer. This is worked out in detail in the Chapters 4 and 5.

3.3.2 Macro stability

As well as instability of the cover layer and migration of fines, instability of the subsoil is also a failure mechanism. This failure mechanism can be the dominant failure mechanism in the case of a permeable revetment (riprap, block mattress with holes in the blocks) on granular subsoil.

Macro stability exists when the weight component of the soil (including pore water) parallel to the friction forces exceeds these friction forces. The friction forces are determined by the soil properties like cohesion, angle of internal friction and packing density. If the soil is densely packed there is a higher probability for shear failure. When the soil is loosely packed there is a higher risk of liquefaction. These two different failure modes are described.

Flow slide

Liquefaction is the effect that appears when a soil mass loses its shear strength. If a soil mass loses its shear strength it behaves like a liquid, which explains the name of the effect. In saturated soils the decrease in pore space causes an increase in the pressure of the pore water present in the soil mass. This pore water is forced to flow off to nearby soil layers or the bed surface. However, if the densification of saturated soil takes place suddenly, as during an earthquake or dredging activities, and the permeability of the soil mass is low, the pore water cannot redistribute quickly.

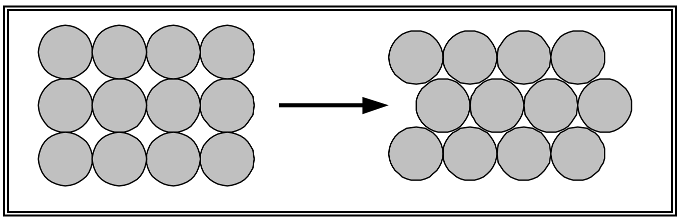

Figure 3.1 Decrease of pore volume

The loss of shear strength in granular soils is related to an increase in pore water pressure in the soil. When the pore water pressure equals the total stress in the

soil mass, the effective stress becomes zero and the soil mass liquefies. Therefore, liquefaction occurs only in saturated soils.
If liquefaction appears in a slope, complete subsidence may result (See Figure 3.2). The process is called a flow slide and can last for hours with recorded displaced soil volumes of hundred thousands cubic meters.

In general, river training works will be constructed in the flood plain area. Along the Jamuna, the soil predominantly consists of silty fine sands, of which the upper 10 to 15m have to be considered as relatively loose packed. Underlying layers have a higher density, which can be classified as medium dense to dense. During construction, while the trench was being dredged, numerous flow slide-like instabilities occurred. This led to the adaptation of the design to incorporate less steep slopes.

Whether or not liquefaction (and thus a flow slide) occurs, depends on the soil conditions. In principle, the steepness of the slope has no influence on the occurrence of liquefaction, but it does have an influence on potential flow sliding and the resulting deformation. In the Dutch delta region, many flow-slides occurred; these were investigated to try to find a relationship [HEETEREN ET AL. 1990]. The general conclusion was that with regard to flow-slides a slope that is steeper more than 1:3 over a height of more than 5m is considered critical.

In addition to a loose saturated packing and a steep slope, a trigger is also needed to start the process of flow sliding. Examples of such triggers include earthquakes, dredging activities or a sudden drop of water level.

Some further considerations:

- A high total stress (in the deeper layers) in the soil mass reduces the potential for liquefaction (the construction level for apron will be in the deeper layers).
- A high water table will decrease the effective stress and thus increase the potential for liquefaction (scour will be effective at high water stages).
- A high initial relative density will lower the potential for density changes.
- A high permeability will lower the potential of pressure built up.

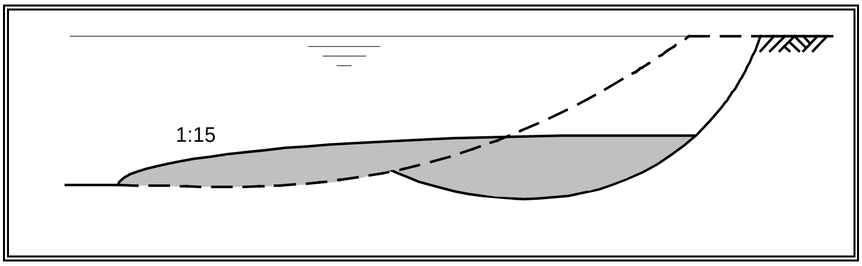

Figure 3.2 Flow slide result

Slip circle
Another form of macro instability is the loss of shear resistance in a circular plane. A complete soil mass will then rotate along a plane. In Figure 3.3 a soil mass with a weight G must be balanced by the shear stress τ.

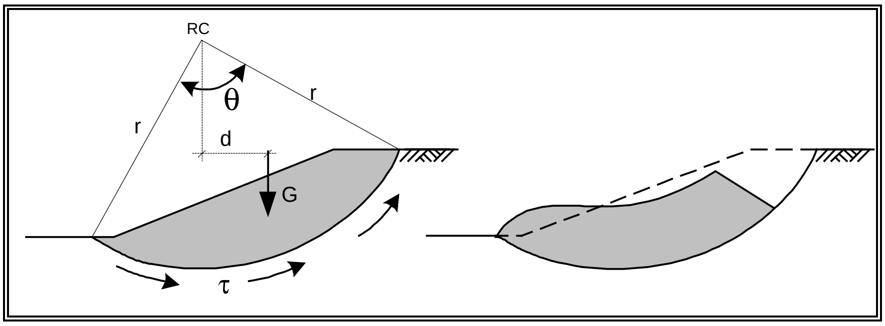

Figure 3.3 Slip circle failure with rotation centre RC

When this shear stress τ is assumed constant, the critical point of stability would be:

$$d \cdot G = \tau \cdot \Theta \cdot r^2 \quad \text{Equation 3.2}$$

in which,

d	=	arm of force	[m]
G	=	weight of soil mass	[kg]
τ	=	shear stress	[N/m^2]
Θ	=	angle	[rad]
r	=	radius	[m]

The normative rotation centre RC must be found experimentally, just as the radius. This can be done with a computer program, which calculates a large number of situations. The Bishop method for the calculation of slip circles also takes into account different values of the shear resistance along the circle. The soil mass is than divided into vertical lamellae which all have their specific weight and shear resistance.

3.4 Presence of clay

There is an important limitation to the applicability of a flexible scour protection.: it can only be used in areas where the bed material consists of non-cohesive material. When cohesive sediments like clay layers are present, the scour will result in steep slopes. In general, cohesive banks erode more slowly than non-cohesive banks with sediments of the same diameter.

A falling apron that consists of loose granular material will not have any pull strength. This means that the material can slide off a slope that is too steep, leaving an unprotected slope.

If a flexible mattress is applied, the mat will remain attached to the revetment, leading to high tensions. To avoid rupture and thus openings in the protection, the design should then be adapted to these forces.

A thorough site investigation should reveal any clay layers. In Bangladesh, however, the river bank material and bed material consist mainly of cohesionless sand.

3.5 Presence of mica

During the construction of the river training works for the Jamuna Bridge, special geotechnical aspects were encountered. During excavation works near the toe of the riverbanks, shallow landslides occurred. The reason for this was that the sand contained mica. Mundegar [1998] did research on the behaviour of sand containing mica. Mica particles, which have a plate-like shape, have an enormous influence on the behaviour of the sand.

It was shown that the presence of sand-size mica plates within sand increases its void ratio, modifies its volume change characteristics and introduces a collapse potential, particularly when under low stress and when sheared in extension. Extension loading under low stress occurs at the toe of a slope being excavated by dredging or by scour.

Shear testing with different mica percentages showed that for low percentages of mica, the sand dictates the failure. Between 20% and 40% lies the transition. In the study the pure sand was found to have an internal angle of shearing resistance of about 30º compared with 24º for the 40% mica sample. The mica also increases the porosity of the sand.

4 Common design practice

4.1 Introduction

Falling aprons were first used during the last century, when the first railway bridges were being built over the Ganges River. The design practice was mainly based on experience. In this chapter, the different aspects of designing a falling apron according to the common design 'rules' and the ideas behind it are presented. This chapter also describes the stability of rock in flow conditions. The information in this chapter is based on literature (mostly Indian) and on consultants reports for various river works in Bangladesh.

Another important function of this method is the retention of soil under the apron. The filter rules, as valid in this situation are treated in Chapter 5.

4.2 Design

4.2.1 Thickness of apron section

Spring [CBIP 1989] recommended (in 1903) a minimum thickness of apron equal to 1.25 times the thickness of stone riprap of the slope revetment. He further recommended that the thickness of apron at the transition of apron and constructed slope[5] should be the same as that of slope stones but should be increased in the shape of a wedge towards the riverbed.

Here intensity of current attack and therefore loss of stone has a higher probability. Because the apron rock will have to be dumped under water and cannot be placed it is therefore necessary that the thickness of the laid apron at the transition should be 1.50 times the thickness of riprap on the slope protection, as suggested by Rao [CBIP 1989]. The thickness of river end of apron in such case must be 2.25 times the thickness of riprap in slope.

These rules are based on geometrical aspects (see Figure 4.1). According to Schiereck [2000], the required thickness of an apron after falling is given as 5 times d_{50}. In this case this thickness is assumed to be sand-tight. From this, the total amount of rock to be stored in the apron can be calculated. A more detailed description of filter rules is given in Chapter 5.

4.2.2 Length of apron section

The general practice, as recommended by Inglis [CBIP 1989], is to lay the apron over a length of 1.5 D, where D is the design scour depth below the position of laying. For the design of the Padma Bridge, the designers assumed that a falling apron could only be installed a certain maximum (safe) 'falling height' [JMPBA 1999, P. C-119]. It states: "the falling height for a falling apron, to be installed at the foot of the slope protection of the guide bund or groyne, is limited to a safe limit of 10 to 15m". For the design of the Paksey Bridge however, a depth of 55m is considered feasible. The quantity of rock stored in the falling apron is therefore in the order of 180 m^3/m^1.

[5] In this study, the term constructed slope is used to distinguish the upper bank protection slope from the scour slope protection by the falling apron.

Figure 4.1 Falling apron design according to Spring, Gales and Rao

4.2.3 Slope after setting

The covered slope of the falling apron after setting can be estimated as 1:2 for loose stones. Observations at guide banks on various rivers in India and Bangladesh [CBIP 1989] have shown that the actual slopes of launched aprons usually range from 1:1.5 to 1:3, but in some cases may even be flatter. However, in most cases the average approximates to1:2.

Ray [CBIP 1989] states: “The materials of the armour on the slope of the shank and in the apron act only as ‘face wall’. The guide bank slopes should, therefore, be stable by themselves, without any external support. To ensure this, the slope should have the same ‘angle of repose’ of the material of which it is constructed. The presence of clay in the sand, (which is always found in the alluvium, of which the bed and banks of the alluvial rivers are composed), at once makes the angle of repose approximate more towards saturated clay. The wet clay mixed with wet sand, apparently acts as a lubricant between the grains of sand, so that the angle of repose of the alluvium is 18° approximating to a slope of about 1 to 3.”

4.2.4 Construction depth

In its original form, the falling apron concept entailed no more than dumping blocks at the low water line when the currents during floods endangered a riverbank. This means that the complete underwater slope is to be protected by the falling apron with its accompanying slope. For the design of the guide bunds of major bridge works, this was considered too high a risk. A compromise had to be found between safety and costs. This is worked out in this section with the use of design considerations on the Jamuna Bridge.

Table 4.1 Comparison of costs per m^1 of guide bund for various levels of the falling apron*

CONSTR. LEVEL [PWD+m]	FALL. HEIGHT [m]	DRED. VOL. [m3]	DRED. COST [$]	ROCK VOL. [m3]	ROCK COST [$]	MATT. AREA [m2]	MATT. COST [$]	TOTAL COST [$]
-3	0	0	0	79	4747	0	0	4747
-4	1	115	172	76	4571	4	98	4841
-6	3	356	533	70	4219	11	295	5047
-8	5	613	919	64	3868	18	491	5278
-10	7	886	1328	59	3516	25	688	5532
-12	9	1175	1762	53	3164	33	885	5811
-14	11	1480	2219	47	2813	40	1081	6113
-16	13	1801	2701	41	2461	47	1278	6440
-18	15	2138	3206	35	2110	55	1474	6790
-20	17	2491	3736	29	1758	62	1671	7165
-22	19	2860	4289	23	1406	69	1867	7563
-24	21	3245	4867	18	1055	76	2064	7985
-26	23	3646	5468	12	703	84	2260	8432
-28	25	4063	6094	6	352	91	2457	8902
-30	27	4496	6743	0	0	98	2654	9397

*) Cost for dredging and slope protection to PWD-3m not included. The figures mentioned are at price level 1989. from: [JAMUNA BRIDGE PROJECT PHASE II STUDY]

In Table 4.1, details of the cost comparison are given. The deeper the construction level, the higher the cost. The uncertainties in the setting process however, will be fewer. The consultants for the Jamuna Bridge proposed a level of PWD-18m; a compromise between cost and safety based on the following considerations:

- The remaining falling height for the apron is large (up to 13m)[6], but not too large to implement any additional measures to protect the slope should this become necessary.
- The dredging depth is very substantial (up to 30m, measured from the level of floodplain), but can be reached by using equipment which is available in the market or which can easily be adapted.
- Though this would require a major effort, it would be possible to complete an entire guide bund within one working season.

Three different parts are discerned in Table 4.1: dredging, rock and mattress costs. The mattress is the slope protection directly above the falling apron. During construction, the slopes were found to be too steep and after several flow-slides the design was adapted. The slopes were made less steep and therefore more slope protection material was needed. In the revised design (and thus the actual structure) the falling apron level was PWD –15m. (Probably a new cost-safety regulation was formulated.)

This example from the design and construction of the JB-RTW is illustrative of the search for an optimum level. It is stressed here that when a falling apron is installed for major works (revetments, groynes or guide bunds), this compromise between safety and costs will always have to be made. For smaller works the low waterline will be taken as apron level, where dry construction is possible.

4.2.5 Grading of rock

A generally applied design rule is to use a wide grading when the apron consists of granular material. The falling apron is then considered to be a self-constructing filter of graded material, the larger sizes of which are resistant to the hydraulic loads induced by the currents. However, to provide material that can form a filter layer, smaller sizes are also required.

In the apron, the fines will be washed out from the top layer. However, in the underlying layer enough fine material to retain the bed material will remain. This filter effect will be highly influenced by the setting behaviour of the apron.

As also a lot of finer particles are required, the d_n, as determined for current resistance (See §4.4), must be taken as the d_{65} in the overall grading for the apron consisting of rock. An extra quantity of 25% is added to cover losses due to material that does not reach its intended place. Most of the latter will be the fine fraction of the grading which washes away in the current. It is clear that 25% is a considerable quantity.

4.3 Alternative materials

In the literature and in practice, different materials are proposed for use as falling aprons. In this section, various alternatives are described. Known results and design considerations are hard to find therefore some general information concerning the behaviour is presented. The number of alternatives described here

[6] Based on model tests, the expected maximum scour level is estimated at PWD-31m.

is probably not complete, but it gives an idea of which materials might serve as a flexible scour protection. A distinction is made between mattress type and granular protections.

4.3.1 Mattresses

Assuming the correct type is used, with geotextile, the sand-tightness is guaranteed,. The bed protection can be made by using concrete blocks that are connected with the textile layer for ballast. Overlaps between two mats have to be constructed with care to prevent openings.

When there is an erosion gradient the bed protection (i.e. differences in soil parameters) 'hanging' of the mat may occur between to points with stronger soil characteristics. In between, the soil can wash out freely. Another disadvantage of using geotextile mats for a falling apron, is the steepness of the slope after the 'falling' process. See Figure 4.2.

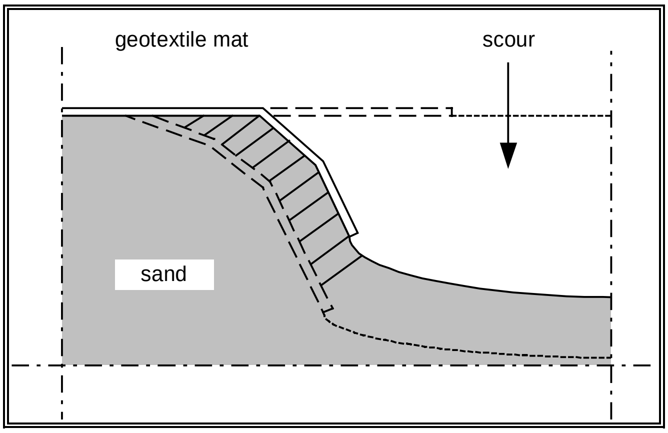

Figure 4.2 Steepness of sand slope beneath a sand-tight mattress, re-drawn from: [De Groot 1988]

De Groot [1988] did tests on the behaviour of a flexible mat consisting of geotextile and concrete blocks in current conditions. He found that the steepness of the slope could become larger than the angle of repose, which endangers the slope above the apron. Nevertheless, designs with geotextile as a falling apron are made.

A way to overcome this disadvantage of mattresses would be to design a structure, which combines the strength of a mattress with the open structure of a granular filter.

As established in real cases and in scale tests [De Groot 1988], sand-tight mattresses lead to very steep slopes at the edges of any (horizontal or sloping) section of the slope protection which has not been installed to the ultimate scour depth. Loose material, such as riprap, provided as current resistant material, when placed on a geotextile, would not have a large enough angle of internal friction to remain on the geotextile in the case of scour at the edge. Dividing the mattress into sections with vertical elements could prevent this sliding off.
In the Dutch hydraulic engineering tradition, much use was made of fascine mattresses made of willow saplings. To prevent the ballast from sliding off, a

trellis is made which divides the mattress into sections. In this way the rock used for ballast is kept in the correct place by the partitions. These mattresses are made on the low water line and towed to the construction site at a higher water level. Modern types of mattresses incorporating geotextile do not have enough buoyancy and have to be placed with special equipment or have to be combined with willow saplings to obtain enough buoyancy.

In the scope of the Flood Action Program (FAP), various studies on river training works were executed. The China-Bangladesh Joint Expert Team [1991] describes different falling apron-like toe structures used on the Yangthze River.

- Flexible mattress formed by cement-soil filled woven bags:
  The mattress is formed by sewing together the bags (1m wide and 0.3m thick) to form long geotextile fabric strips (total length is 36m). Theses bags are filled with cement-soil (cement content 10%). Then the strips are then sewn together and are enclosed by rope nets made of artificial fibre. The longitudinal ropes are fixed to anchor piles, which are embedded beneath the revetment. After the mattress has been laid down, 0.5-1.0 m thick soil is placed on top, to protect it from damage and deterioration. This kind of structure is suitable for the construction on dry land.

- Mattress toe protection formed by earth filled synthetic material tube bags: This kind of mattress consists of two parts. One is a scour resistant mat laid on the riverbed and another is the long earth filled tube bag put on top of the mat to prevent it from being scoured away. The tube bags are around 40m long and 0.6m in diameter and have a unit weight of 297kg/m^3. The scour depth is about 15m. This kind of structure is suitable for construction in the water, and can be completed in one operation.

According to the designs the anticipated slope is 1 V:2H, for both alternatives. At Chandpur, Bangladesh, mattresses made of sand-filled woven bags were used. The bags were tied together with nylon ropes to form a mattress. Two layers were laid with some overlaps. The diameter of one bag is 1.2m and its length is 1.40m. Each bag is filled with approximately 0.5m^3 sand [CBJET 1991].

4.3.2 Granular material

The most secure method to provide coverage of the slope of the scour hole would be to use loose granular material (TE SLAA 1995). The quantity should be sufficient to cover the entire eroded slope. The thickness and the grading of the granular material should be such that at the end of the falling process, the protective layer retains the underlying soil. The design of a falling apron consisting of rock is described in Chapter 5. For the first applications of falling aprons, the available construction equipment limited the size of the stone. This meant that the size of stone could not exceed the ‘one-man-stone’ (the size of stone that a man could carry). Although today state-of-the-art equipment is available in the market for this purpose, one should not forget the financial limitations when designing a structure located in a developing country like Bangladesh.

In Bangladesh, concrete cement blocks (CC blocks) are also used. These blocks are uniform in size. The advantage of using CC blocks is that they can be manufactured on site with local materials. The logistical problems of transporting huge quantities of rock can thus be avoided. However, the porosity and interlocking of these blocks differs from that of graded rock. One can assume that this will have consequences on the behaviour of a falling apron. Some alternatives to rock materials are mentioned here:

- Graded boulders.
  These are almost as resistant as rock, but less expensive (because small quantities are available in Bangladesh). A problem might arise when large diameters are required. The angle of internal friction can also be different from that of quarriedrock.

- Uniform sand cement blocks (SCB).
  Sand cement blocks can be produced on site and thus high transportation costs are avoided. Making a normal grading with this material is not considered an option because it is mainly uniform. However, it is possible to make and mix a number of sizes. The benefit of using this material is that it can be made on site, using local material; the problem is that it is not very wear-resistant and also breaks easily. The model tests showed that the rock used in the experiments did not 'fall' but that the loose rocks were 'transported' onto the establishing slope. Furthermore, the sand-laden current will cause wear on the individual blocks. In addition, the construction method (dumping) requires the use of wear- resistant blocks.

- Uniform concrete cement blocks (CCB)
  Concrete cement blocks are stronger than sand cement blocks. The disadvantage is that aggregates have to be brought to the site. Instead of small boulders, which still have the disadvantage of transport costs, it might be possible to use of broken bricks as aggregate. However, this would decrease the strength of the blocks, so a compromise will have to be found.

- Uniform Sand filled bags
  Although not really a granular material, bags made of jute or geotextile can be filled with sand and used as scour protection. Individually, these bags retain the underlying sand but, because of sliding on the slope, the distance between the bags will probably lead to gaps where the bed material can escape.

4.3.3 Description of some applications

Various river works have been executed in Bangladesh, many involving graded rock. One of the oldest river works in Bangladesh, is the riprap protection (using Indian rock) for the Hardinge Bridge. It was constructed in 1912. The performance of the falling apron section was at first found to be good, however, a breach occurred in 1933. Based on the experience from this falling apron structure and its collapse, many other designs have been made.

In 1933 a breach occurred in the Right Guide Bank of the Hardinge Bridge. Probably this was because the angle of attack changed in a short time. From the reports of the Hardinge Bridge Staff at the time of the breach, the following extracts are given in Annual report 1937-1938 [CWPRS 1938]:

"Early in September a definite change in the direction of the main current was observed after it had left the Damukdia Guide Bank and […] the current impinged on the head of the Right Guide Bank at about chainage 27".
"Dangerous eddies were observed in front of ch. 14 to 17 […] and on the 26th September at about 04.00 hours this guide bank was breached between ch. 19 and 22 on a rapidly rising river. During the course of the day the breach extended from ch. 14 to ch. 25 by erosion from inside the embayment."

Research afterwards showed that the current carried the stones at the toe (the falling apron section) away. This failure can be ascribed to instability of the individual stones. At present, more is known about the stability of rock in currents (see §4.4). The river training works for the Hardinge Bridge have been used as an example for the design of later falling apron applications: little information on the functioning of these structures is available. Some applications are given in Table 4.2.

Table 4.2 Types of materials used at different locations

LOCATION	MATERIAL USED AS 'FALLING APRON'
Bahadurabad	Geotextile bags filled with sand
Bhuapur	Cellular Geotextile Mattress
Bhairab	Dumped boulder (D 50-350)
Chandpur Town	Geotextile bags filled with sand
Hardinge Bridge	Rock
Jamuna Bridge	Rock, 1-100 kg
Padma Bridge (**)	Rock, 0-250 kg
Paksey Bridge (*)	Rock, 0-120 kg
Sirajganj	CC Blocks
Yangthze	geotextile bags filled with sand cement
Yangthze	Long tube bags filled with earth

*) Feasibility study stage
**) Under construction

The reason for the difference in weight between the rock size used at the Jamuna Bridge and at the proposed Padma Bridge is that the Padma River has generally higher flow velocities.

4.4 Stability of apron rock

The individual stones in the apron layer derive their stability from their own weight and from contact with other rocks. The design of this layer is such that minimal transport occurs under maximum current attack. Some transport always occurs, but the quantity of stones transported in a certain period is restricted by the selection of the average dimension of the rock (d_{50}). The width of the grading will also influence the (minimal) transport. Two different methods to determine the stability are described in this section: Izbash and Shields.

4.4.1 Izbash

According to Schiereck [2000], Izbash expressed a relation between the flow velocity and the grain diameter as follows:

$$u_c = 1.2\sqrt{2\Delta d} \qquad \text{[m/s]} \qquad \textit{Equation 4.1}$$

or,

$$d = 0.7\frac{u_c^2}{2g\Delta} \qquad \text{[m]} \qquad \textit{Equation 4.2}$$

in which,

d	=	diameter	[m]
u_c	=	critical velocity	[m/s]
Δ	=	relative density	[-]

There is no influence of depth in this relationship. It is considered a tool for a first approximation in cases where the velocity near the bed is known but the relation with the water depth is not clear (this is because Izbash did all his experiments with a water depth of 1m). This stability relation is used in most designs for falling aprons.

4.4.2 Shields

Shields derived a criterion for the initiation of movement of uniform granular material on a flat bed. The experimental data used by Shields was mainly obtained by extrapolating curves of sediment transport versus applied shear stress to the zero transport condition. This so-called ‘Shields curve’ is actually a broad belt because of the difficulty of pinpointing the actual initiation of movement.
WL|Delft Hydraulics [1976] gives, after extensive research, 7 different criteria of movement:

- Cr.1 occasional particle movement at some locations
- Cr.2 frequent particle movement at some locations
- Cr.3 frequent particle movement at many locations
- Cr.4 frequent particle movement at nearly all locations
- Cr.5 frequent particle movement at all locations
- Cr.6 permanent particle movement at all locations
- Cr.7 general movement

A graphical representation of the Shields diagram is given in Figure 4.3, where the 7 different criteria are drawn.

Figure 4.3 Shields diagram

$$\Psi_s = \frac{\tau_c}{(\rho_s - \rho_w)gd} = \frac{u_{*c}^2}{\Delta gd}$$ *Equation 4.3*

in which,

ψ_s	=	Shields parameter	[-]
ρ_w	=	density of water	[kg/m^3]
ρ_s	=	density of stone	[kg/m^3]
τ_c	=	critical shear stress	[N/m^2]
u_{*c}	=	critical shear velocity	[m/s]

Instead of using the Shields diagram, it is also possible to use the empirical relations given by Van Rijn [RAUDKIVI 1993]. These are presented in Table 4.3.

Table 4.3 Empirical relations for Ψ_c according to Van Rijn

Ψ_c AS FUNCTION OF D_* (= $d(\Delta g/v^2)^{1/3}$)		
$\Psi_c = 0.24D_*^{-1}$	for	$D_* \leq 4$
$\Psi_c = 0.14D_*^{-0.64}$	for	$4 < D_* \leq 10$
$\Psi_c = 0.04D_*^{-0.10}$	for	$10 < D_* \leq 20$
$\Psi_c = 0.013D_*^{0.29}$	for	$20 < D_* \leq 150$
$\Psi_c = 0.055$	for	$D_* > 150$

From the Shields diagram, it can be seen that small grains will start to move more quickly than larger grains; with wide graded sizes is this difference is less. The smaller grains will end up in the lee of the larger grains. Therefore, a higher momentum is needed to lift them into the current.

Another mechanism that relates to this is called armouring. Because of washing out of the small grains from the top layer, only the larger stones are left. This layer of larger stones will protect the underlying mixed layer. The design philosophy of applying a wide grading of rock is based on this mechanism.

4.4.3 Sloping bed

During the falling process, a side slope will develop. A stone on a side slope will be less stable than one on a horizontal plane. On the other hand, during this resettling process, the depth will increase and the flow velocity will decrease. The situation (horizontal plane with high velocity or side slope with lower velocity) that is normative for the stability, has to be determined. For a side slope with angle α, the reduction factor is [SCHIERECK 2000]:

$$K(\alpha_\perp) = \sqrt{\frac{\cos^2\alpha \tan^2\phi - \sin^2\alpha}{\tan^2\phi}} = \sqrt{1 - \frac{\sin^2\alpha}{\sin^2\phi}}$$ *Equation 4.4*

in which,

α	=	slope gradient	[°]
ϕ	=	angle of internal friction of protective material	[°]

It can be expected that the slope occurring after the falling process of the apron depends on the material used or on other parameters. The angle of internal friction of the protective material can be estimated from Figure 4.4 or be determined by testing with a tilting board.

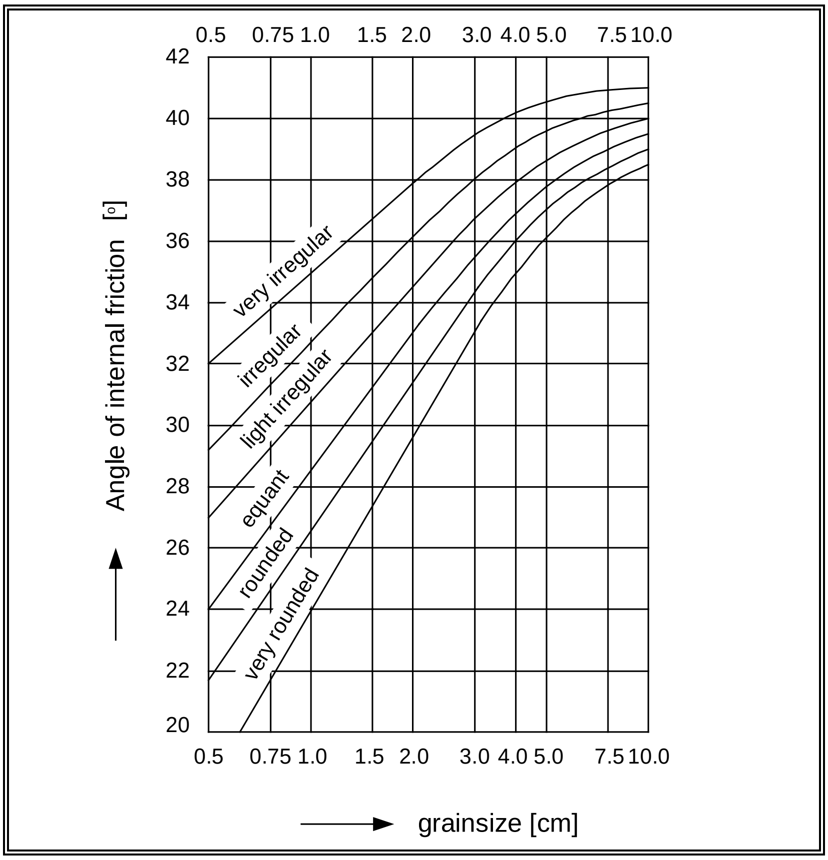

Figure 4.4 Angle of internal friction for different grain diameters acc. to Lane

From: [Jansen 1979]

5 Granular filters

5.1 Introduction

Filters are used widely and for different purposes in hydraulic structures. A filter layer is usually referred to as the layer between top (or armour) layer and the base material. In the case of a falling apron, the top layer is placed directly on the bed material. It has to be heavy enough to be stable in the current and it has to retain the soil.

Much of the theory summarised in this chapter is based on the CUR-report 161 [CUR 1993] and the work of Schiereck [2000].

5.1.1 Filter function of a falling apron

When a falling apron is installed, the function of the apron is to cover the side slope of a deepening river until the equilibrium water depth is reached. After this deepening phase, the slope should have sufficient armour protection against current conditions. Per definition, erosion of sand from under the *waiting apron*[7] is allowed. However, the amount of sand and the manner in which the erosion is taking place should be within limits. In particular the side-slope that is forming is important to the above-lying structure and should not become too steep.

When determining the size of rocks to be used the filter rules that apply to bed protections are important. It is not intended that the model should conform to these rules, which are based on the design philosophy that no sand can pass the filter. This is schematised in Figure 5.1, where three areas are discerned. Area 1 is the area of geometrically closed filters. The rock size is small enough to trap the sand grains. Transport is therefore impossible. Area 2 is the area of stable geometrically open filters (hydraulically closed). Here, theoretically, the sand can pass through the pores of the filter, but the driving force (gradient) is kept under the critical value. Area 3 is the area of unstable geometrically open filters, where transport of sand through the filter is possible.

The falling apron would fit into area 3 and therefore, in a model, two conditions should be met simultaneously:

1. The sand grains should be geometrically able to pass through the rock layer.
2. The load on the sand grains should be high enough to actually move the grains.

ad 1. For the sand to pass the rock layer, the pores should be wider than the individual sand grains. This condition for geometrically open filters is given as $\frac{D_{f15}}{D_{b50}} > 5$.

ad 2. To comply with this condition, the drag force on the individual sand grain should be high enough. This drag force is dependent on the water velocity along the rock layer and the thickness and grading of the rock layer.

[7] In this study, the term waiting apron is used, to distinguish the unaffected stack of material in the apron from the material that has already *launched* onto the slope.

The scour depth of the riverbed will reach equilibrium when the cross-section becomes large enough. The current velocity will be less than the critical value for transport. Whether or not the second condition is fulfilled, can only be verified after the setting process, when the thickness of the apron on the slope can be determined.

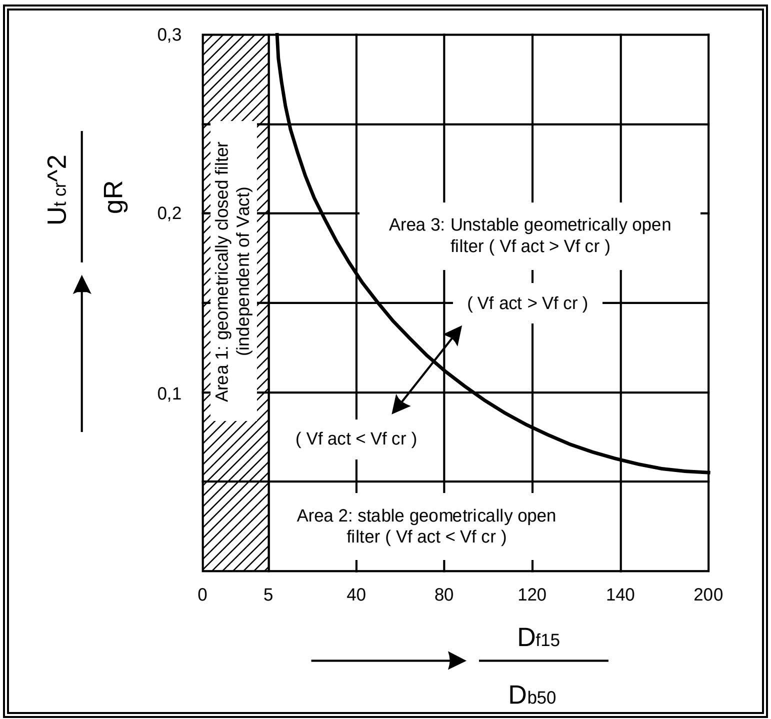

Figure 5.1 Relation between different types of filters

5.1.2 Geometrically closed filters

In a geometrically closed filter, the space between packed grains is much smaller than the grains themselves. For spheres with equal diameter D, this space can be blocked by a sphere with a diameter of about 6 times smaller than D (0.15D). The largest grains of the base layer get stuck in the pores of the filter layer and block the passage of all other grains. The base layer should be internally stable, which means that the range of grain diameters in the base layer should not be too large, so that the larger grains of the base layer can block the smaller ones. It is obvious that a falling apron can not be designed as geometrically closed.

5.1.3 Geometrically open filters

The idea behind a geometrically open filter (or hydraulically closed filter), is that the grains of the base layer can erode through the filter layer, but that the gradient occurring is lower than the critical value. The gradient is related to the velocity in the filter, which is again related to the forces on a grain. When the loading forces on a grain of the base layer are smaller than the resistant forces, there will be no erosion. This is the general idea behind a falling apron.

With perpendicular flow, there is a serial system where the flow through base and filter layer has to be the same, causing a much larger gradient in the base layer, because of the greater permeability of the filter layer. Erosion of the base layer will take place due to fluidisation. This situation is found when there is seepage through a body of sand.

When the water flows parallel to the interface, the gradient in both layers is about the same, causing the flow velocity in the filter layer to be much higher than in the base layer, because of the greater permeability. At the interface there will be a velocity gradient, inducing a shear stress at the upper grains in the base layer. This is the situation in a falling apron.

5.2 Basic equations

To derive the filter velocity and the gradient, calculations can be made. The turbulent flow inside a grain structure is described by taking average values over the rock layer and turbulence coefficients are used. The values calculated with these formulas can therefore not be exact, but give insight into the order of magnitude. The relations between the different parameters are given in this section.

5.2.1 Navier Stokes

The basic equation used here is the Navier-Stokes equation for fluid motion (conservation of momentum and mass). This is valid for laminar as well as turbulent flow. The complete equation is not used here but it is written in the Reynolds-form for the x-direction as worked out in [SCHIERECK 2000].

$$\frac{\partial u}{\partial t}+u\frac{\partial u}{\partial x}+\frac{\partial u}{\partial z}=-\frac{1}{\rho}\frac{\partial p}{\partial x}+\upsilon\frac{\partial^2}{\partial z^2}-\frac{\partial\overline{u'^2}}{\partial x}-\frac{\partial\overline{u'w'}}{\partial z} \qquad \textit{Equation 5.1}$$

With this equation, the flow in a porous medium can be calculated. For practical reasons (not considering every individual pore), the velocity is averaged. This filter velocity is defined as:

$$u_f=\frac{1}{A}\iint_A u\cdot dA=n\cdot u \qquad \left(n=\frac{V_p}{V_T}\right) \qquad \textit{Equation 5.2}$$

The porosity n is the pore volume, V_p, divided by the total volume, V_T. Averaging over many pores, the term ∂u/∂z in Equation 5.1 has no meaning. Combined with Equation 5.2, it can according to van Gent, be rewritten to:

$$\frac{1}{\rho g}\frac{\partial p}{\partial x}=i=au_f+bu_f\left|u_f\right|+c\frac{\partial u_f}{\partial t} \qquad \textit{Equation 5.3}$$

in which,

i	=	water level gradient	[-]
u_f	=	flow velocity in filter	[m/s]

For stationary flow: $\partial u_f/\partial t=0$. When this last term is left out, the classic Forchheimer equation appears.

5.2.2 Forchheimer

The flow over a bed protection consisting of large stones, which are stable them selves, will also cause flow through the protection. The permeability of granular filter material can be determined relatively simply by laboratory tests. Both laminar and turbulent flow play a role. The influence of both components can be expressed with the Forchheimer relation (Equation 5.4).

$$i = au_f + bu_f^2 \qquad \text{Equation 5.4}$$

with,

$$a = \alpha \cdot \upsilon(1-n)^2 / \left(gn^3 D_{15}^2\right)$$
$$b = \beta / \left(gn^2 D_{15}\right) \qquad \text{Equation 5.5}$$

in which,

i	=	water level gradient	
u_f	=	flow velocity in filter	[m/s]
n	=	porosity	[-]
D_{15}	=	characteristic diameter of filter material (15% is smaller)	[m]
g	=	gravitational acceleration	[m/s^2]
υ	=	kinematic viscosity	[m^2/s]

For the coefficients the values $\alpha \approx 160$ and $\beta \approx 2.2$ can be used for a first approximation. The flow in fine material is laminar; the relation between i and u is linear (first term in Equation 5.4). For rock, the relation is quadratic, indicating that the second term dominates. In intermediate materials, both terms play a role. It is obvious that the smaller part of the stone grading determines the flow conditions.

5.3 Calculation of gradient inside the filter

The water discharge induces a load on the bed protection. The gradient above the bed in turbulent flow is primarily dictated by turbulent vortices. Inside a vortex, the head varies. Because the vortices are transported in the current, the head varies in space and time. The variation in space generates a gradient along the bed.

To calculate the gradient in the situation of stationary uniform flow, with a completely developed boundary layer, Equation 5.6 can be used [CUR 1993].

$$\left(\frac{d\phi}{dx}\right)_{bottom} = C_0 \bar{i} \qquad \text{Equation 5.6}$$

with,

$$C_0 = 1 + 0{,}5\beta r^2 \frac{C^2}{g} \qquad \text{Equation 5.7}$$

or,

$$C_0 = 1 + 25\beta r^2 \left(\frac{R}{d_{n50}}\right)^{1/3} \qquad \text{Equation 5.8}$$

in which,

C	=	Chézy coefficient	[$m^{1/2}/s$]
β	=	Empirical coefficient (β≈3.0)	[-]
r	=	Relative turbulence (r=0.1 to 0.15)	[-]
U	=	Average flow velocity	[m/s]
R	=	Hydraulic radius	[m]

With Chézy, the formula can be written as:

$$i_{act} = \left(\frac{d\phi}{dx}\right)_{bottom} = \frac{U^2}{RC^2} + \frac{1}{2}\frac{\beta r^2 U^2}{Rg} = \frac{U^2}{RC^2} + \frac{U}{g}\cdot\frac{\partial U}{\partial x} \qquad \text{Equation 5.9}$$

This gradient can be compared with the critical gradient to assess the stability of bed material under a geometrically open filter.

5.4 Stability of bed material

5.4.1 Critical gradient

When a geometrically open filter is applied, the transport of material is theoretically possible, but the load is kept smaller than the strength. In other words, the gradient should be smaller than a critical value. When the gradient exceeds this value, the filter velocity will generate transport. To determine the critical flow condition for stationary parallel flow, as over a falling apron, Equation 5.10 can be used [CUR 1993].

$$u_{f,cr} = \left\{\frac{n_f}{c}\left(\frac{D_{f15}}{\upsilon}\right)^m \left(\psi_s \Delta_b g D_{b50}\right)^{0,5}\right\}^{\frac{1}{(1-m)}} \qquad \text{Equation 5.10}$$

in which,

$u_{f,cr}$	=	critical filter velocity	[m/s]
n_f	=	porosity of filter material	[-]
Δ	=	relative density of sediment	[-]
e	=	empirical coefficient; $e=c*Re^{-m}$	[-]
ψ_s	=	Shields parameter	[-]
g	=	gravitational acceleration	[m/s^2]
D_{b50}	=	size of bed material	[m]
c	=	coefficient (see Table 5.1)	[-]
m	=	coefficient (see Table 5.1)	[-]

Table 5.1 Parameters according to Klein Breteler

D_{b50} [mm]	c [-]	m [-]	ψ_s [-]
0,10	1,18	0,25	0,11
0,15	0,78	0,20	0,073
0,20	0,71	0,18	0,055
0,30	0,56	0,15	0,044

The formula is valid for bed materials with characteristic diameter $D_{b50,}$ between 0.1 and 1.0 mm. With the calculated value of the critical filter velocity from this formula, the critical water level gradient can be derived from the Forchheimer relation. On the basis of experiments, another formula is derived. This formula can be used to calculate the critical gradient in porous flow (Equation 5.11).

$$i_{cr} = \left[\frac{0.06}{n_f^3 d_{f15}^{4/3}} + \frac{n_f^{5/3} d_{f15}^{1/3}}{1000 d_{b50}^{5/3}} \right] u_{*cr}^2 \qquad \textit{Equation 5.11}$$

in which,

i_{cr}	=	critical gradient	[-]
n_f	=	porosity of filter material	[-]
d_{f15}	=	characteristic diameter of filter material (15% smaller)	[m]
d_{b50}	=	characteristic diameter of bed material (50% smaller)	[m]
u_{*cr}	=	critical shear velocity	[-]

The two terms between brackets are a laminar part and a turbulent part, as in the Forchheimer equation. For a given ratio of $n_f d_{f15}/d_{b50}$, the critical gradient is greater for fine than for coarse material. This might be explained by the lower filter velocities in fine pores, because of which a relatively steeper gradient is needed in the filter layer to reach the critical velocity. There is no influence of layer thickness in this formula, and neither in equation 5.9.

5.4.2 Thickness

The velocity and turbulence decrease inside the rock layer, but remain constant from a distance of $1.5d_{50}$ inside the layer [CUR 1993]. Because of the constant value in the lower part of the rock layer, the better protection against scour of a thicker layer does not derive from of the decrease of the turbulent velocities inside the filter. The explanation is found in the longer path for the sand grains through the rock layer.

From tests with the top layer directly placed on the bed material, it seemed that the bed material was transported through the top layer when the latter was less than 1.5 times the stone diameter. To calculate the apron thickness, Equation 5.12 can be used.

$$\frac{d_{f15}}{d_{b85}} = 5 \frac{(1-n_f)}{n_f} \frac{t}{d_{f50}} \qquad \textit{Equation 5.12}$$

in which,

t	=	layer thickness	[m]
n_f	=	pore number filter material	[-]
d_b	=	characteristic diameter bed material	[m]
d_f	=	characteristic diameter filter material	[m]

In the falling process, the falling apron is expected to move vertically as well as horizontally (see Figure 5.2). The apron layer will become thinner because the quantity of rock per unit area will decrease.

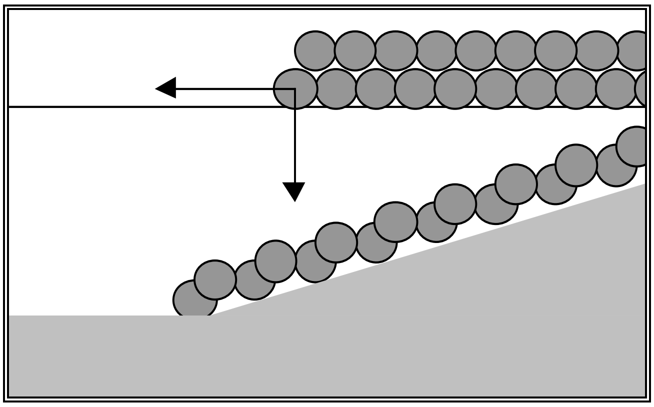

Figure 5.2 Decrease of apron thickness during setting

During all stages, the retaining function must be fulfilled. The gradient in the apron layer should therefore be sub-critical at all times. In the model, the apron material must be chosen such that this condition is fulfilled during the falling process. However, during the scouring process it can be expected that only small amounts of rock will fall at a time. This will leave openings between the stones, where scour can continue.

6 Model

6.1 Introduction

From the start of this study, it was evident that a scale model experiment would significantly contribute to the knowledge on falling aprons. In this chapter, a description of two alternative models and the aspects of scaling is given. To investigate the different aspects, various tests are to be executed. Because of the relatively small load on the sand, it was not considered necessary do the model tests in a geo-technical centrifuge.

The two experimental tests in this chapter are:

- Suction pipe test (SPT): In a model of a falling apron, the scour process is simulated by means of a suction pipe.
- Flume test (FT): In a flume, a stretch of guide bund is constructed which is exposed to a current.

The decision whether or not to do tests with flowing water was an important one. First the two different experimental alternatives are described. Then follows the decision to use which of the flume tests, which was made on the basis of possible results and feasibility.

6.2 Information required from the model tests

A study of the action of an apron during the falling process, though simple, is essential to the understanding of the behaviour of a falling apron protection. The literature described in the previous chapters gives only design assistance based on geometrical aspects. Only initial and (estimated) final situations can be found, leaving open questions on what happens during the setting process.

In the foregoing, the different aspects of a falling apron are summarised and described. The emphasis was on flow conditions and stability, rather than on soil mechanical aspects. The reason for this, is that the soil mechanical behaviour is very complicated (especially because of the mica content), and therefore demands separate attention. The liquefaction aspect cannot easily be investigated in a model, largely because of size limitations. This aspect is therefore not a subject of investigation in the model, but should be taken into account when conclusions are drawn.

In §1.3, the aim of the project was formulated. In the model some of the same aspects have to be investigated, as the literature does not give satisfactory answers to the questions. For the experiment, the following objectives were set:

- To get insight in the falling process and the successive phases (what happens?),
- To determine whether different configurations influence the final slope (special care during dumping necessary?),
- To determine the thickness and slope angle of the settled apron.

To get insight into the behaviour of the falling process, relative simple testing can be adequate. Because the successive phases of the falling process of a falling apron are not known, the process is difficult to simulate. The combination of scouring and the resettling of stones should therefore be reproduced. To do this, tests could have been conducted either with flowing water to simulate the scouring effect as in real situations, or the sand could have been removed manually, as with a suction pipe.

6.3 Extent of the model

6.3.1 Borders

At the shore side, a falling apron is placed along the constructed slope. The function of the falling apron is primarily to provide protection from scour. Secondly, the established slope of the falling apron should form the foundation of the above-lying slope. For this, the slope should not become to steep. However, the rock layer on the upper slope is stable in itself and is not supported by the falling apron section. In the case of the Jamuna Bridge, this slope is 1:6. For the model, the assumption is made that the upper slope does not influence the falling process, although the scouring process will be influenced. The constructed slope in a real situation is schematised as a vertical wall in the model.

At the side of the river, the sand bed stretches out for several 100 metres (in the case of the Jamuna even several km) over the bed of the river. Here different flow channels and sandbars (locally known as chars) can be recognised. This morphological geometry is not implemented in the model, because it was the setting of an apron and not the scour process that was the subject of research. Directly along the apron section, the riverbed seems to subside evenly and therefore this part of the model is kept quite narrow.

For tests with flowing water, a flume that is wide enough for an apron section to be placed and to have enough space left for the unprotected riverbed. Because of flow conditions and disturbances at the boundaries, the test section also has to be long enough. For tests with a suction pipe, the length of the section is less important. However, for practical reasons the same flume is to be used. To test larger sizes of rock, the apron should be placed perpendicular in the flume (suction pipe tests). The location chosen for the tests was the research facility of HAM at Moerdijk. The width of the flume is 1.15m, the depth 1.35m and the length is over 11.00m. It has a glass wall, which allowed viewing of the process (especially with the suction pipe tests).

6.3.2 Boundary conditions

For an experiment without flowing water, a ‘slice’ of a falling apron can be modelled. A 2-dimensional situation can then be investigated in a relatively small model. The width should be such that the side walls do not influence the area of interest. Sand and rock will create friction along these walls and therefore the setting will be influenced directly along the glass.

For tests with flowing water, for a 2-dimensional situation a long model area is also needed. The model should extend far enough upstream and downstream to include all features that will significantly affect the flow at the points of prime interest in the model. Of course, the area of the model should be kept to the minimum area necessary, to allow the use of the largest scale possible within the test facility.

One limitation of doing experiments in a flume, is the influence of the sidewalls. The rivers in which a falling apron is installed, like the Ganges or Brahmaputra River, are so wide (order of magnitude: several km) that the hydraulic conditions on one side will not be influenced by the other side. This will not hold for the hydraulic conditions in a small flume. The scour along the glass wall should therefore be interpreted with caution. The upstream boundary condition is the discharge and its distribution over the width of the flume. The discharge is kept constant during all tests. At the downstream termination, where the submersible pump is placed, the discharge is also constant.

6.4 Similarity

The quality of a model is determined by the reliability of the test results, which is again determined by the similarity of the processes studied. Similarity is characterised by scaling rules, based on physical laws. When there are deviations, scaling effects are introduced. There are three kinds of similarity:

Geometric similarity
Two systems are geometrically similar when the proportionality of corresponding parameters is equal. Examples of geometric parameters are area and volume.

Kinematic similarity
Two systems are kinetically similar when corresponding distances are covered in corresponding time intervals. Examples are velocity and acceleration.

Dynamic similarity
Two systems are dynamically similar when corresponding masses under influence of corresponding forces are dynamic similar. Examples are density, force and energy.

In general, two different systems can only be similar (geometrically, kinetically and dynamically), when the relevant dimensionless parameters have the same value in model and prototype. However, as long as the studied process represents a real situation it is not necessary to reproduce all aspects. As the model is primarily used to get insight into the behaviour of a falling apron, only the relevant parameters have to comply with these scaling rules. The scaling factor for a parameter x is determined as the value of x in prototype, divided by the value of x in the model, see Equation 6.1.

$$n_x = \frac{x_p}{x_m} \qquad \textit{Equation 6.1}$$

For both the suction pipe tests and the flume tests, the scaling is important. The former is mainly a way of visualising the behaviour during the scour development. In this case the primary importance is to simulate the scour process (with a suction pipe) realistically. Therefore different scenarios are developed. This is completely different approach than that used for the tests with flowing water. Here the scour development should comply with prototype situations; otherwise it is difficult to interpret the rules.

For both test options the soil parameters should comply with a prototype situation. It is especially important to model the ground mechanical instability with care. Because of size limitations, these instabilities are not likely to occur in the model, so experiments should be done in a geo-centrifuge to take into account these failure modes .

Finally, it must be remembered that the model in which the setting is visualised, is not meant to represent the prototype exactly.

6.5 Considerations on suction pipe tests

Before doing suction pipe tests (SPTs), the way of eroding the sand bed has to be determined. Unlike the case in which flowing water is used to erode the sand, here the use of a suction pipe will influence the falling process considerably. In the introduction to this chapter, it was already mentioned that it is difficult to erode the sand between the different ‘stacks’ of stones. Some considerations on this problem and different scenarios of attack are described in this below.

6.5.1 Suction distance

As well as the determination of the setting result, the setting process itself is to be investigated.. To get this insight into setting behaviour, simple tests can be done with a suction pipe. For different scenarios (worked out in §6.5.2), the process of launching can be simulated by taking sand away. The advantage of doing this without flowing water is that:

- What happens is visible (no sand in suspension),
- It is possible to ‘erode’ in different ways (scenarios),
- Problems with flow conditions are avoided.

The only real problem, or disadvantage, is that it is difficult to simulate the scour development well. This can be illustrated by Figure 6.1, which shows a possible intermediate phase. Here a subsiding foreshore attacks the edge of the apron (cross-section over the edge). The first group of stones has shifted into the scour pit. The new configuration that appears loses its sand-tightness. Over the length of the edge, the protection against scour varies at different locations. The problem with a suction pipe, as opposed to a current, is that is difficult to erode the sand between the stones that have shifted, in a natural way.

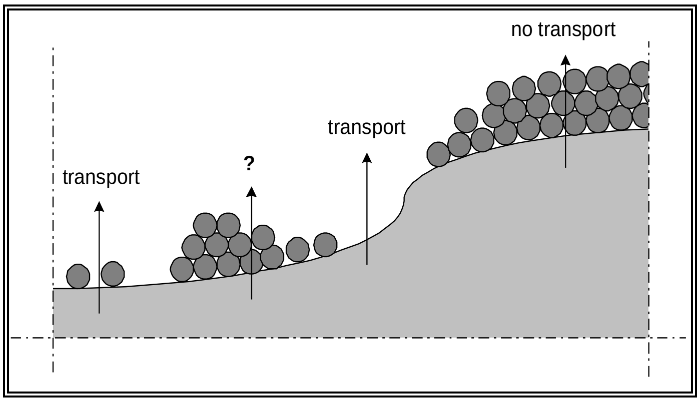

Figure 6.1 Sand transport at different locations of the cross-section

To erode sand between parts of the apron that have already fallen, a simple aid must be applied. Sand should only be eroded at places were the river flow would erode it as well. Therefore, the mouth of the suction pipe should be kept at a specific distance from the sand and/or stones. This can be done by using a distance holder made of steel wire at the mouth of the pipe.

This distance has to be found experimentally, i.e. by calculating the transport of sand through the rock layer with the aid of the theory in Chapter 6. It depends on suction velocity and on the open filter rules. The sand transport capacity (in this case into the suction pipe) should then agree with the prototype.

6.5.2 Scenarios

Besides the technical manner in which the sand was eroded, also the mode of attack is to be reproduced. There are different possibilities. Survey data from the JB-RTW show that the riverbed in front of the apron seems to subside evenly. However, the falling height of the apron has not been reached. It is also possible that the river attacks a guide bund at an angle and that the apron is locally undermined. Two different ways of (possible) attack are shown in Figure 6.2. and these have to be investigated.
The first is an even, horizontal subsidence of the river bed (A). The second is the simulation of a deep channel that travels horizontally towards the apron (B).
The stones are coloured in strips parallel to the toe (perpendicular to the flume). In this way, it is possible to tell how far the stones moved in a horizontal direction. When the tests seem to give a reasonable result, the slopes will be measured, by means of a rod with a half sphere. This will be done according to the CUR manual. A compromise has to be found between the number of measuring points and accuracy.

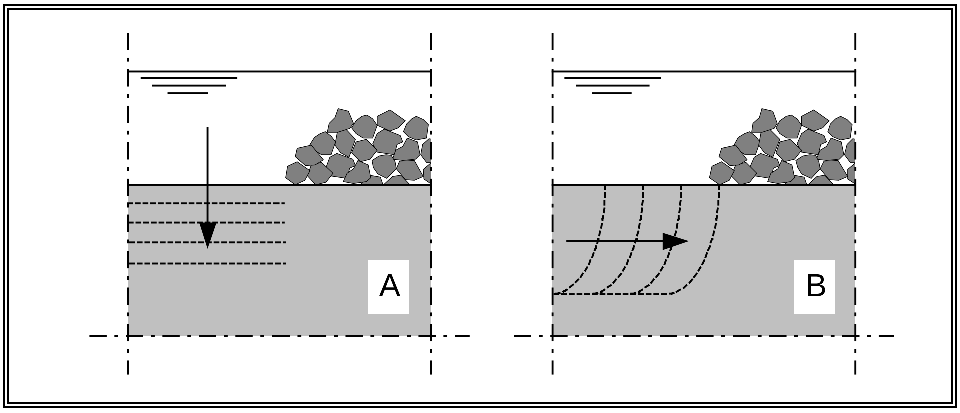

Figure 6.2 Attack scenarios

The slopes can be compared with the angle of repose, for example determined from tests on a tilting board. With such a board, the friction angles for sand-rock and rock-rock, can be determined relatively simply.

6.5.3 Apron material

The stone size for the apron section in the model should have a characteristic diameter d_{50} in the order of 0.03m. This choice was made on basis of the size of the testing facility. With this size, it is possible to apply several layers of rock and several apron configurations. Because the apron is placed perpendicular in the flume, the width can be chosen freely.

In the design practice, use is made of different geometrical configurations in which the apron is laid (see Figure 6.3). The SPTs provide a good way to determine the influence of these different forms on the falling behaviour.

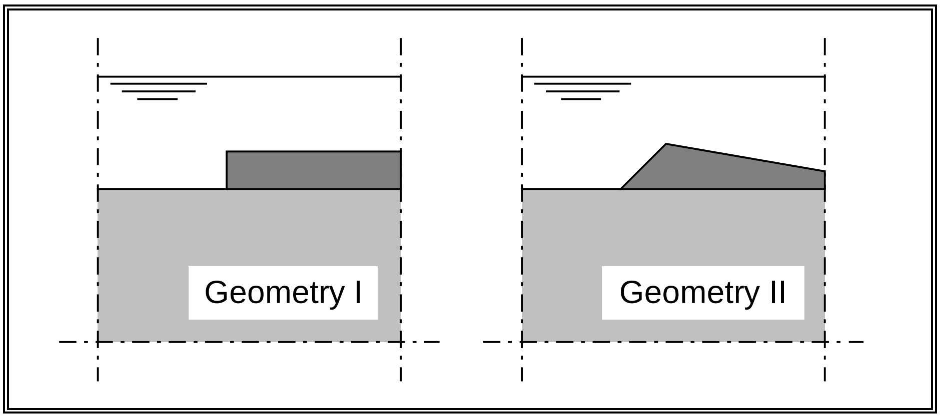

Figure 6.3 Different geometrical configurations

In Figure 4.1, different apron forms, as suggested by different authors are given. The sizes (such as thickness) are entirely based on geometrical conditions. Placing the apron in the form of a wedge towards the riverbed seems logical, because the stones at the outer (river) side of the apron will have to move a longer distance to reach their final position (see Figure 5.2). The stones at the bank side are already at their final position. The falling apron is considered to fail when these stones come off their place, because then the toe of the slope has already lost its protection against scour.

Another aim of the study with SPTs is to try to determine how an apron that contains insufficient rock, can be replenished when the scour depth has been underestimated (i.e. in design). Or, in other words, is it possible to start with a smaller (and thus cheaper) apron and supply extra material when needed? This question arises with the design of the Paksey Bridge guide bunds (180 m^3/m^1!).

6.6 Considerations on flow tests

Apart from demonstrating/visualising the behaviour of the falling process with the SPTs, it is also possible to try to simulate the scour development under flow conditions. This simulation would be simplified and schematic, but could add substantially to insight into the behaviour. The aim of these tests was to try to let the current dictate the scour development. In this chapter, the different materials and flow velocities chosen for the flow tests are considered. These are primarily the bed material, the apron material and the flow velocity. The model sand should be as fine as possible and the apron material as coarse as possible.

6.6.1 Froude

The Froude number gives the relation between gravity and stationary inertial force. For a correct representation of the flow field, the value should be the same for model and prototype. Because the flow field in the model is mainly determined by model boundaries and the hydraulic roughness, the Froude number representation is not of primary importance. However, the value of the

Froude number in the model flow, has to be smaller than the critical value of Fr=1 for stationary flow.

$$Fr = \frac{U}{\sqrt{gh}} \qquad \textit{Equation 6.2}$$

in which,

u	=	velocity	[m/s]
g	=	gravitational acceleration	[m/s^2]
h	=	water depth	[m]

For the model the flow velocity must chosen such that the sand transport is substantial. Using different flow velocities gives insight in the influence of flow velocity in the scour development. However, every velocity used should be high enough. The maximum discharge and the used water depth will determine the velocity.

When the water depth in the flume is 0.50m (above the sand bed), the value for u_{cr} is 2.21 m/s. The flow velocities used (below 1.0m/s), are thus low enough for stationary flow. The roughness of the sand bed is dependent on the flow velocity. This is worked out in §6.6.4.

6.6.2 Reynolds

In the conditions encountered by a falling apron, with large rock (d_{50}≈0.30m) and high flow velocities (u≈3.0m/s), the flow around the rock will certainly be turbulent. When small stones are used in the model and the flow velocities therefore have to be smaller, the flow should still be turbulent. The Reynolds number gives the relation between momentum and viscosity. For values of Re>1200, the flow is turbulent and the influence of the viscosity becomes negligible.

$$Re = \frac{uD}{\nu} \qquad \textit{Equation 6.3}$$

in which,

u	=	characteristic velocity	[m/s]
D	=	characteristic diameter	[m]
ν	=	viscosity	[m^2/s]

With a flow velocity of 0.5 m/s, for coarse sand the flow already becomes turbulent.

6.6.3 Bed material

For an undistorted model in which sand is the bed material, the sediment transport can be reproduced in the model to scale if the d_{50} is reproduced at the length scale. The bed material of the Jamuna River is fine sand. If this sand is scaled at the length scale, the diameter of the model sand will become equal to diameter of silt or clay. However, the properties of silt and clay particles are completely different from those of sand. Clay particles, with a much smaller size than sand grains, attract each other and form a cohesive mass[8].

The most important characteristic of the Jamuna bed material is that it is cohesionless material. Therefore, the sand cannot be scaled at length scale. The smallest diameter to be used is sand with a diameter of 100 μm; this is about half the size (in diameter) of the Jamuna bed material (see Table 3.1). Little significance is attached to using the smallest possible sand. In §3.2 it was indicated that the smaller the grain diameter, the smaller the fall velocity. This implies that there is more sand in suspension and thus poorer visibility.

The size of sand used will also influence the sediment transport rate. Bed material movement may occur in two transport modes: (1) bed-load and (2) suspended load. As the value of ψ increases for flow over a loose bed, sediment movement as bed-load (for which particles tumble and bounce along the bed) intensifies and progressively establishes a substantial suspended-load component (for which particles are carried in suspension over the full depth of flow). Although the transport process evolves more or less smoothly from one mode to the other, the mechanics of suspended transport differ from bed-load in that particle fall velocity is highly influential in characterising suspended transport. Fall velocity, though, is less relevant for describing the tumbling of particles as bed-load.

The flow velocity required to erode the sand is determined by using the Shields relation, which gives the threshold of motion (see Figure 4.3). Because the threshold of motion is hard to determine, Delft Hydraulics makes a distinction of 7 criteria. Criterion 1 is when some individual grains lose their stability and criterion 7 is when “the march of the grains” begins. Because the sand should be washed away in a relatively short time, the velocity for ongoing transport of grains (criterion 7) is calculated.

6.6.4 Roughness

The roughness of the riverbed can be divided into two types. The first is the surface or grain roughness. The second is the roughness due to bed features. Two types of bed features are distinguished, ripples and dunes. The size of the ripples is independent of flow depth; it depends only on grain parameters and flow velocity. Dunes are generally larger bed features and develop at higher bed shear stresses than ripples. The height of dunes is dependent on depth.

Whether bed forms appear is determined by flow conditions. Three flow regimes are distinguished [RAUDKIVI 1990]:

Lower regime	$\psi< 1.1$
Transition regime	$1.1< \psi< 1.5$
Upper regime	$\psi>1.5$

The influence of bed features is especially important with smaller transports (lower regime, $\psi< 1.1$). In order to try to predict the bed form, the Shields

[8] These attracting forces are known as the Van der Waals-forces. These consist of electro-chemical bindings between the particles.

parameter can be used. It can be scaled, according to WL|Delft Hydraulics [1988A], with

$$n_{\psi_s} = \left(\frac{n_h}{n_D}\right)^{2/3}$$

In this equation, the subscript *h* stands for depth and the subscript *D* for (grain) diameter. For an identical bed form in model and prototype, this scaling factor should be equal to 1. Because the bed material is not scaled with diameter, deviations are introduced. In the Stokes region, the fall velocity is proportional with D^2 (See §3.2). The scaling factor for the Shields parameter can therefore be written as:

$$n_D^2 = n_w$$
$$n_w = n_h^{1/2}$$
$$n_D = n_h^{1/4}$$
$$n_{\psi_s} = \left(\frac{n_h}{n_h^{1/4}}\right)^{2/3} = n_h^{1/2}$$

From this, it can be concluded that it is not possible to produce the same bed form in the model when the depth is scaled.

The bed form in the model can be predicted with Equation 6.4. Van Rijn [1982] gives a formula for flow over bed features of height η and length λ, based on flume and field data:

$$\frac{k}{\eta} = 1.1\left(1 - e^{-25\eta/\lambda}\right) \qquad \textit{Equation 6.4}$$

in which,

k	=	grain roughness	[m]
η	=	ripple height	[m]
λ	=	ripple length	[m]

The data covered values of 0.08 < h <0.75 m, 0.25 < U <1.1 m/s and 0.1 <d50< 4,4 mm. Therefore it can be used for calculations on the model. The total hydraulic roughness of a sand bed stream is expressed as:

$$k = 3d_{90} + 1.1\eta\left(1 - e^{-25\eta/\lambda}\right) \qquad \textit{Equation 6.5}$$

With the flow velocity to be used (between 0.5 and 1.0m/s), ripples in the bed can be expected. The calculations on bed forms in the model, based on these relationships, are described in Appendix 2. The calculated ripple size is given in Table 6.1. The ripple height depends only on the diameter (approx. $1000d_{50}$).

Table 6.1 Ripple sizes for sand 100μm and different flow velocities

	U=0.50m/s	U=0.75m/s	U=1.0m/s
Ripple height η	0.025	0.039	0.035
Ripple length λ	0.10	0.10	0.10

In real situations, with high flow velocities, the transport of bed material will be such that ripples do not appear. The ripples in the model therefore distort the scour process. When the falling process is disturbed too much during testing, the sand bed can be smoothened artificially (i.e. with a suction pipe).

6.6.5 Apron material

The size of rock in the model should be such that it is much larger than the base material. Another consideration is that the rock should be small enough to fit the flume. To investigate the falling process, there should be a real apron of stones, a few layers thick. Because of limitations on the testing facility, the choice was made to use different sizes of apron material. This meant that more tests had to be done, but at the same time produced more results that could be compared.

In the model tests little emphasis was placed on the hydraulic stability of individual stones. Transport of rock in the direction of the current was not permitted during the tests. With the aid of the Shields formula, rock sizes were determined that were stable in the current.

The space available for the apron section was 0.60m wide. With a d_{n50} of 0.01m, this meant (depending on grading and packing of material) a width of approx. 60 stones. An apron consisting of 10 layers would be 0.10m high. This is considered enough to determine the process of resettling. When the stones are coloured, this process can be visualised.

The larger their size, the fewer stones can be placed in the apron section. To compare the results for small stones of 0.01m, larger sizes were also tested. The size of the stones chosen was (d_{50}) of 0.025m and 0.045m. An option is to test different gradings in the falling apron section. The grading can be changed, while the characteristic size remains the same.

The difference in size between sand and rock should be large enough (as in the prototype); a comparison is given in Table 6.2.

Table 6.2 Sand and rock size

	SAND (d_{50})	ROCK (d_{50})	SIZE FACTOR
Prototype	200 μm	0.30m	1500
Model	100 μm	0.010m	100
Model	100 μm	0.025m	250
Model	100 μm	0.045m	450

The critical flow velocity was also calculated for the apron material. Only this time, it was not the ongoing transport that had to be calculated, but the start of movement (criteria 1). For values of Re_* of more than 500, the Shields parameter becomes a constant, because the viscosity is negligible. For the three sizes, the Shields factor is a constant. With a value of Ψ of 0.055 (approx. criteria 6), the critical flow velocity for rock with d=0.03m, is 1.89 m/s. For a value of the Shields parameter of 0.040 (criteria 1), the critical flow velocity is 1.60 m/s.

The calculations of stability were made for the different sizes, and the outcome is given in Table 6.3.

Table 6.3 Critical velocities for proposed rock sizes (h=0.50m)

	0.01m	0.025m	0.045m	UNIT
C	45	36	33	$[m^{1/2}/s]$
$\sqrt{g}/C$	0.070	0.087	0.095	[-]
ψ	0.040	0.040	0.040	[-]
U_{cr}	1.15	1.60	1.80	[m/s]
ϕ	33	38	39	[°]
$U_{cr}(\phi)$	0.86	1.20	1.35	[m/s]

The value for U_{cr} (ϕ) is the critical velocity [m/s] for rock on a side slope of 1:2 (see §4.4.3). The angle of internal friction (ϕ) was determined with Figure 4.4, assuming irregular shaped rock. The possible flow velocity in the model is limited by the discharge capacity. For a flow velocity of 1.0 m/s, the stability of rock with d=0.01m is not guaranteed with a side slope of 1:2. It was therefore decided that with the small size rock of 0.01m, the flow velocity should be under 0.75 m/s. The two other sizes could be tested with a maximum flow velocity of 1.0m/s.

6.6.6 Thickness of apron section

Besides the diameter, the thickness of the apron is also important. For the starting situation as well as for the end situation, the thickness should be such that the turbulent fluctuations are damped inside the rock layer and that the transport of sand though the layer is stopped (see §5.4.2).

With the small size of rock, 10 layers are feasible (like in real situations). But for the rock with a diameter of 0.05m, only a maximum of 4 layers is possible.

To investigate the possible influence of the apron thickness on the setting behaviour and resulting slope; different initial apron heights can be tested. The thickness should be such that for the different rock sizes the same height can be used, making a comparison possible.

6.7 Choice of model

After previous consideration of both test methods, it is clear that both have advantages and disadvantages. These are summarised in Table 6.4.

Table 6.4 Comparison of test alternatives

	ADVANTAGE	DISADVANTAGE
SPT		
	Visibility (no sand in suspension)	'Sand transport' perpendicular to the apron edge.
	Less complex model	'Scour' imposed on model
	Larger scale possible	Uncertainties on scour development
FT		
	Scour determined by model	Smaller scale necessary
	Time dependent development	No visibility during testing
	Sand transport in the direction parallel to the apron	Scaling according to kinematic scaling rules

As the slope angle is expected to be influenced by the flow velocity, it cannot be measured correctly in a model without flowing water. The setting mechanism will also be influenced by the current. Because this study is a first exploration, it was considered more useful to do experiments with flowing water.

7 Experiment Set-up

7.1 Introduction

This chapter describes the model and the test conditions. All the aspects of the experiments, as far as they were the same for the different tests, are worked out here. The test results and the specific test parameters, as measured during the tests, are presented in the next chapter.

7.2 Test facility

The *Merwelanden Flume* at the research facility of HAM at Moerdijk was used for the tests. The tank is approx. 13m long, 1.10m wide and 1.30m high and has one glass side (see the drawings in Appendix 3 for details). The first part of the flume (3m) is separated from the rest by a weir. In this part the water is pumped. The weir distributes the water over the entire width into the flume.

In the flume section two slopes, made of wood, were placed. The central, horizontal, section (5m long) consists of sand. This is the measuring area. The sand body was 0.5m high. Together with the slopes it makes a sill on which the apron can be placed.

The discharge was generated by a submersible pump, which was placed at the end of the flume. The submersible pump has a capacity of approx. 100 l/s (0,100 m^3/s) when the head difference is kept small (horizontal water displacement). This is the reason why the return-pipe for the water was placed directly on the side wall of the flume and was kept as short as possible. A diameter of 125mm was used for this pipe.

The end part of the flume has a pit with a depth of 0.50m below flume bottom. The pump was placed partly above this pit. Because of the flow conditions in this end part and the closed bottom of the pump, most of the transported sand settles in this pit. It serves as a sand trap.

7.3 Materials used

7.3.1 Sand

Falling aprons are used along riverbanks where the riverbed consists of a homogeneous sand layer. At the site of the Jamuna Bridge, the bed material consists of loose uniform sand with a diameter of approx. 210 μm. It is not possible to scale this sand (scaling sand would lead to the use of clay, which has a completely different behaviour) as was done in the case of the apron rock. The choice made was to use sand with a characteristic diameter of 170 μm. This sand, which was already present at the test facility, is considered small enough and has a uniform size. An advantage was that this sand had been used in previous model tests and therefore the fines had already been washed out. See sieve curve in Appendix 4a.

7.3.2 Rock gradings used

The choice of rock size was made on basis of scaling rules and on the limitations of the testing facility. To avoid possible scaling effects, three different rock gradings were used. In Table 7.1, the most important characteristics of the rock that was used are summarised below.

	8/16 mm	15/30 mm	30/60 mm	UNIT
Material	Basalt	Greywacke	Basalt	[-]
Density	2850	2650	2850	[kg/m^3]
d_{15}	7.2	17.8	29.7	[mm]
d_{50}	10.7	24.3	45.0	[mm]
d_{85}	14.8	32.7	58.4	[mm]
d_{85}/ d_{15}	2.05	1.83	1.97	[-]
d_{60}/d_{10} (=u_c)	1.70	1.67	1.71	[-]
shape class	Irregular	irregular	irregular	[-]
batch size	24	33	47	[litre]

Table 7.1 Rock characteristics

These three different gradings were chosen such, that the ratio d_{85}/d_{15} was almost equal (approx. 2.0, see Table 7.1). The small sizes of rock used in the model are classified as 'fine gradings'. For these gradings, often the uniformity coefficient (U_c) is used to characterise the width of the grading [CUR/ CIRIA 1991]. According to this, they can be classified as normal (wide) gradings.

In §5.1.1, the filter function of a falling apron is described. Here the relation d_{f15}/d_{b50} was found to be important for the classification of the type of filter relation. In Table 7.2 the relation between sand and rock is presented.

Table 7.2 Relation between rock gradings and sand size

	8/16 mm	15/30 mm	30/60 mm	UNIT
d_{f15}/d_{b50}	42	105	175	[-]
d_{f50}/d_{b50}	63	143	265	[-]

Sieving of the samples took place according to the CUR guideline, which gives a rule of the thumb for the batch size [CUR/ CROW/ NNI 1993]. The minimum batch-size is given as:

$$V = 6\sqrt{D} \qquad \textit{Equation 7.1}$$

in which,

V	=	Volume	[litre]
D	=	largest nominal grain size	[mm]

Sieving (with standard sieve set) was done for 10 minutes, after which the sieves were cleaned with a brush. Finally the sieving was continued for another 3 minutes. The sieve curves are given in Appendix 4.

7.4 Test conditions

7.4.1 Water depth

A serious limitation encountered during the first try-outs of the model set-up was the pump capacity. Although a discharge of over 90 l/s could be generated, this was still very modest in relation to the required discharge (order of 300 l/s) to reach a deep scour pit. To overcome this deficiency, the originally planned test conditions were adapted.
The primary aim of the experiment was to visualise the adapting of the apron to a developing scour hole. The asymptotic (clear water scour) development of scour as described in §2.5.3, is repeated in Figure 7.1. Because the critical velocity of the sand was exceeded, sand transport took place and the scour depth increased. Because of deepening of the scour hole, the velocity decreased (and therefore the transport of sand) and the growth of the scour hole declined. An equilibrium scour depth ($h_{s\ eq}$) was found after time t_s. If a lower flow velocity is used, this equilibrium value will be lower.

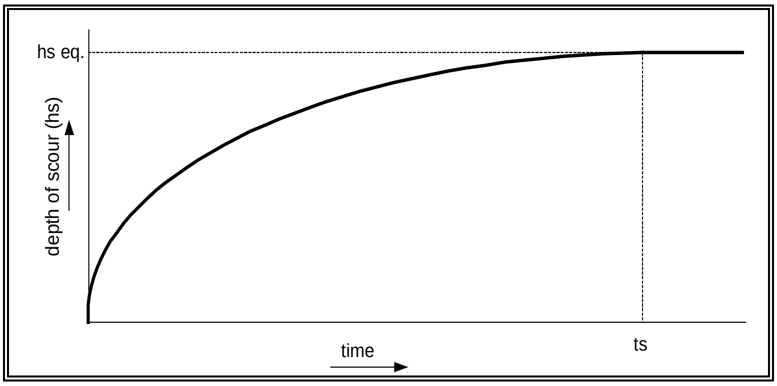

Figure 7.1 Scour development

The pump capacity was limited to a discharge of approx. 100 l/s. If tests are carried out with an average flow velocity of 0.5 m/s, the cross-section has to be limited to 0.1/0.5=0.2 m^2. Because of the deepening of the sand bed, the (asymmetric) cross-section area increases in time. The result is that the flow velocity decreases in time (assuming a constant discharge). Therefore, a choice was made to adjust the water level to the velocity at the start of each run.

The scour development was approached as shown in Figure 7.2: the scour process is split up into discrete steps. The discharge was constant during all tests. When the transport of sand started to stagnate, the water level was lowered to decrease the cross-sectional area and thus to increase the flow velocity, so the scour could continue. This lowering of the water level was synchronised with the start of the different runs.

In Figure 7.2 the development of scour is given in a qualitative way, the quantification is given in Chapter 8 where the experimental results and the measuring data is described. There the scour development during the experiments is also given to make a comparison.

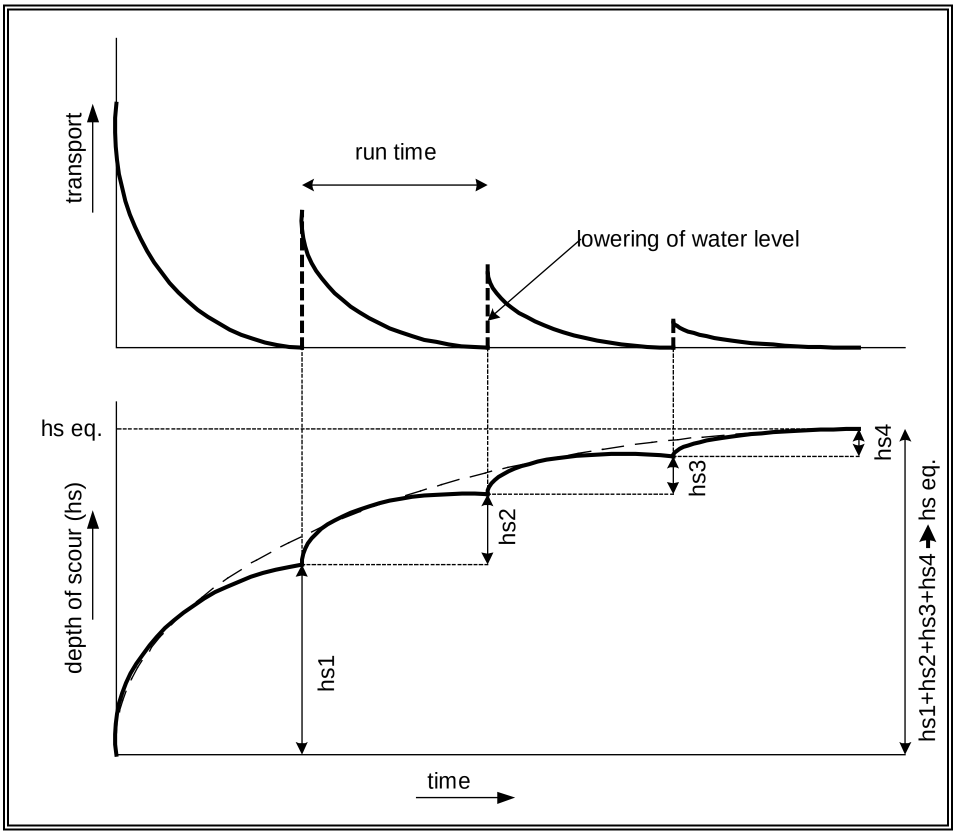

Figure 7.2 Method of approach of scour development

7.4.2 Curvature of flow lines

Because the apron was placed on top of the sand bed and therefore protruded into the current, the flow lines were curved around it. The up and downstream terminations were rounded to avoid extra turbulence. This is schematised in Figure 7.3. The higher flow velocity around the apron section generates extra erosion at the apron toe. This leads to a lower position of the sand bed directly in front of the apron. This can be compared with a prototype, where a river channel 'hangs' on to the revetment or guide bund. In the supplement report for FAP 21/22 [NEDECO 1996] where the scour development along a guide bund in a scale model is described, the same development is seen.

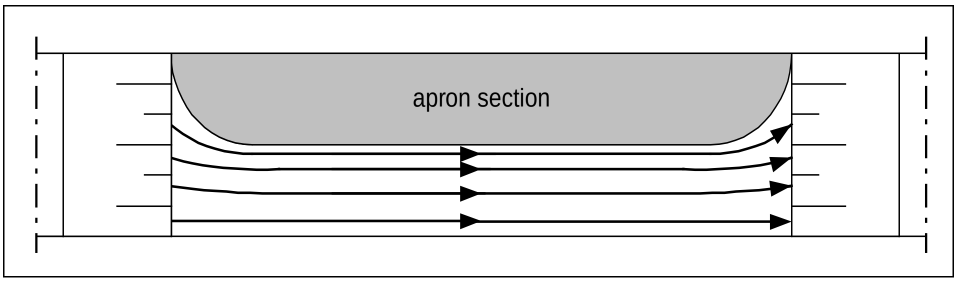

Figure 7.3 Curvature of flow lines (top view)

7.4.3 Roughness and bed features

In §6.6.4, a description of the possible bed features in the model is presented. In this section, the theory is applied to the material used and the flow conditions. The important formulae are repeated:

$$\frac{k}{\eta} = 1.1\left(1 - e^{-25\eta/\lambda}\right) \qquad \textit{Equation 7.2}$$

The validity of this formula is: 0.08m < h < 0.75m, 0.25m/s< u < 1.1m/s and 0.1mm < d_{50} < 4.4mm. Therefore it can be used for calculations on the model. The total hydraulic roughness of a sand bed is expressed as:

$$k = 3d_{50} + 1.1\eta\left(1 - e^{-25\eta/\lambda}\right) \qquad \textit{Equation 7.3}$$

With the flow velocity of 0.60 m/s and sand size of 170 μm, for a number of depths the shape of the bed form and the roughness was calculated. This is summarised in Table 7.3.

Table 7.3 Theoretical bed form and roughness for different depths

	h=0.20m	h=0.30m	h=0.40m	h=0.50m	UNIT
ripple height η	0.0037	0.0056	0.0075	0.0095	[m]
ripple length λ	0.17	0.17	0.17	0.17	[m]
k	0.0023	0.0040	0.0062	0.0083	[m]
C	54	53	52	51	[$m^{1/2}$/s]

It can be seen that the height of the bed formations is negligible, with a maximum value of approx. 1cm at a depth of 0.50m. Even relative to the smallest rock grading, this is only 1*d_{50}. It also implies that the total hydraulic roughness is almost equal to the ‘normal’ Chézy value: the surface or grain roughness.

7.5 Experiment programme

In total 4 tests were conducted. In each experiment, it was attempted to keep all parameters, except one, constant. The bed material (sand) was kept constant for all tests, as were the current conditions and the discharge. Only two parameters were altered during the experiments: the thickness of the apron, and the rock size. It was decided that the experiment with an apron thickness of 0.12 cm and a rock size of 15/30 mm should be taken as the benchmark (FT02) and that the two parameters should be adjusted to make a comparison possible. This led to an experiment outline as given in Table 7.4.

Table 7.4 Experiment Outline

TEST NUMBER	THICKNESS	ROCK SIZE
FT01	**0.20 m**	15/30 mm
FT02	0.12 m	15/30 mm
FT03	0.12 m	**30/60 mm**
FT04	0.12 m	**8/16 mm**

The parameter that differs from that of the reference experiment is printed in bold type here.

7.6 Description of experiment outline

In this section the order of the different operations is given; in principle this is the same for the four experiments. Each experiment consisted of a number of operations. These had a total time span of about 8 to 9 days per test.

1. Flume section between slopes filled with sand (0.50m thick).
2. A filling rack, which was used to place and paint the rock in the flume, was placed on top of sand in the middle of the flume (see Figure 7.4).
3. Thin layer of rock (1 to 2 times d_{50}) was placed in all compartments of rack.
4. Spray painting of rock layers (each compartment having its own colour).
5. Repeating steps 3 & 4 until the desired (0.12m or 0.20m) apron thickness is reached (see Figure 7.4).
6. Removal of rack with crane.
7. Measuring of profile according to predefined grid.
8. Filling with water.
9. Start of pump and discharge.
10. Adjusting (lowering) water level until desired velocity is reached.
11. 90 minutes running.
12. Stopping of pump and removal of water.
13. Back to step 7 (until sand transport stops).

In the experiments, runs of 90 minutes were used. This duration was long enough to permit substantial sand transport and a noticeable setting of the apron. The sand trap was large enough to store the amount of sand and had to be emptied after each run. The quantity of sand in the sand trap was approx. 0.15 m^3/ 90 min. The experiments consisted of 5 to 6 runs of 90 min, and had a total duration of 390 to 480 minutes. By doing measurements after each run, the setting process could be visualised in 5 to 6 consecutive steps. In Chapter 8, a detailed description of each experiment is given.

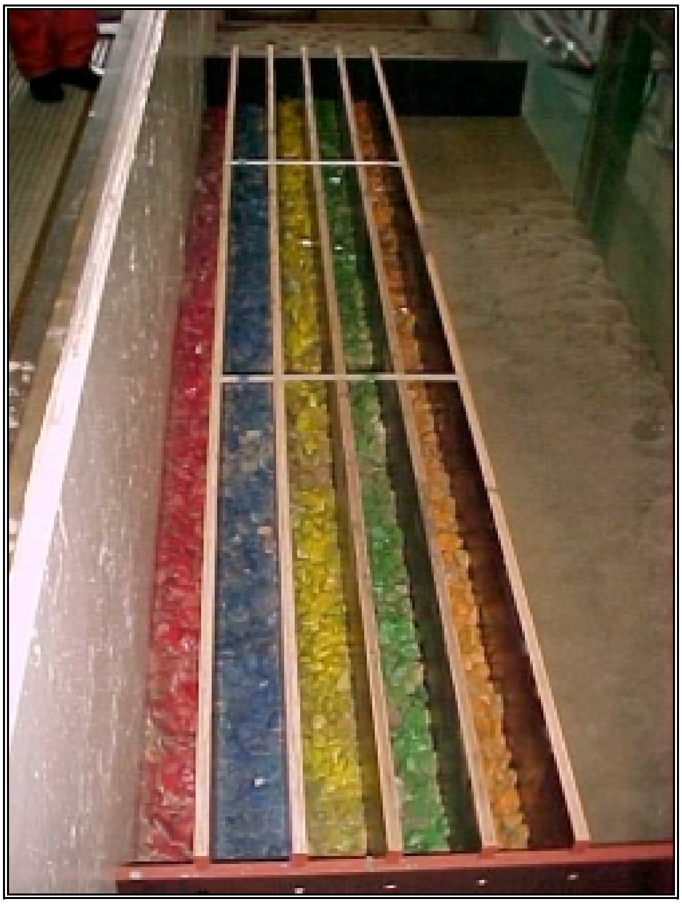

Figure 7.4 Filling rack with its 5 compartments

7.7 Measurements

Before, during and directly after the tests, different measurements were executed. These measurements are divided into the following four categories:

1. Bathymetric survey of the area of interest before and after the different runs.
2. Water level in the flume during pumping.
3. Discharge in the pipe during pumping.
4. Velocity measurements during pumping.

7.7.1 Co-ordinate system for measurements

For the different measurements and graphs, a co-ordinate system, as shown in Figure 7.5, was used. The three directions are defined as follows:

X. Horizontal, in the flow direction, starting at the end of the wooden slope.
Y. Horizontal, perpendicular to the flow direction, increasing towards the glass side of the flume.
Z. Vertical, perpendicular to the flow direction, origin at the top of the wooden slope (initial sand level, flume bottom +0.50m).

The profiles were measured from the top of the flume and were later converted to the co-ordinate system as shown here. In this way, the reference level is the *Initial Sand Level* (I.S.L).

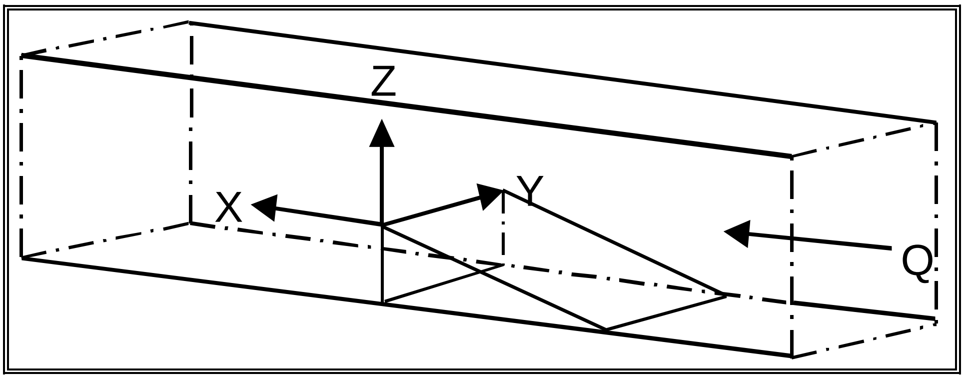

Figure 7.5 Co-ordinate system

7.7.2 Velocity

The flow velocity is determined by using a propeller current meter, also known as an Ott-meter. The propeller current meter works on the principle that a propeller of a certain pitch is turned by the water particles passing along. Each revolution of the propeller corresponds with a travelling distance of a water particle equal to the pitch of the propeller. The number of revolutions in a certain time interval gives then the velocity of the current in a unit of time, according to the calibration formula of the propeller (see §8.6.2).

The velocity measurements are executed in the vertical to determine the velocity distribution over the depth. The location will be at x=2.50m. At this location, in the middle of the flume, the flow is considered to be the least influenced by the model boundaries.

7.7.3 Bed profile

The profile of the apron, as well as that of the sand bed, was measured before and after every run. In 9 cross-sections (every 50cm) the profile was recorded. Measurements were made by using a measuring rod with half a sphere. The diameter of this sphere was always $0.5d_{50}$. This means that for every rock size, a different sphere was used.

According to [CUR/CIRIA 1991] the distance between the measuring points should be kept to 0.5 to 1.0 times d_{50}. Considering the size of rock and the size of the flume, this was not feasible. Instead, distances of 10cm in y-direction and 50cm in x-direction were chosen, mainly based on the number of measuring points (100 per run). Some considerations on the accuracy are described in §8.6.3.

7.7.4 Water depth

A variable water level was used to establish the desired current velocity in the flume, while the discharge from the submersible pump was kept constant during all tests.
The water level was measured at the start of each run. The level is relative to the initial sand level (I.S.L). It was measured at the glass side with a ruler at different locations along the flume.

7.7.5 Discharge

The discharge was measured with an altometer (Electro-magnetic discharge meter) in the return pipe. Because the water is assumed to be incompressible and there is no storage of water, the discharge is assumed constant along the system. The output of the altometer is given as the averaged velocity in the pipe, which can be multiplied with the area.

$$Q = v \cdot \pi \cdot r^2 \qquad \textit{Equation 7.4}$$

The radius of the pipe (r in equation 2.4) is 62.5mm.

The discharge from the pump was kept constant during all tests. Measurements were executed constantly with the altometer, mainly to detect possible loss of pump-capacity.

Table 7.5 Location and time of different measurements

MEASUREMENT	LOCATION	TIME
Velocity	x=2.50m, y=0.90m z=-0.05m z=-0.10m z=-0.15m z=-0.20m z=-0.25m	every 90min
Profile	x=0m through x=4.0m over entire width	before and after every run
Water depth	x=2.0m, y=1.15m and x=4.0m, y=1.15m	start of run
Discharge	return pipe	continuously, recorded at start run

8 Description and interpretation of results

8.1 Introduction

In this chapter, the results of the experiments are described and discussed. For every experiment the description is split into two parts. First the scour development described and after that, the behaviour of the apron as a consequence of this imposed scour. Although the apron behaviour is the investigated part, the scour should comply with the development as described in section 7.4.1.

With regard to the figures in this section, it should be noted that to show the profiles, the measuring points are connected. This does not imply that the actual values between two points lie on the lines shown. In addition to a description based on measuring points and observations, the effect of errors on these results is also discussed here. Measuring errors are discussed in Chapter 8.6.

8.2 Experiment FT01 (rock: 15/30 mm, thickness: 0.20m)

8.2.1 Set-up

The first experiment (Flume Test 01, FT01) was executed by using the middle size rock grading 15/30 mm. The thickness of the chosen apron section was 0.20m, which corresponds with a thickness of approximately 8 times d_{50}. After measuring the apron section before the first run, the actual height was found to be 18.5cm.

The filling rack was used to place the rock onto the sand bed. Five compartments were filled, resulting in an apron width of 0.70m at the initial sand level and 0.50m at the top of the apron. The rock was given 5 different colours in 5 strips parallel to the flume.

After measuring the starting profile, the pump was turned on. The discharge during all runs was kept constant at (7.6m/s $*0.125^2*\pi$) 0.093m^3/s, or 93 l/s.

8.2.2 Development of scour

As expected, the scour hole started to develop directly downstream of the wooden slope. During run #1 (which lasted 150min) the maximum scour depth was 12,5 cm below initial sand level (x=0.50m). Table 8.1, shows that although the scour develops very rapidly in the scour hole at first , the scour depth at x=2,5m catches up in the following runs. In Figure 8.1 the maximum scour depth and the scour depth at x=2.50m are plotted for the different runs. It can be clearly seen that the growth of the scour depth (maximum as well as local) declines in time. This agrees nicely with the scour development in real situations, where an equilibrium scour depth is also found (see also section 7.7.4). In Appendix 6, the development of the scour profile is given in the flow direction.

A scour depth of 20cm was reached during this experiment (approx. 8 times d_{50}). The scour process could be maintained for 4 runs with a total running time of 7 hours (420 minutes). Table 8.1 gives a summary of the different parameters for each run.

Table 8.1 Characteristic parameters from experiment FT01

	RUN #1	RUN #2	RUN #3	RUN #4	UNIT
Start	0	150	240	330	min.
End	150	240	330	420	min.
Duration	150	90	90	90	min.
Water level	+0.20	+0.18	+0.17	+0.14	m
Discharge	0.091	0.094	0.092	0.093	m^3/s
Average velocity	0.54	0.65	0.58	0.60	m/s
Max scour depth	0.125	0.175	0.200	0.210	m
Scour at x=2.5m	0.050	0.100	0.165	0.190	m

Figure 8.1 Development of scour depth FT01

In Figure 8.1, the open dots represent the maximum observed scour depth in the flume at a given moment. These points do not necessarily lie at the same co-ordinates. It can be seen that the maximum scour depth after the first run was 12.5cm and after the last run, it was 21.0cm.

The black dots also represent the maximum scour depth, but now at x=2.50m. This is in the middle of the measuring area. Here scour depth also converges to a maximum.

8.2.3 Behaviour of apron

In this chapter a description of the observed apron behaviour is given. Before every run and after the last run, the bed profile was measured. This leads to 5 matrices with data, which are given in Appendix 5a. To record where sand and where rock were found during the measurements, the sounding on rock are printed in bold numbers (and the sounding on sand in normal typing).

It can clearly be seen that the apron follows the bed profile as it is supposed to do. At the edge of the settled apron the stones are more exposed to the flow. Here it was obvious that extra erosion had taken place, in addition to the general lowering of the sand bed, the imposed scour. It appears that the flow around the individual stones caused turbulence around them, like that around a bridge pier. Because of this, the stones were sinking into the sand. The rock at the edge of the slope is therefore constantly ahead of the sand bed position. This mechanism causes a complete covering and therefore there is no unprotected sand slope at any moment. This is shown in Figure 8.2, which is the top view of the edge of the settled apron with one individual stone on the sand bed just in front of this edge.

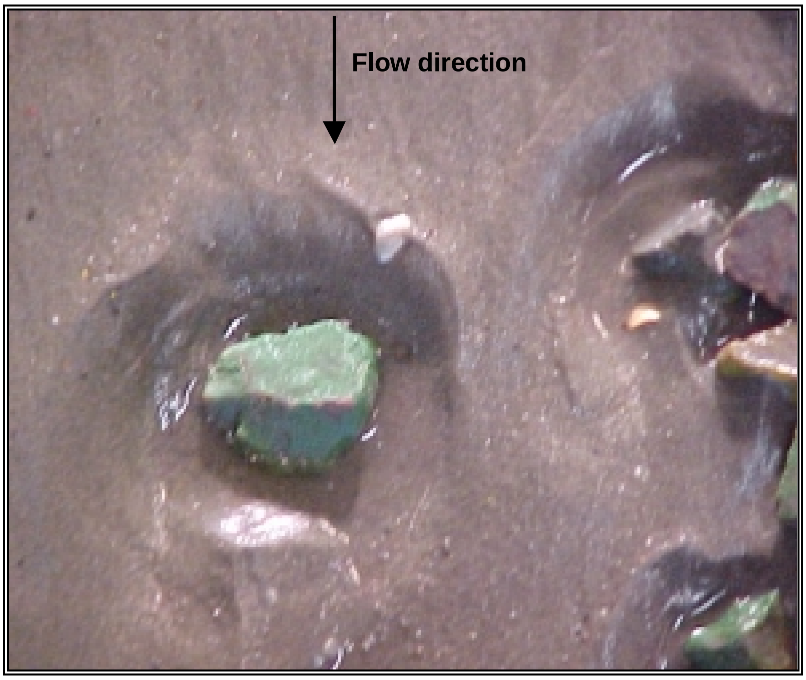

Figure 8.2 Erosion around an individual stone and along the apron edge (on the right).

The rock-layer on the establishing slope remained limited to a very thin layer. Only a single layer of rock ended up on the slope. The edge of the apron retreated only 0.10m, which implies that a very small amount of apron stone is really used. The larger part was unaffected. This can also be seen in the cross-sectional profiles. A difference in angle can be observed between the slope were the rock lies directly on the sand and the slope of the toe of the waiting apron.

In Appendix 7a the cross-sectional profiles are given for the different runs at x=2.50m. This shows the development of the side slope. In Figure 8.5 a simplified version with only the beginning and final situation is given. With a linear fit, based on the original measuring data, the angle is determined. This came to 27° (1V:2H) for this experiment after run number 4 (after run 3 the angle is also 27°). This result seems reasonable, considering the angle of repose of sand under water (approximately 1V:2H). The profile shows a steeper part between y=50.0cm and y=60.0cm. This is the part of the slope were the stones were piled on top of each other. Here the friction between the individual stones determines the angle, which in this case was approx. 1.2V:1H. In Figure 8.4 lines are drawn to accentuate this difference in angle.

Although not the area of interest, the setting of the apron at the upstream termination is also even. The fact that the flow attacks the rounded termination front, instead of flowing along it, does not seem to influence the setting process. This seems to agree with the use of a falling apron at locations where the water does not always flow parallel to the apron.

Figure 8.3 Settled apron at t=420min

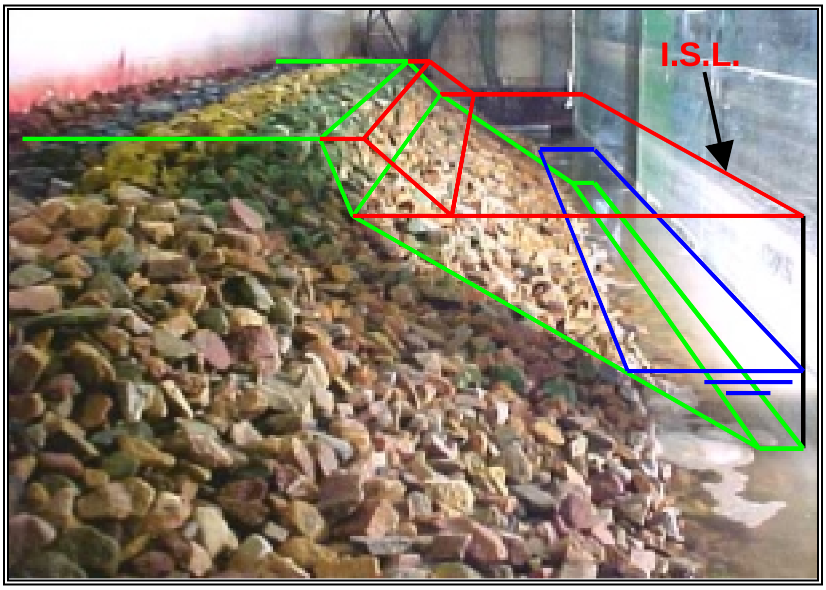

Figure 8.4 Settled apron at t=420min with lines to accentuate the difference in slope angle (initial sand level in red)

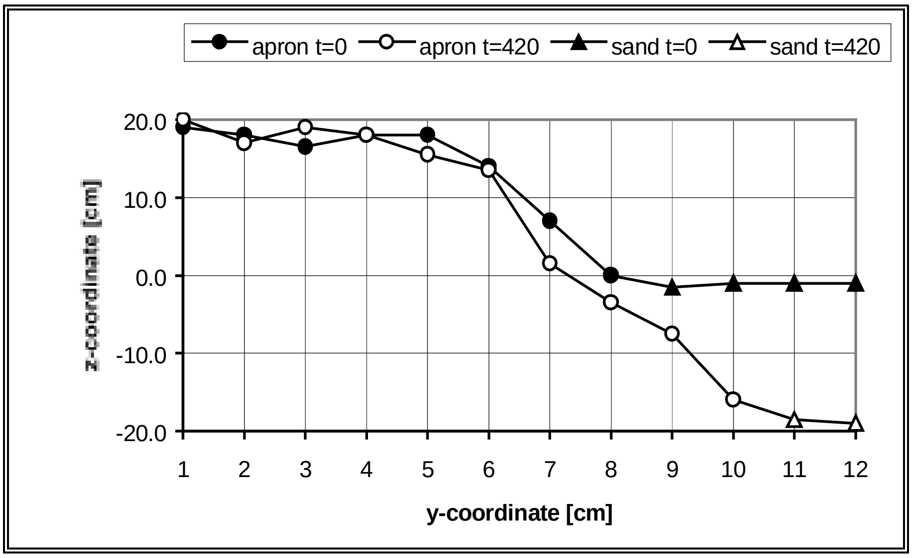

Figure 8.5 Profile of apron and sand before and after setting (FT01, x=2.50m)

8.3 Experiment FT02 (rock: 15/30 mm, thickness: 0.12m)

8.3.1 Set-up

During experiment FT01, only a small amount of rock was actually *launched*. It was therefore decided that during the following experiments the width of the apron section would be limited to 0.50m (4 compartments of the filling rack, instead of 5).

In experiment FT02, the same rock grading was used: 15/30 mm. However, the thickness of the apron (0.12 m) and the width (0.50m, as described above) were adjusted. Applying a less thick apron was expected to have two effects:

1. The underlying sand would pass more easily through the rock-layer, leading to subsidence of the waiting apron.
2. The apron, when called upon, would retreat more rapidly because of the smaller volume of rock per unit of length.

re 1. The thickness applied was 0.12m, or 10 times d_{50}. This is still considered thick enough to retain the sand. Applying an open apron would lead to subsiding, which is undesirable, considering the scope of these experiments.

re 2. When the waiting part of the apron retreats more rapidly, the horizontal displacements will be larger. This should be visible in the results of this experiment.

In this experiment also, the stones were coloured, in 4 different strips parallel to the flume. After measuring the apron section before the first run, the actual average height was 12.50cm (10*d_{50}).

8.3.2 Development of scour

The scour hole started to develop directly downstream of the wooden slope. During the first run (which lasted 120 min) the maximum scour depth was

14.5cm below initial sand level. It can be seen in Table 8.2 that although the scour develops very rapidly at first in the scour hole at the start of the experiment, the scour depth at x=2,50m catches up in the following runs. In Appendix 7b, the development of the scour profile in the flow direction is given.

A scour depth of 25 cm was reached during this experiment (approx. 10 times d_{50}). The scour process could be kept in operation for 5 runs with a total running time of 8 hours (480 minutes). Table 8.2 gives a summary of the different parameters for each run.

	RUN 1	RUN 2	RUN 3	RUN 4	RUN 5	UNIT
Start	0	120	210	300	390	min.
End	120	210	300	390	480	min.
Duration	120	90	90	90	90	min.
Water level	+0.19	+0.18	+0.17	+0.15	+0.13	m
Discharge	0.091	0.091	0.092	0.091	0.091	m^3/s
Average velocity	0.61	0.62	0.54	0.55	0.56	m/s
Max scour depth	0.145	0.145	0.205	0.245	0.250	m
Scour at x=2.5m	0.035	0.095	0.160	0.165	0.200	m

Table 8.2 Characteristic parameters from experiment FT02

In Figure 8.6 the scour development is presented. It can be seen that the maximum scour depth did not increase during the second run. The deep scour pit at the start (14.5 cm below initial sand level) only widens. In this figure the decrease of the scour growth is also visible in the following runs.

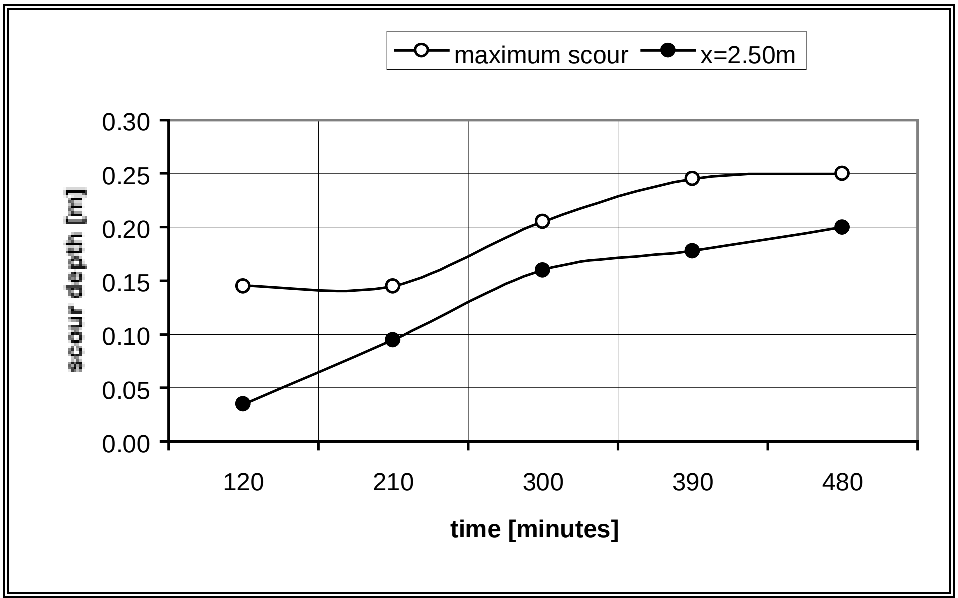

Figure 8.6 Development of scour depth FT02

8.3.3 Behaviour of apron

In this section the description of the observed behaviour is given. Before and after every run, the bed profile was measured. For experiment FT02, this led to 6 matrices with data, which are given in Appendix 5b. The sounding on rock is printed in bold numbers. Photographs were also made before and after every run. In Figure 8.8 and Figure 8.9 these photo series are presented.

Just as in the first experiment, the rock-layer on the developing slope remained limited to a very thin layer. Only a single layer of rock ends up on the slope. The edge of the apron now retreated 0.15m, 1.5 times the distance seen in experiment FT01. This was expected because in this experiment the apron placed was thinner. Even so, very little of apron stone was really used. The greater part remained unaffected. This can also be seen in the cross-sectional profiles.

In Appendix 7b, the cross-sectional profiles are given for the different runs. This shows the development of the side slope. Figure 8.7 gives a simplified version with only the beginning and final situations. Here the retreating apron toe (at initial sand level (z=0)) can be seen and the slope developed after 480 minutes.

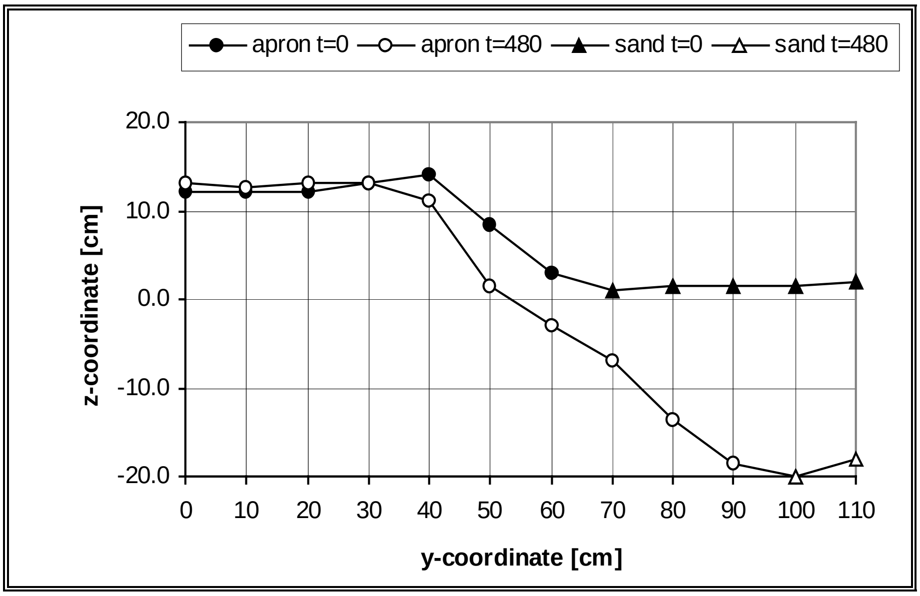

Figure 8.7 Profile of apron before and after setting (FT02)

The slope at x=2.50m is 27º after run 5, which corresponds with 1V: 2.0H (after run 4 the angle is also 1V:2.0H). Again a difference in angle can be observed between the slope where the rock lies directly on the sand and the slope of the toe of the waiting apron. Just as in experiment FT01, the apron toe, where the stones are piled on top of each other, shows a steeper part (approx. 1:1).

Figure 8.8 Top view of setting FT02 (x=2.50m)

Figure 8.9 Side view of setting FT02

8.4 Experiment FT03 (rock: 30/60 mm, thickness: 0.12m)

8.4.1 Set-up

In this experiment a different rock size was used: 30/60mm. Again only 4 of the 5 compartments of the filling rack were used, leading to an apron width of approx. 0.55m at initial sand level.

The thickness of the apron chosen was equal to that of the previous experiment, again 0.12 m. However, this is only 3 times d_{50} for this rock size. The apron section was measured before the first run and the average height was 11.7cm. (The rock is coloured in 4 strips.)

8.4.2 Development of scour

During the first run of this experiment, the sand bed did not subside at x=2.50m. It was therefore decided to continue for 3 hours (180 minutes). After this extended run, the first setting of the apron could be recognised. The apron rock was already retreating noticeably.

This retreating led to a widening of the flow cross-section. Therefore the flow velocity decreased more quickly than in the other experiments and only 3 runs were possible. Nevertheless, The scour process here showed an even development, with the different profiles parallel to each other.

The sand bed stayed relatively horizontal, except in the first run. Here two flow branches could be distinguished. One along the apron section and one along the glass wall. These disappeared after run 2.

The different parameters during the three runs are presented in Table 8.3.

Table 8.3 Characteristic parameters from experiment FT03

	RUN #1	RUN #2	RUN #3	UNIT
Start	0	180	270	min.
End	180	270	360	min.
Duration	180	90	90	min.
water level	+0.20	+0.15	+0.12	m
Discharge	0.093	0.091	0.093	m^3/s
average velocity	0.56	0.61	0.60	m/s
max scour depth	0.165	0.185	0.200	m
scour at x=2.5m	0.055	0.100	0.125	m

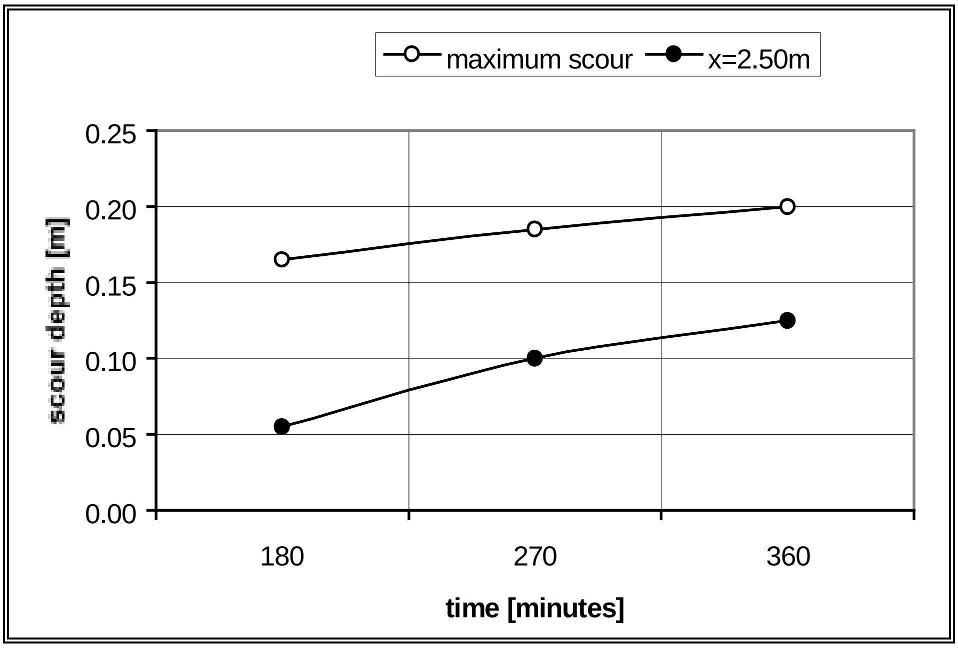

Figure 8.10 Development of scour depth FT03

8.4.3 Behaviour of apron

Because of the larger size of the rock, a larger volume per area is needed to cover slope. It can be clearly seen in Appendix 7c that the waiting part of the apron retreated more quickly than it did in the other experiments. The profiles after the different runs lie parallel with a distance of approximately 5cm (approx. the characteristic diameter, d_{50}).

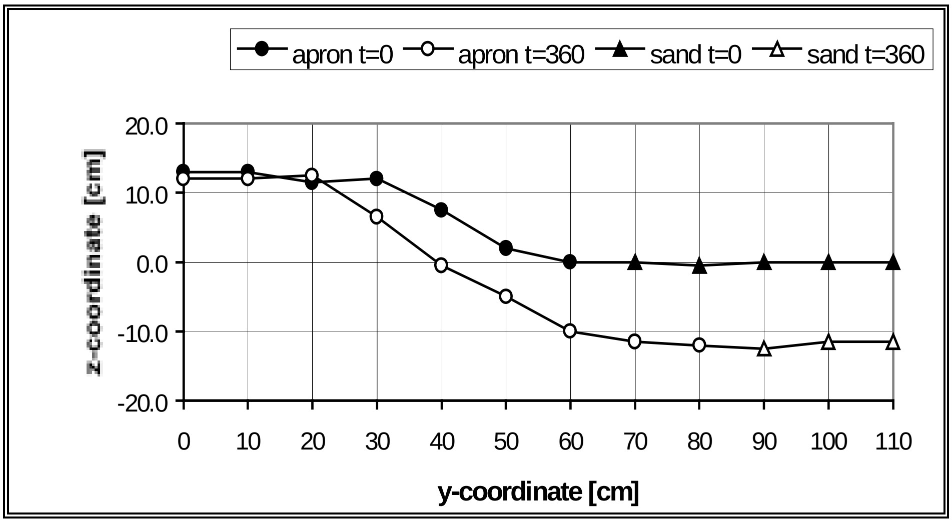

Figure 8.11 Profile of apron before and after setting (FT03)

The slope at x=2.50m was determined at 26º after run 3, which corresponds with 1V: 2.1H (after run 2 the angle is also 1V:2.1H). Again a (small) difference in angle was observed between the slope where the rock lies directly on the sand

and the slope of the toe of the waiting apron. The slope angles measured were 27° and 33° respectively, which is too small a difference to be observed.

8.5 Experiment FT04 (rock: 8/16 mm, thickness: 0.12m)

8.5.1 Set-up

In this final experiment, the smallest rock grading was used: 8/16 mm. Again the thickness of the apron layer chosen was 12.0 cm. This corresponds with approximately 12 times d_{50}. Considering the size of the small stones, it was decided not to colour it for this experiment. The apron section was measured before the first run and the average height was 13.6cm.

8.5.2 Development of scour

The scour hole started to develop directly behind the wooden slope. During the first run (which lasted 90 min) the maximum scour depth was 13.5cm below initial sand level. It can be seen in Table 8.4, that although at the start of the experiment the scour develops very rapidly in the scour hole, the scour depth at x=2,5m catches up in the following runs. In Appendix 6d, the development of the scour profile is given in the flow direction.
A scour depth of 19 cm was reached during this experiment (approx. 19 times d_{50}). The scour process could be kept in operation for 4 runs with a total running time of 6½ hours (390 minutes). Table 8.4 gives a summary of the different parameters for every run.

Table 8.4 Characteristic parameters from experiment FT04

	RUN #1	RUN #2	RUN #3	RUN #4	UNIT
start	0	90	180	270	min.
end	90	180	270	390	min.
duration	90	90	90	90	min.
water level	+0.19	+0.16	+0.14	+0.12	m
discharge	0.095	0.095	0.094	0.094	m^3/s
average velocity	0.64	0.64	0.61	0.57	m/s
max scour depth	0.135	0.165	0.175	0.190	m
scour at x=2.5m	0.035	0.085	0.160	0.160	m

In Figure 8.12 the scour development is presented. It can be seen that the maximum scour depth developed as in earlier experiments. The scour growth at x=2.50m however, was almost linear during the first 3 runs. After run #4, a decrease in the rate of scour growth was visible. When the scour depth ceased to increase the experiment was stopped.

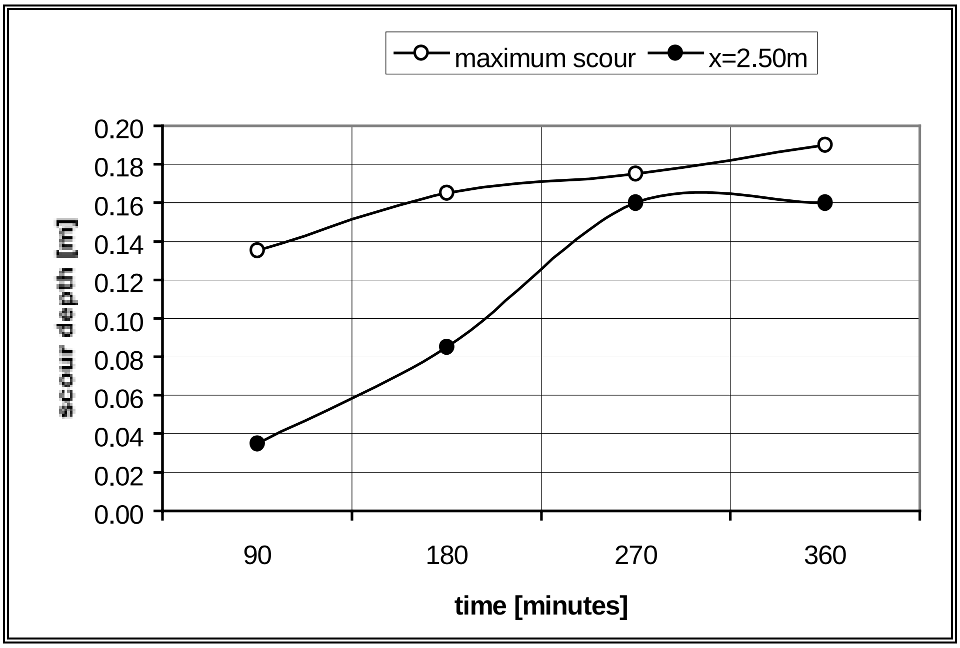

Figure 8.12 Development of scour depth FT04

8.5.3 Behaviour of apron

After the first run, the toe of the waiting part of the apron (at x=2.50m) had moved 5.0cm in the positive y-direction. This can be explained by the steepness of the slope directly after placing the rock onto the sand bed. Owing to exposure to the current, the rock shifted and took on a less steep configuration. After this first run, the apron retreated as it did in the other experiments.
Compared with the other experiments, only a small volume was needed to cover the slope. Of course this is because of the smaller rock size. It can be seen from the profiles, that there is hardly any retreat of the apron slope. The slopes for the different runs lie parallel with a distance of only 2cm, or 2 times d_{50}.

The slope measured after run 4 (t=390 minutes) is exceptional, as it is very straight. This can be explained by the fact that for smaller rock the deviations in measured level will also be smaller. This is described in section 8.6.

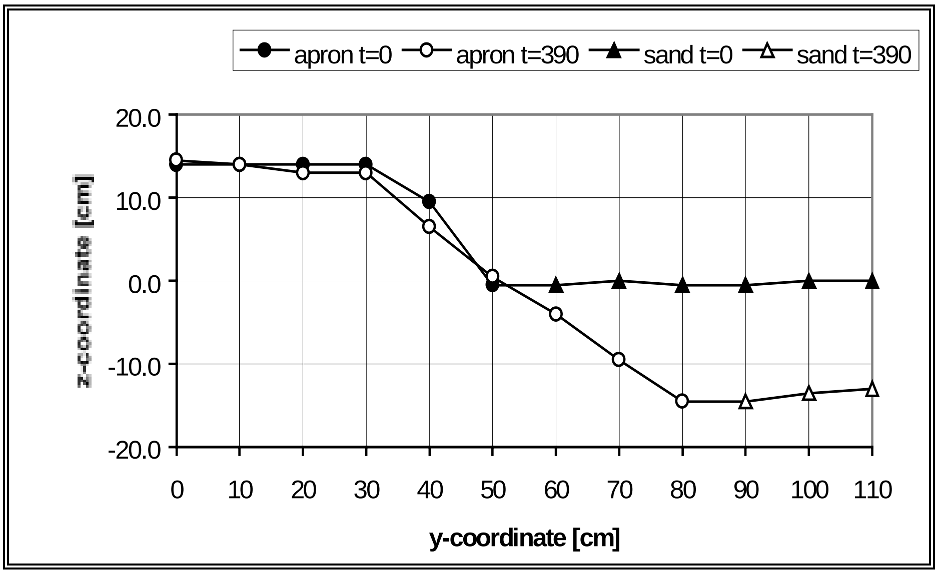

Figure 8.13 Profile of apron before and after setting FT04

From z=0 to sand bed (at z=-14,5) the angle is again 27º, which corresponds with 1V:2H. Above z=0, the slope is 32º (1V:1.6H). After run 4, glass plates were carefully inserted into the settled apron, perpendicular to the flow direction (in the z-y-plane) at x=2.50m in order to visualise and measure the apron thickness. A picture of this cross-section is given in Figure 8.14.

Figure 8.14 Cross-section of apron after run #4 (FT04)

8.6 Influence of measuring errors

During the execution of measurements, errors are introduced; these can result in deviations in the values of the parameters. For every parameter the measuring error is described. Three different types of errors are distinguished in this chapter:

1. Reading error,
2. Deviation in measuring device,
3. Accuracy of number of measuring points.

8.6.1 Reading error

A reading error is interpreted here as the difference between the actual value and the measured value. The recorded value can sometimes deviate from the true value and therefore lead to a deviation of the actual values of the parameter.

Profile measurements
To avoid apparent accuracy, the soundings are rounded off to half centimetres. This means that the soundings can deviate to a maximum of 2 mm, compared to readings in millimetres. However, soundings in millimetres would not contribute to a better, more precise, picture of the apron slope. This is because the dimensions of the flume were such, that taking a precise reading in millimetres was not feasible.

The deviation in the profile measurements occurs because of this built-in relaxation and is not a reading error, but it depends on the number of measuring points. The deviation is calculated in §8.6.3.

Discharge measurements
The velocity gauge (Altometer) in the pipe was used to determine the discharge. It gives the output on a digital (LCD-) display. Because of fluctuations of the velocity in the pipe and the number of digits (up to 1/1000th), the value could not be read clearly. Therefore, an extra analogue display was installed, which was not as sensitive to fluctuations. The reading error of this meter is estimated at 0.1 m/s, because of the scale on the face of the analogue meter.

Water level measurements
The water level during the experiments was adjusted to a ruler, which was drawn on the glass. This level was rounded off to centimetres. Because of small fluctuations in the water level, the maximum reading error was estimated at 0.5cm.

Velocity measurements
The propeller current meter gives pulses, which are recorded by a counting device. This device gives its output in integers and therefore, the deviation is not a matter of reading error.

8.6.2 Deviation of measuring device

A deviation of a measuring device is interpreted here as the deviation that must be ascribed to the device. It is therefore a limitation that cannot be overcome by increasing the number of measurements.

Measuring rod
To measure at the correct location the measuring rod should be exactly vertical. Because this cannot be guaranteed over the considerable height (order of 1m) a deviation is introduced. Assuming an angle of 1 degree out of the vertical position, introduces a deviation of 1.7cm.

Propeller
The calibration of the propeller was executed under the assumption that the pitch (calibrated by the manufacturer) had not changed. In a flume in which the current velocity was adjustable, two different propellers were calibrated. This led to the following two calibration formulae:
For the propeller with a pitch of 100mm:

$$u = \frac{n \cdot 100.103}{t} + 0.012 \qquad \text{[mm/s]}$$

For the propeller with a pitch of 50mm:

$$u = \frac{n \cdot 50.31}{t} + 0.080 \qquad \text{[mm/s]}$$

In which n is the number of revolutions in time interval t [s]. The propeller with a pitch of 50mm is best used in current velocities of 0.3 to 0.6 m/s. The propeller with a pitch of 100 mm is best used in velocities of 0.6 to 1.2 m/s. The calibration curves are given in appendices 9a and 9b.

8.6.3 Deviation in measured planes

The direct aim of the experiments was to visualise and measure the development of the side slope. Therefore it was not possible to choose random points (done when measuring a horizontal level) to determine the level. It was necessary to measure the profile in lines perpendicular to the flume (x-direction). The average deviation was calculated for a distance of 5cm (22 points in the y-direction) and for the used 10cm distance (11 points in the y-direction).

For a particular profile, the points are split into 2 groups: the points on a horizontal line (the waiting part of the apron) and the points on the slope (the settled part of the apron). For the horizontal part, the average value is automatically the average level, see Figure 8.15a. The individual deviations from this average level were determined, which led to the average deviation.

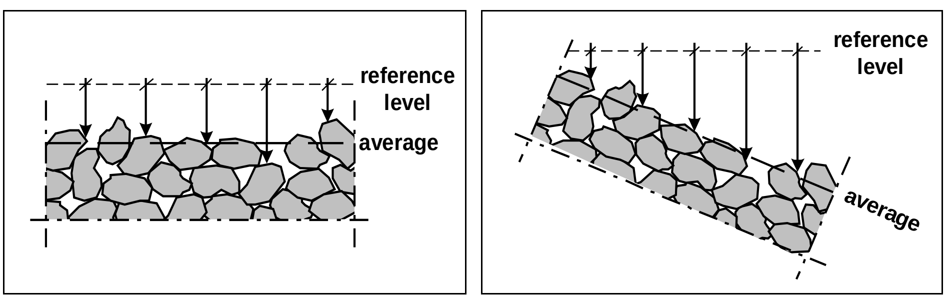

Figure 8.15 a&b Measuring of average rock level

For the points on the slope the average deviation was calculated by determining the deviation between an individual point and a trend line through the points, see Figure 8.15b. This calculation is worked out in Appendix 10. To check the number of points used in the x-z-plane (11 points), one profile was measured at 22 points. The differences in average deviation and in slope angle were determined and given in Table 8.5. The average deviation for twice as many points is almost the same, which justifies the chosen distance of 10cm.

The chosen distance between the profiles in the y-direction was 0.50m. This led to 9 profiles over the length of the flume per run. This was considered enough to visualise the scour development in the x-direction. By measuring different profiles the irregularities over the length of the flume could be recorded.

Table 8.5 Deviations in measured planes

	Δ HORIZONTAL PART		Δ SLOPE	
FT01	12.1 mm	1/2 d_{50}	8.8 mm	1/3 d_{50}
FT02 (5cm interval)	7.6 mm	1/3 d_{50}	5.5 mm	1/5 d_{50}
FT02 (10cm interval)	11.4 mm	1/2 d_{50}	4.0 mm	1/6 d_{50}
FT03	18.5 mm	1/2 d_{50}	8.5 mm	1/5 d_{50}
FT04	3.0 mm	1/3 d_{50}	1.8 mm	1/5 d_{50}

In Table 8.5 it can be seen that the average deviation is smaller for the slopes than for the horizontal parts. This can be explained by the thinner layer on the slope. Surprisingly, the deviation on the slope is smaller with a measuring distance of 10cm. However, the difference is small and it is stressed here that this was just one random check and not too much significance should be attached.

8.7 Model observations

The observations in this section reflect only to the behaviour in the model and cannot be directly translated to prototype situations. This translation is made in Chapter 9. A summary of the different results is given in Table 8.6.

Table 8.6 Summary of experiment results

	FT01	FT02	FT03	FT04	UNIT
rock size	15/30	15/30	30/60	8/16	[mm]
apron height	18.5	12.5	11.7	13.6	[cm]
$\Delta_{avg,height}$	1/2 d_{50}	½ d_{50}	1/2 d_{50}	1/3 d_{50}	[-]
Slope	26.6	26.6	25.6	27.0	[°]
V:H	1:2.0	1:2.0	1:2.1	1:2.0	[-]
$\Delta_{avg,\ slope}$	1/3 d_{50}	1/6 d_{50}	1/5 d_{50}	1/5 d_{50}	[-]

The following observations are given here on basis of the observed and described behaviour of the apron in the model.

- The slope in the model came to 1:2 after setting.
- The setting of the falling apron was a continuous and even process.
- The flow conditions, which are not a macro instability process, dictate the setting process.
- The slope angle was not dependent on the size of stone
- Uneven scour along a guide bund (as with attack under an angle) did not seem to jeopardise the working of the apron.
- Because of turbulent current around the individual stones, the stones ‘sink’ into the sand and against the surrounding stones. The layer, however thin, is therefore closely packed.
- The flow around the individual stones causes erosion around them and therefore the stones sink into the sand. Because of this mechanism, there is no unprotected sand slope at any moment.
- Applying a thicker apron does not lead to a thicker protection on the establishing slope.

9 Relation between model and prototype

9.1 Introduction

The general idea behind the model test was to visualise the behaviour of a falling apron. In Chapter 8, the observations in the model were given. The results of the model have to be translated to a full-scale application in order to make the study useful for future design tasks. In this chapter, this translation is made.

Firstly, the model is described in terms of scaling rules and effects. The different scales used in the model are fitted to the prototype, making a comparison possible. Here also the observations on the prototype are described.

Secondly, various influences that were neglected in the model are described. These side-effects, not considered of primary importance in the model, are assumed to have some influence on the prototype behaviour. These are called secondary influences and briefly mentioned in § 9.5.

9.2 Parameters of prototype

The term prototype is used in this report to distinguish the full-scale apron application from the model. However, the model parameters, are not scaled exactly according to the scaling rules. The primary aim of the experiments was to visualise the behaviour in a more general context, but in order to make a comparison a prototype has to be chosen.

Because of the available data, the Jamuna Bridge River Training Works were the most obvious example to use for this comparison. The relevant structure parameters are listed below. The scour and setting results are described in §9.4.

Table 9.1 Falling apron parameters of JB-RTW

PARAMETER	VALUE	UNIT
Water level		
LWL	6.2	[m +PWD]
HWL	13.0	[m +PWD]
Construction depth	-15.0	[m +PWD]
Apron width	12	[m]
Apron height[1]	2.0-4.0	[m]
Diameter	0.30	[m]
Flow velocity[2]	3.0	[m/s]

[1]The falling apron is constructed in the shape of a wedge and therefore the height increases from 2.0m at the revetment side to approximately 4.0m at the riverside.
[2]This is the maximum flow velocity expected (by the designers) and not a measured value.

Unlike those of the model, the water levels at the location of the Jamuna Bridge are not exactly known. In a natural river the discharge, velocity and water levels fluctuate during the year. These parameters where described in §2.2. No measurements of flow velocities along the guide bunds are available. Here the minimum and maximum values are presented, to give an order of magnitude.
The rock grading used for the falling apron at the JB-RTW was 0-100kg (see §4.3.3). Here a characteristic diameter of 0.30m is adopted, which neglects the

fact that a wide grading had been used with a very fine fraction. This grading aspect is treated separately in §10.2.

9.3 Scaling effects

Scaling effects are the unwanted side effects produced in a model by variables that are not scaled in accordance with similitude requirements. In Chapter 6 the scaling rules are described. Geometric, kinematic (time and velocity), and dynamic (force) similarity should be maintained between model and prototype. Practical considerations make this difficult to achieve. Explicit satisfaction of two, dynamic-similitude criteria associated with a flow would require the model fluid to be different from the full-scale liquid. The satisfaction of two, dynamic-similitude criteria associated with particle transport would require the use of a model particle with a density different from that of the full-scale particle.

Because of the context of this project, it was not considered necessary to make a precise translation from the prototype to the model. However, the fulfilling of the Froude and Reynolds numbers are worked out here.

Froude number
The Froude number gives the relation between gravity and the stationary inertia force. For a correct representation of the flow field, the value should be the same for model and prototype. Because the flow field in the model is mainly determined by model boundaries and the hydraulic roughness, the Froude number representation was not of primary importance. However, the value of the Froude number in the model flow, has to be smaller than the critical value of Fr=1 for stationary flow.

$$Fr = \frac{U}{\sqrt{gh}} \qquad \textit{Equation 9.1}$$

For the model the flow velocity chosen was such that the sand transport was substantial. When the results of the model tests have to be translated to full-scale applications, the value of the Froude number should theoretically be the same. Because the gravitational acceleration is equal, it depends only on the depth and the flow velocity (assuming similar density, shape and surface roughness).

For example, the Froude number for two experiments is calculated (FT03 and FT04).

$$Fr_{FT03} = \frac{U^2}{g \cdot h} = \frac{0.56^2}{9.81 \cdot 0.20} = 0.16$$

$$Fr_{FT04} = \frac{U^2}{g \cdot h} = \frac{0.64^2}{9.81 \cdot 0.19} = 0.22$$

If the model results were to be translated to prototype values, the depth would be in the order of 20m. This would mean a velocity of 5.6 m/s for FT03 (and a d_{50} of 4.5m). For FT04 it would mean a velocity of 6.6 m/s and a d_{50} of 1.0 m. Of course other depths and velocities are also possible as long as the relation U^2/h is kept constant.

Reynolds number
In the case of a falling apron, with large stones and high flow velocities, the flow around the rock will certainly be turbulent. When small stones are used in the model and therefore the flow velocities have to be smaller, the flow should still be turbulent. The Reynolds number gives the relation between gravity forces and viscosity. For values of Re>1200, the flow is considered turbulent and the influence of the viscosity becomes negligible.

$$Re = \frac{uD}{\nu}$$

With a flow velocity of 0.5 m/s, for coarse sand the flow already becomes turbulent.

Prototype flow is, almost without exemption, turbulent. If, the model flow is also turbulent, the model will be suitable for the study of flow conditions. This condition was assured in the model.

Main scale factors
The length scale and the Froude condition determine the main scale factors for the reproduction of the flow field. The length scale and the condition that the mean flow velocity is about twice the critical flow velocity for the sediment determine the main scale factors for a reproduction of the local scour holes in the model. To compare flow velocities with the Froude condition, measurements were conducted.

Table 9.2 Main scale factors

PARAMETER	PROTOTYPE	MODEL	UNIT	SCALE FACTOR
Diameter	0.30	0.010	[m]	30
	0.30	0.025	[m]	12
	0.30	0.045	[m]	6.7
Depth	28.0	0.2	[m]	140
Flow velocity	3.0	0.5	[m/s]	6
Bed material	210	170	[μm]	1.25

9.4 Survey information Jamuna Bridge

The contract for the Jamuna Bridge River Training Works (JB-RTW) included a maintenance contract with the obligation to supply satellite photographs and to conduct bathymetric surveys after every monsoon discharge. The satellite images are described in a qualitative way and the survey profiles are described in a more quantitative way.

9.4.1 Satellite images

As an illustrative example of the changing character of the Jamuna River, three satellite images are presented dated 10-4-‘98, 3-28-‘99 and 2-19-‘00. Because of the different seasons, the water levels differ and are respectively (m+PWD) 11.5m, 6.5m and 6.0m. In this relatively short period of 16 months, differences can already be observed in the course of the river at the location of the bridge.

The most obvious development is the formation of a char between the two guide bunds. On the satellite image of November 4th 1998 only a small char upstream of the bridge can be observed. On the next image (March 28th 1999) this char has grown significantly and moved further downstream, leaving two channels, each lying along one of the guide bunds. It can be seen that the east guide bund (EGB) lies parallel to the flow channel, which attacks straight from the north. A year later (February 19th 2000) this flow channel is coming upstream from a northwest direction, making a turn towards the south just upstream the EGB.

At the west guide bund (WGB) in 1998, no real attacking flow channel can be distinguished. Because of the developing char, in March 1999 such a flow channel is present, which impinges at the north-western corner of the guide bund. This channel makes a bend in front of the guide bund at the north-western corner and follows the guide bund over the remaining length. A year later, February 2000, this bend has shifted downstream, attacking at the location of the bridge.

9.4.2 Survey results

When the apron is attacked, the rock at the edge will launch onto the slope. This was observed at the JB-RTW. The idea was to measure the area of rock in the cross-section and to subtract it from the area of rock, which was present after the completion of the works. In this way the volume of rock, which is launched per metre of bund length can be determined. When an even distribution over the developed slope is assumed, the thickness of the layer is known. In comparing the latest surveys with the completion survey, it should be kept in mind that some inaccuracies are introduced, because:

- Some cross-sections of the completion survey recorded some sand/ silt sediment cover that had already accrued on top of the rock protection,
- The accuracy of the maintenance surveys (no RTK-DGPS[9]) is less than the accuracy of the completion survey,
- Subsoil settlement may have occurred,
- It cannot be guaranteed that no transport of apron material has taken place.

Summarising, it is difficult to draw firm conclusions from small differences in levels; therefore it is not considered useful to make volume balances to determine the layer thickness on the scour-hole slope. However, a more general description of the scour development is given. Here the scour depth and the slope angle are presented. It can be seen that the slope approximates, just as in the model, to 1V:2H.

The deepest scour hole along the east guide bund was observed in 2000, three years after the completion of the river training works. This was at cross-line 2300 (see Appendix 11 and the summary in Table 9.3).

After the monsoon of 2001 however, there was again 10m sand cover at critical EGB sections. This illustrates that the 2000 scour was an incidental occurrence, which is important to keep in mind in considering sand-tightness, lifetime and maintenance requirements for a falling apron.

[9] RTK-DGPS: Real Time Kinematic-Differential Global Positioning System. As ‘normal’ GPS, but enhanced with a fixed shore station that continuously sends out the error, which is enclosed in the satellite messages. An accuracy of cm’s instead of meters is reached.

Table 9.3 Scour characteristics from survey data October 2000

CROSSLINE	MAX.DEPTH	RELATIVE TO APRON LEVEL	SLOPE
2150	PWD -17m	-2m	1V:2H
2200	PWD -17m	-2m	1V:2.3H
2250	PWD -18m	-3m	1V:1.3H
2300	PWD -19m	-4m	1V:2H
2350	PWD -18m	-3m	1V:1.9H
2400	PWD -15m	0m	-

9.5 Considerations on secondary influences

In this section, secondary influences on the setting behaviour of a falling apron are briefly mentioned. They were not included in the model but are considered to play a role in prototype situations. Four different influences are distinguished here:

- Secondary flow
- Bank slope
- Multiple river branches
- Curved areas

These are aspects that should be taken into account in the design of a falling apron. Because no data is available on these influences, a more general description is given.

Influence of secondary flow on slope steepness
In a river bend, the water mass will tend to spin outwards because of momentum (centrifugal force). This leads to an inclination of the water surface and an increase of the water depth at the outer bend. Because of the establishing gradient, water at the surface will start to flow towards the inner bend. The introduced secondary flow generates an upward directed flow at the outer bend. See Figure 9.1.

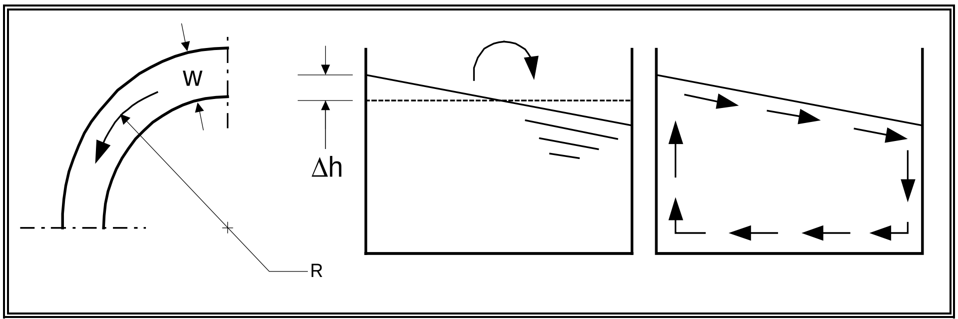

Figure 9.1 Secondary flow in river bend

The secondary flow induces an upward directed current at the outer bank and a downward directed current at the inner bank. These currents influence the angle of repose of the bed material. It is the same mechanism that gives a river its meandering character.

In the model, the angle of the settled apron came to 1:2. This angle was not determined by the rock size, but by bed material and flow conditions. Secondary effects, as described here, did not influence the flow conditions in the model. The small width of the flume causes the flow to be straight and parallel to the apron. In a prototype situation it is possible that a curved flow channel ‘hangs’ on to the bank protection. The slope of the outer bank will then adapt to this ‘new’ angle of repose, which is possibly steeper.

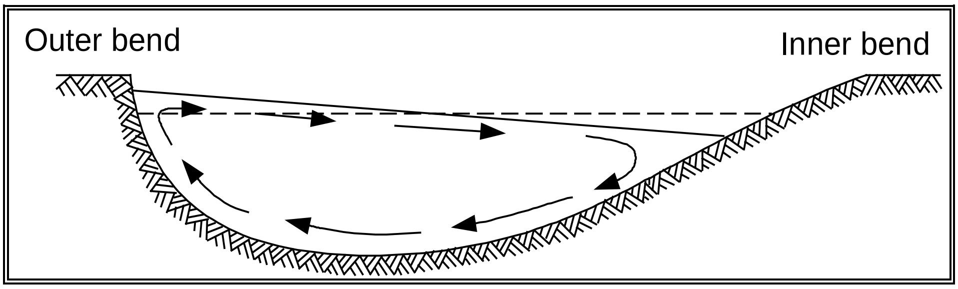

Figure 9.2 Change of bank steepness as result of secondary flow

Influence of multiple river branches
In Chapter 2, a description was given on the various forms of scour. It was concluded that for the purpose of calculating the maximum scour depth, the local scour is dominant. This local scour is determined by flow conditions at a specific location. It will therefore be different from the local scour in the model. The width of the river permits different flow channels to exist in the cross-section.

In the model the scour process stopped because an equilibrium scour depth was reached. This gave an anticipated final situation. Even if there is a real equilibrium depth in the prototype situation, there will always be a certain risk of the occurrence of more heavy flow conditions.

For example, a char could form between the two guide bunds. The river discharge would then be split into two branches each along a guide bund. A higher flow velocity would result.

Influence of bank slope on scour depth
No attempt was made to reproduce the prototype scour and scour depth exactly in the model. However, some characteristics should agree well with the prototype. In Chapter 8 the development of the scour depth in time was described for the different experiments.

From other experiments [NEDECO 1996], it is known that the steepness of the guide bund or riverbank influences the scour depth. In general, without quantifying, it can be stated that the scour depth is larger for a vertical wall. In the experiments for FAP21/22, also, different slopes were examined. The scour depth was minimised by the flattest slope, or in other words, the steeper the deeper.

Curved areas
In the foregoing, the falling apron along a bank protection or guide bund was described. In the model, the 2-dimensional situation of a straight stretch of apron was investigated. It will be clear that in a prototype situation, the guide bund

could be curved, while when a falling apron is positioned at the head of a groyne or along a revetment, the apron will certainly be curved.
Because of this curvature, the length of the edge will increase during setting: this is termed ‘out-fanning’. In Figure 9.3 this out fanning is schematised. The quantity of rock stored in the apron has to be adapted to this different distribution of material.

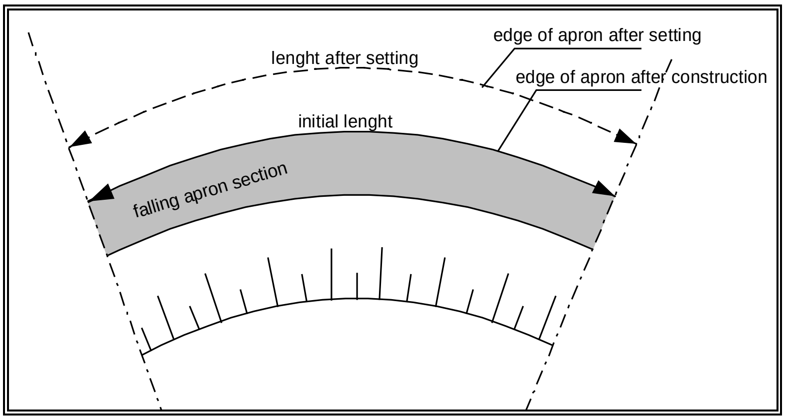

Figure 9.3 Outfanning of apron in bend.

If a curved river branch is adjacent to a straight part of a revetment, the opposite will occur.

10 Description of apron behaviour

In this chapter a general overview of the observed apron behaviour is presented. It summarises the behaviour of a falling apron as observed in this study. The considerations are given in a qualitative way and should apply for both model and prototype. The three aspects that are discussed are:

- Setting result
- Filter function
- Durability

10.1 Apron dynamics

In the model it was found that the rock size did not influence the steepness of the slope. In both the model and the prototype situation, the slope after setting is 1:2 (27º, see also Table 8.6). This angle should be flat enough to prevent macro instability of the slope. Ground mechanical collapse mechanisms were not observed in the model or prototype. It was already mentioned in §9.3 that the size of the model would be too small for these kinds of failure modes to occur.

At the JB-RTW the recorded scour depths (below the falling apron level at PWD –15m) are also not deep enough to expect flow slides in front of the apron. In §3.5 it was indicated that flow slides occurred during construction along slopes steeper than 1:3. For the settled apron with a steepness of 1:2 this could have consequences on the stability. However, at the time the height was still modest.

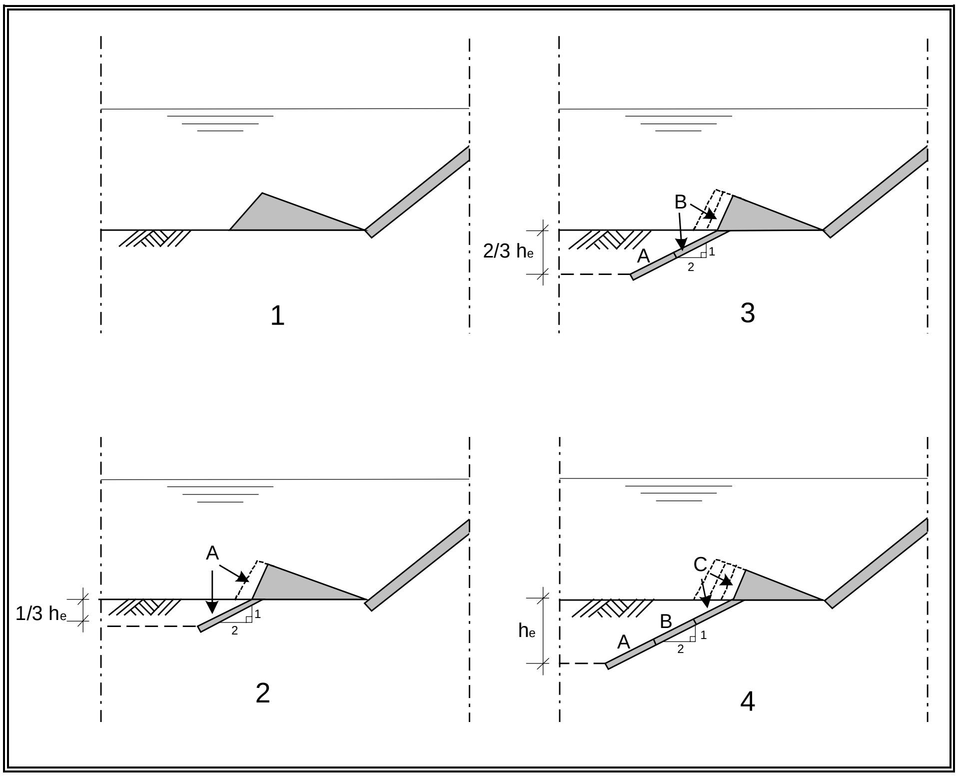

Figure 10.1 Setting process of the apron

In Figure 10.1 the setting process due to scour at four different times is shown. The single layer is located at the edge of the waiting part of the apron. When the bed material is eroded, the rock on the slope *slides* downward and more material from the waiting part is drawn upon. At all times, the top of the slope coincides with the outer edge of the waiting part of the apron.

Theoretically the rock should be stable on a slope of 1:2, both statically and hydraulically. With the, modest, flow velocity in the model even the grading 8/16mm is theoretically stable. This sliding can therefore only be explained by erosion of the sand layer directly under the rock layer. Apparently, the gradient inside the rock layer is high enough to transport the sand. When this transport takes place, the sand grains in the top layer lose contact with surrounding grains and loss of friction will result. The rock layer can slide into this fluidised sand-water mixture layer, thus following the subsiding riverbed.

In Figure 10.2, the expected and the observed setting results are presented (not to scale). For both situations the slope is approximately 1:2. The difference is found in the layer thickness and the location of the slope. In both situations, an equilibrium depth is assumed, which is drawn in the figures. When this depth is reached, the flow velocity is expected to be under the critical value and the transport of bed material stops.

The layer thickness, which was expected to be 5 times d_{50} (A) remains limited to a single layer (B). A consequence of this single layer is that only a small amount of apron material is really used. The greater part of the waiting apron remains unaffected. The consequences of this single layer for the soil retaining function are worked out in §10.2.

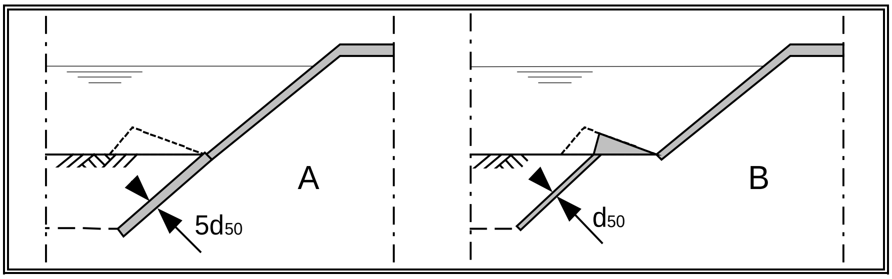

Figure 10.2 The expected (A) and the observed (B) setting result

The developing slope was expected to start from the toe of the constructed slope downwards. In Figure 10.2, these slopes are drawn in line, but of course a flatter or steeper constructed slope is also possible, depending on the design.

As far as the macro-stability is concerned, the observed setting has an advantage. In the observed situation, a horizontal part is still present, this being by means of 'waiting' part of the apron. This can be compared with a berm in a breakwater or dyke. The stability for slip circle failure is influenced positively by this 'berm'.

Two remarks are made here concerning these observations:

- The observed setting behaviour is only an anticipated final situation.
- Although the macro-stability for the slope as a whole (apron and constructed slope) is influenced positively, the slope at the edge of the waiting part is

steep. Here a considerable amount of apron material per m^1 is present. Small instabilities might occur, which would lead to more apron material falling on the slope.

In §9.4 the survey data were described. These results do not seem to contradict the setting observed in the model. Here also the waiting (horizontal) part of the apron can be seen and also at the JB-RTW, the slope angle stays limited to 1:2.

As far as the anticipated final situation is concerned, both in the model and in the prototype, more setting can be expected. This setting could occur because the equilibrium depth is not reached, or because sand material is transported through the single layer. Also a more severe flow condition could occur. When it is assumed that the equilibrium depth is reached, no more transport of the bed material takes place. Two possibilities then remain:

- The transport of bed material stops *and* the transport of sand through the rock layer stops because the gradient is below the critical value. A stable situation is reached (until the flow conditions are again more severe).
- The transport of bed material stops *but* there is still transport of bed material through the rock layer. When this happens, the rock layer will subside and more rock from the waiting part will reach the slope until the transport stops.

In a real situation the probability always exists that the stable situation is loaded by more severe flow conditions. This could result from a higher discharge or because of a more direct attack of the apron by a river branch. However, because of the natural character of the river, the load could also decrease. This should be realised when interpreting the outcome of this study; the apron is an extra protection for the maximum possible flow conditions that may occur from time to time. It is not likely that the apron will be heavily loaded constantly.

10.2 Filter function

The setting behaviour of the apron, which was observed in the model, has a significant influence on the soil retaining function. Two different aspects are mentioned here:

- Single layer on the slope
- Continuous setting process

In the model, only a single layer of rock was found on the developed slope. Slope protection by a single layer does not comply with the normal filter rules, treated in Chapter 5. Here it was stated that for geometrically open filters, the layer thickness should be such that the gradient inside the apron is smaller than the critical value. With only a single layer this condition can not be assured.

As seen in the model and described in the previous section, the developed slope retreats with the edge of the waiting part of the apron. In Figure 10.3 it can be seen that the slopes at different intervals lie parallel. The slopes are linear, which means that the setting is even over the entire slope. The fact that the complete slope retreats implies that sand is transported *through* the apron.

It can therefore be stated that the apron does not fulfil its function to retain the bed material. However, the erosion of sand is slowed down significantly (relative to the erosion of the unprotected bed). Another important feature is that this single layer seems to distribute the erosion evenly over the entire slope. Instead of steep scour hole slopes, the slope stays limited to 1:2.

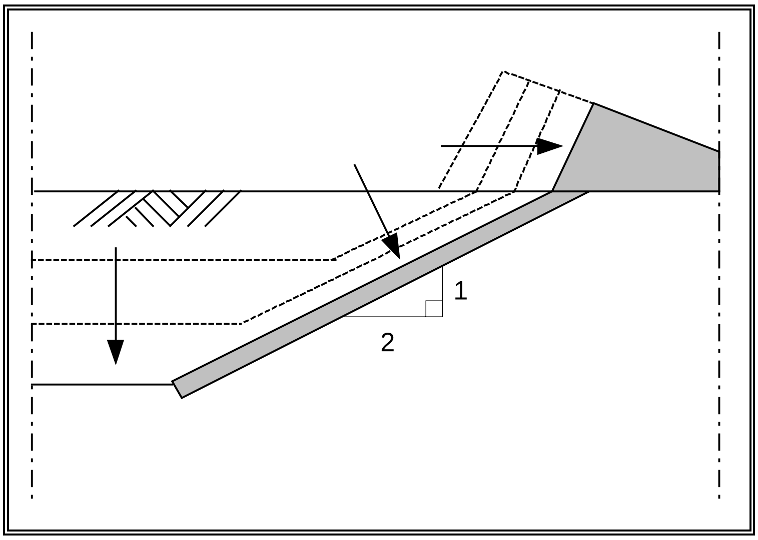

Figure 10.3 Retreat of slope

The setting process, as observed in the model, is expected to have an influence on the final grading of rock on the slope. When a wide grading is used with a very fine fraction, these fines are washed out easily. This washing out is in fact the idea behind the application of wide gradings (see § 4.2.5). However, in the filter design it is expected that a layer of about 5 times d_{50} will cover the scour slope. If then some fine material is washed out from the top layer, a filter structure will develop.

One can imagine that when the individual stones in a cross-section reach the slope one by one, *all* the grains that are small enough could theoretically be transported with the current. Instead of a thick layer with larger rock in the upper layer and more fines underneath, only the rock that is stable in the current will remain on the slope. In addition to this, it has been observed that apron material is only launched onto the slope when the current is eroding the toe (scour) or when sand is transported through the covering layer. Both mechanisms are only present during the higher flow velocities and thus the fines are likely to be transported.

10.3 Durability

It was observed in the model and seen on the survey results from the Jamuna Bridge that the apron settles nicely and uniformly over the slope. This is one of the outstanding features of the falling apron protection. The setting will take place at the most protruding part along the guide bund and therefore the face wall of the apron will always be flat. Thorough site investigations should be made to ensure that there are no clay layers, which will disturb this even setting process.

When the equilibrium scour depth is reached, a single layer of granular material will cover the slope. This will not sufficiently retain the soil. But when still sufficient apron material is stored in the waiting part, this will not endanger the protective function. When sand is transported from under the slope cover, the rock will subside. The above lying material will then shift downwards and fill the hole. Here the sand transport is stopped and it will take place at another location where the cover layer is not sand-tight. The slope will retreat and more rock will reach the slope from the waiting stack of material.

In this way, the erosion of sand is slowed down significantly and the stability of the slope is secured. Besides this, it was noticed that the flow conditions in rivers like the Ganges and Brahmaputra show extreme fluctuations (see Appendix 12). The scour depth, with the attendant need for a falling apron, are therefore not present year-round and not every year. Only during the periods with high flow velocities, does the probability of scour exist.. During the period 1998-2001, the apron at the Jamuna Bridge was attacked only once

This seems to agree nicely with the observed behaviour. When the toe is attacked by scour, an even covering of the slope appears. This might not be sand-tight, but it does slow down the toe erosion.

Another aspect of the durability is the existence of macro-stability along the revetment or guide bund. On the basis of model and prototype, it can be stated that the steepness of the slope stays limited to the angle of repose of the bed material in the flow condition present at location. This includes the secondary influences and will be in the order of 1V:2H for sand. When the soil conditions are well known, this should not give a problem relating to the stability of the slope as a whole.

However, problems relating to micro-stability could occur, especially when the constructed upper slope consists of a thick filter layer or sand-tight mattress, with a very low permeability. If the water level in the river drops quickly, a steep groundwater gradient will be present in the bund. Because of the open structure of the covered apron slope, the water can flow out in this part of the slope and transport of sand through the apron could occur.

The most probable failure mechanisms are summarised. It can be stated that the falling apron does not fulfil its functions if the following events occur:

- Hydraulic instability of rock in the current (transport),
- Presence of clay layers which will form steep slopes,
- Usage of all material present in the apron and the uncovering of the toe of the constructed slope. When this happens, the scour will continue at the toe of the constructed slope, eventually leading to slope failure,
- Apron material, which does not easily *launch* is used. The scour slope should be covered with a layer of material at all times.
- Flow slide due to a high and steep slope.

11 Conclusions and recommendations

11.1 Introduction

In this chapter, the conclusions that relate to the setting behaviour of a falling apron are drawn. In the introduction to this report on page 16, the objective of the project was presented in the form of four separate project aims:

- To obtain insight into the falling process and the successive phases (what happens?),
- To determine whether different configurations influence the final slope (is special care during dumping necessary?),
- To determine how an apron with insufficient rock should be re-strengthened,
- To determine whether the use of a falling apron will provide a durable protection against scour.

The descriptions of the model and the prototype provide answers to some of these questions. However it should be kept in mind that this study was only a pilot study and therefore a first exploration of the falling apron behaviour. The experiments that were executed fulfilled this purpose, but cannot be regarded as a perfect representation of the prototype.

In addition to the conclusions, recommendations are also made. These include recommendations concerning the design of future structures incorporating a falling apron and recommendations concerning supplementary research.

11.2 Conclusions

The following conclusions can be drawn concerning the setting process and setting result:

- A falling apron settles evenly and over the entire slope. In the model, the scour hole slope was covered with rock at all times.
- The slope angle is approximately 1:2. This seems to hold for both model and prototype and agrees with the expected steepness described in the literature.
- The resulting protective layer stays limited to a single layer of granular material.
- The rock size does not influence the angle of the slope.
- Applying a thicker apron does not lead to the formation of a thicker protective layer on the slope. It will however slow the retreat of the apron edge.
- When the falling apron is constructed in the form of a wedge towards the river, more material is stored at the outer side. This will retard the retreat of the apron at the beginning of the setting process.
- The slope protection is not sand-tight. Because of the single layer and the relatively large rock used, the openings between the rock are such that the layer cannot retain the sand.
- The slope protection retards the transport of bed material through the layer. Although not sand-tight, the protective layer will limit the transport of sand from under the layer.

- After reaching an equilibrium depth, the larger part of the falling apron is still unaffected. This extra buffer quantity will be necessary, however, when a greater depth occurs or when a river branch is adjacent to the revetment.
- The falling apron is a flexible protection, which can adapt to flow conditions when the river attacks at an angle. In the upstream part of the model the apron was attacked at an angle. Here the setting was also even and showed the same behaviour.
- When it is necessary to replenish a falling apron, the extra volume of rock should be dumped on the horizontal part of the apron. The setting mechanism can then distribute the rock over the slope. Because of the relatively steep slope of 1:2 and the modest rock layer on the slope, trying to place the extra quantity directly on the slope is not considered an option.

11.3 Recommendations

The recommendations following from this study are subdivided in two different categories: recommendations on additional research and recommendations on future design practice.

For additional research

- The execution of a duration experiment should give more information on what happens after the equilibrium depth is reached and when flow conditions are still such that sand transport from under the rock layer occurs.
- The execution of an experiment with a wide rock grading should give more insight into the actual transport of the fines in the grading, as expected from the results of this study. Such an experiment should be executed with a high velocity (fine fraction not stable, large fraction stable).
- When additional model experiments are to be executed, it is recommended that a flume model should be used. This seems to give satisfying results. The size chosen, however, should be wider and longer. The scale of the model used in this study was limited by the width and length of the flume; however, larger flumes are in use, in which a larger rock size can be tested. The relation between small sand grains and large apron material would then be represented more accurately.
- A study of the behaviour of alternative materials such as sand filled geotextile bags and uniform CC-blocks might contribute to more innovative design. The problem is that using quarried rock in a country like Bangladesh will always lead to logistical problems and therefore high project costs. It must be kept in mind however, that the use of materials such as, CC-blocks will not automatically lead to lower costs. The costs have to be calculated for each individual project, but it is also essential to consider the behaviour of the alternative material in the conditions in question.

For design practice

- Wedge-shaped design is recommended above a rectangular cross-section. More material in the riverside of the apron slows the retreat and therefore keeps the scour hole slope at a larger distance from the revetment.
- The use of a wide grading is expected to lead to high losses and therefore is not considered a good option. The design consideration of applying a wide grading which should form a filter structure (fines washing out from the top

layer) is not valid when the rocks in the apron reach the scour hole slope one by one.

- A falling apron always requires maintenance, but how often will depend on the frequency of its attack.

Bibliography

ASCE (2000), “Hydraulic Modeling, Concepts and practice”, ASCE, Reston, USA, ISBN 0-7844-0415-1.

Barnes, Jr. R.C. (1971), “Erosion control structures”, Chapter 28 in H.W. Shen “Rivermechanics”. Fort Collins, Colorado State University, U.S.A.

Best, J.L. and Bristow, C.S. (1993), “Braided Rivers”, The Geological Society, London, U.K, ISBN 0-903317-93-1.

Breusers, H.N.C., Raudkivi, A.J. (1991), “Scouring”, Balkema, Rotterdam, The Netherlands.

CBIP (1989), “River behaviour management and training”, CBIP, New Delhi, India.

China-Bangladesh Joint expert team (1991), “Study report on flood control and river training project on the Brahmputra River in Bangladesh”. Vol 3, FAP 24-3.

CUR/ CIRIA (1991), “manual no 169, Manual on the use of rock in coastal and shoreline engineering”, CUR/ CIRIA, Gouda, The Netherlands.

CUR (1991), “rapport 91-1, Toegepast filteronderzoek, inventarisatie van ontwerpregels voor filterconstructies in de waterbouw (in Dutch)”, CUR Gouda, The Netherlands.

CUR (1993), “rapport 161, Filters in de waterbouw (in Dutch)”, CUR Gouda, The Netherlands, ISBN 90-3760-029-8.

CUR/ CROW/ NNI (1993), “Rapport 93-4Handleiding voor de monsterneming van loskorrelige materialen” (in Dutch), Gouda, The Netherlands.

Central Board of irrigation and power (1994), “River behaviour management and training, vol. I and II”, Malcha Marg, New Delhi, India.

Central Water and power research station (1938), “Annual Report 1937-1938”, pp 68-76, Govt of India, Pune, India.

CWPRS (1944), “Annual Report 1944”, pp 74-81, Govt of India, Pune, India.

CWPRS (1946), “Annual Report 1946”, pp 6-15, Govt of India, Pune, India.

CWPRS (1947), “Annual Report 1947”, pp 54-57, Govt of India, Pune, India.

Duivendijk, J.V.(1997), “Building the Jamuna Bridge in Bangladesh. Land & Water International, 89, 15-18.

De Groot (1988), “Gedrag van een bodemverdegingsrand bij een over- en langstrekkende stroom, verslag modelonderzoek Q771” (in Dutch), WL| Delft Hydraulics, Delft, The Netherlands.

Elling, R. et.al (1994), “Rapportage techniek” (in Dutch), Wolters-Noordhoff, Groningen, The Netherlands, ISBN 90-01-29131-7.

FAP 21/22 (1993), “Bank protection and River Training pilot project, final report planning study”, Dhaka, Bangladesh.

Gemeentewerken Rotterdam (2001), “Construction and Survey Accuracies for the execution of dredging and stone dumping works”, Rotterdam, The Netherlands.

Heeteren, J. et al. (1990), “Verweking van zand en zettingsvloeiing” (in Dutch), Grondmechanica Delft, Delft, The Netherlands.

Hemphill, R.W. and Bramley, M.E. (1989), “Protection of river and canal banks”, CIRIA, Cambridge, U.K.

Hight, D.W, e.a.(1998), “Flow slides in micaeous sands” article.

ICE (1985), “Flexible armoured revetments incorporating geotextile” Proc. of the Int. Conference organised by the Institution of Civil Engineers, London, U.K., ISBN 0-7277-0226-2.

Jamuna Multipurpose Bridge Authority (1999), “Padma Bridge Feasibility Study- Phase I, Draft final report”, RP-NEDECO, BCL, Peoples Republic of Bangladesh.

Jansen, P.Ph. (1979), “Principles of river engineering”, Pitman Publishing Company, London, U.K.

Kolkman, P.A. et.al. (1988), “Modelling Soil- Water- Structure interactions”, Balkema, Rotterdam, The Netherlands.

Maynord, S.T. et.al. (1995), “River, Coastal and Shoreline Protection: Erosion Control using Riprap and Armourstone”, John Wiley & Sons, U.S.A.

Mott MacDonald (1996),”Paksey bridge construction project, Design report”. Gov. of Peoples republic of Bangladesh.

Mundegar, A.K. (1998), “Engineering in micaeous sands: the practical significance of mica content”, In: Ground Engineering, Nov. 1998, p34-36.

Nedeco (1989), “Jamuna Bridge project, Phase II study, River Training Works, design report”, Dhaka, Bangladesh.

Nedeco (1996), “River training works for Jamuna Bridge Report on 1996 design of east guide bund re-assessment of slopes, updating of lay out” Experiment report FAP 21/22. Gov. of Peoples republic of Bangladesh.

Oostinga, H. and Daemen, I., “Construction of the River Training Works for the Jamuna Bridge Project in Bangladesh”. In: Terra et Aqua 69 (1997), p.3-13.

Przedwojski, Blazejewski, Pilarczyk (1995), “River training techniques”, Balkema, Rotterdam, The Netherlands.

Raudkivi, A.J., 1993, “Sedimentation, Exclusion and removal of sediment from diverted water”, IAHR, Balkema, Rotterdam, The Netherlands, ISBN 90-5410-132-6.

Rendel Palmer & Tritton (1997), “Bhairab Bridge Appraisal Study. Phase 2, Final Report”, Dhaka, Bangladesh.

Rendel Palmer & Tritton, (1999), “Padma Bridge Study. Phase I, Prefeasibility, Draft Final Report”, Dhaka, Bangladesh.

RWS (1991), “Handboek uitvoering bodemverdedigingscostructies van losgestorte granulaire materialen (Dutch). Bouwdienst RWS, The Netherlands.

Sarkar, K.A. (1995), “Experience of using Riprap Works in Bangladesh”, article, appendix in: [Maynord et.al. 1995].

Schiereck (2000), “Introduction to Bed, Bank and Shore protection”, Delft University of Technology, Delft, The Netherlands.

Second Flood Restoration Project (1990), “Consultancy services for protection of Megnha River Railway Bridge at Bhairab Bazar, Final report”, Dhaka, Bangladesh.

Sir William Halcrow & Partners Ltd. (1993), “River Training Studies of the Brahmaputra River”,Dhaka, Bangladesh.

Slaa, B. te (1995), “River training works for a bridge across the Brahmaputra River, Bangladesh”, article, appendix in: [Maynord et.al. 1995].

Stephenson, D. (1979), “Rockfill in Hydraulic Engineering”, Elsevier, Amsterdam, The Netherlands.

Tappin, R. Duivendijk, J.V. and Haque, M. (1998), “The design and construction of Jamuna Bridge, Bangladesh”. Proc. Inst. Civ. Eng., 126, nov, 150-162, paper 11704.

Delft University of Technology (1984), “Flexibele waterbouwkundige constructies, collegedictaat f13A”(in Dutch), Delft, The Netherlands.

U.S. Army Engineers Waterways Experiment station (1984), “Shore Protection Manual, fourth edition”, Vicksburg, U.S.A.

Verruijt, A. (1993) “Grondmechanica”, Delftse Uitgevers Mij., Delft, The Netherlands, ISBN 92-6562-045-1.

Vriend, H.J. de (1999), “Rivierwaterbouwkunde”, Delft University of Technology, Delft, The Netherlands.

Vries, M. de (1976) ”Waterloopkundig onderzoek (in Dutch)” collegehandleiding, Delft University of Technology, Delft, The Netherlands.

WL|Delft Hydraulics (1976), “Inleiding fysisch modelonderzoek, schaalregels” (in Dutch), rapport V26, Delft, The Netherlands.

WL|Delft Hydraulics (1988), “Ontgrondingsproeven, verslag modelonderzoek H298” (in Dutch), Delft, The Netherlands.